

The Pennsylvania State University
The Graduate School
Department of Electrical Engineering

**THE NEW ARECIBO HF INTERACTIONS FACILITY
DUAL ARRAY CASSEGRAIN ANTENNA DESIGN**

A Thesis in
Electrical Engineering
by
Kyle Lawrence Labowski

© 2009 Kyle Lawrence Labowski

Submitted in Partial Fulfillment
of the Requirements
for the Degree of

Master of Science

May 2009

The thesis of Kyle Lawrence Labowski was reviewed and approved* by the following:

James K. Breakall
Professor of Electrical Engineering
Thesis Advisor

Lynn Carpenter
Associate Professor of Electrical Engineering

Ken Jenkins
Professor of Electrical Engineering
Head of the Department of Electrical Engineering

*Signatures are on file in the Graduate School

ABSTRACT

A new HF facility at Arecibo will replace prior facilities that are no longer in operation. The location of the observatory at Arecibo is perfect for HF studies. It will provide the ability to study the upper atmosphere, study plasmas, and several other uses.

The facility will make use of the infrastructure already in place at the Arecibo Observatory. One of two arrays of cross dipoles, operating at 5.1 MHz or 8.175 MHz respectively, will project energy onto a mesh net with 5 foot openings. The energy will then reflect back onto the 305 m diameter dish already in place at Arecibo. Together they will form a cassegrain system for the HF facility. The arrays will be either RHC or LHC polarized.

A combination of GNEC and FEKO was used to model and analyze this design. The design was examined for VSWR, gain, cross polarization rejection, and near field effects. The final design is predicted to have less than 2:1 VSWR across a 100 kHz band at each center frequency. The predicted gains are 22.16 dBi at 5.1 MHz and 25.46 dBi at 8.175 MHz. The antennas will be fed with six, 100 kW sources for a total of 600 kW. This corresponds to an ERP of 98.6 MW at 5.1 MHz and 210.9 MW at 8.175 MHz. There will be no danger to visitors to the facility due to field levels. It is, however, recommended that workers at the facility do not stay on the platform while the facility is in use.

TABLE OF CONTENTS

LIST OF FIGURES	vi
LIST OF TABLES	ix
ACKNOWLEDGEMENTS	x
Chapter 1 Background	1
1.1 General Background	1
1.2 Atmospheric Heating	1
1.2.1 Aeronomy	2
1.2.2 Electron Thermal Balance in Ionosphere	3
1.2.3 Resonant Langmuir/Ion Oscillations Study	3
1.2.4 Electron Acceleration Process Study	4
1.2.5 Structuring of the Ionospheric Plasma at Sub-Kilometer and Meter Scale Lengths	4
1.2.6 HF Radar Studies	5
1.3 The Need for a New HF Heating Facility	5
1.4 Current Design	6
1.4.1 Previous Cross-Dipole Study	6
1.4.2 Current Array Study	6
Chapter 2 Theoretical Background	7
2.1 Method of Moments	7
2.1.1 Weighting Functions	10
Chapter 3 Project Design	12
3.1 Software Modeling	12
3.2 Antenna Specifications	13
3.3 Phased Dipole Array Model	13
3.4 Subreflector Modeling	17
3.4.1 The Original Cassegrain Model	17
3.4.2 The Refined Cassegrain Model	19
3.5 Source Modeling	22
3.5.1 Single Array Design	22
3.5.2 Dual Array Design	25
3.6 Size and Dimensions	26
3.7 Additional Facility Components	32
3.7.1 Transmitters	32
3.7.2 Transmission Lines	33
3.7.3 AC Power Transmission and Switching	33

Chapter 4 Array Modeling Results	34
4.1 Impedance and VSWR	34
4.1.1 Single Array Results at 5.1 MHz.....	35
4.1.2 5.1 MHz Array with 8.175 MHz Array Shorted	38
4.1.3 5.1 MHz Array with 8.175 MHz Array Open	42
4.1.4 Single Array Results at 8.175 MHz.....	45
4.1.5 8.175 MHz Array with 5.1 MHz Array Shorted	48
4.1.6 8.175 MHz Array with 5.1 MHz Array Open	51
4.2 Far Field Results	54
4.2.1 Far Field 5.1 MHz Array with 8.175 MHz Array Shorted and Open ..	55
4.2.2 Far Field 8.175 MHz Array with 5.1 MHz Array Shorted.....	58
4.2.3 Far Field 8.175 MHz Array with 5.1 MHz Array Open.....	61
4.3 Near Field Levels.....	64
4.3.1 Near Field Levels at 5.1 MHz with 8.175 MHz Shorted.....	64
4.3.2 Near Field Levels at 5.1 MHz with 8.175 MHz Open	67
4.3.3 Near Field Levels at 8.175 MHz with 5.1 MHz Shorted.....	70
4.3.4 Near Field Levels at 8.175 MHz with 5.1 MHz Open	73
4.4 Field Levels and Safety	76
4.4.1 Field Levels at Gregorian Dome	78
4.4.2 Field Levels at Upper Platform	81
4.4.3 Field Levels at Visitors Center	83
4.4.4 Field Level Summary	85
Chapter 5 Conclusion.....	88
Bibliography	90
Appendix A FEKO Model Input File for Dual Array Design with 5.1 MHz Active.....	91
Appendix B FEKO Model Input File for Dual Array Design with 8.175 MHz Active.....	103
Appendix C NEC File for the Upper Platform	115
Appendix D Graph of Maximum Permissible Exposure Levels for Controlled Environments in terms of Field and Power Density	119
Appendix E Graph of Maximum Permissible Exposure Levels for Uncontrolled Environments in terms of Field and Power Density	120

LIST OF FIGURES

Figure 1-1: Proposed HF Facility Uses.....	2
Figure 3-1: Proposed dual frequency tower design	14
Figure 3-2: Six tower array design before rotation.....	15
Figure 3-3: Six tower array design after rotation.....	16
Figure 3-4: The original cassegrain subreflector design.....	18
Figure 3-5: Surface Currents at 5.1 MHz on Subreflector Mesh.....	20
Figure 3-6: Cut Down Cassegrain Subreflector.....	21
Figure 3-7: Single Crossed Dipole with Sources and Phase Labeled.....	23
Figure 3-8: Top View of the Three Tower Array	24
Figure 3-9: FEKO Model of the HF Facility at Arecibo	26
Figure 3-10: Dipole Ends with Balls	28
Figure 3-11: 5.1 MHz and 8.175 MHz arrays.....	29
Figure 3-12: Side View of Dish (transparent), Dipole Arrays and Subreflector	30
Figure 3-13: Top view of subreflector	31
Figure 3-14: Transparent Subreflector with Dipole Arrays Underneath	32
Figure 4-1: Input Resistance for 5.1 MHz Array Alone	36
Figure 4-2: Input Reactance for 5.1 MHz Array Alone.....	37
Figure 4-3: VSWR for 5.1 MHz Array Alone	38
Figure 4-4: Input Resistance at 5.1 MHz with 8.175 MHz Array shorted.....	39
Figure 4-5: Input Reactance at 5.1 MHz with 8.175 MHz array shorted	40
Figure 4-6: VSWR at 5.1 MHz with 8.175 MHz array shorted.....	41
Figure 4-7: Input Resistance at 5.1 MHz with the 8.175 MHz Array Open.....	42
Figure 4-8: Input Reactance at 5.1 MHz with the 8.175 MHz array open	43

Figure 4-9: VSWR at 5.1 MHz with 8.175 MHz Array Open.....	44
Figure 4-10: Input Resistance for 8.175 MHz Array Alone	45
Figure 4-11: Input Reactance for 8.175 MHz Array Alone.....	46
Figure 4-12: VSWR for 8.175 MHz Array Alone	47
Figure 4-13: Input Resistance at 8.175 MHz with the 5.1 MHz Array Shorted.....	48
Figure 4-14: Input Reactance at 8.175 MHz with 5.1 MHz Array Shorted.....	49
Figure 4-15: VSWR at 8.175 MHz with 5.1 MHz Array Shorted.....	50
Figure 4-16: Input Resistance at 8.175 MHz with the 5.1 MHz Array Open.....	51
Figure 4-17: Input Reactance at 8.175 MHz with 5.1 MHz array open	52
Figure 4-18: VSWR at 8.175 MHz with 5.1 MHz open.....	53
Figure 4-19: HF Facility Design with Coordinate Axis.....	55
Figure 4-20: Comparison of the Far Field Gain at $\Phi = 0^\circ$ and $\Phi = 90^\circ$ at 5.1 MHz ...	56
Figure 4-21: Comparison of the LHC and RHC Gain Patterns at 5.1 MHz	57
Figure 4-22: Comparison of the Far Field Gain at $\Phi = 0^\circ$ and $\Phi = 90^\circ$ at 8.175 MHz.....	59
Figure 4-23: Comparison of the LHC and RHC Gain Patterns at 8.175 MHz	60
Figure 4-24: Comparison of the Far Field Gain at $\Phi = 0^\circ$ and $\Phi = 90^\circ$ at 8.175 MHz.....	62
Figure 4-25: Comparison of the LHC and RHC Gain Patterns at 8.175 MHz	63
Figure 4-26: Near Field Plot of 5.1 MHz Active Dipole Tip.....	65
Figure 4-27: Near Field on Subreflector Edge with 5.1 MHz Active Array	66
Figure 4-28: Near Field Levels on the passive 8.175 MHz Array (shorted)	67
Figure 4-29: Near Field Levels on 5.1 MHz Active Array.....	68
Figure 4-30: Near Field Levels on Subreflector Edge while 5.1 MHz Array Active..	69
Figure 4-31: Near Field Levels on 8.175 MHz Passive Array (open).....	70

Figure 4-32: Near Fields on the 8.175 MHz Active Array	71
Figure 4-33: Near Field Levels on the Subreflector While 8.175 MHz Array Active.....	72
Figure 4-34: Near Field on 5.1 MHz Passive Array (shorted).....	73
Figure 4-35: Near Fields on the 8.175 MHz Active Array	74
Figure 4-36: Near Fields on subreflector while 8.175 MHz Array Active.....	75
Figure 4-37: Near Fields on 5.1 MHz Passive Array (open)	76
Figure 4-38: Transparent Model of Gregorian Dome Showing Near Field Slice Location	78
Figure 4-39: Near Field Values at 5.1 MHz in Gregorian Dome	79
Figure 4-40: Near Field Values at 8.1 MHz in Gregorian Dome	80
Figure 4-41: Side View of Upper Platform Showing Near Field Location	81
Figure 4-42: Near Field Values on Upper Platform at 5.1 MHz	82
Figure 4-43: Near Field Values on Upper Platform at 8.175 MHz	83
Figure 4-44: Near Field Levels at Visitors Center at 5.1 MHz.....	84
Figure 4-45: Near Field Levels at Visitors Center at 8.175 MHz.....	85

LIST OF TABLES

Table 3-1 : Array Phasing.....	25
Table 3-2 : Antenna Dimensions	27
Table 4-1 : Table of Max. Permissible Exposure Levels for Controlled and Uncontrolled Environments.....	77
Table 4-2 : Comparison of FEKO Calculated Field Levels with Maximum Permissible Exposure Levels.....	87

ACKNOWLEDGEMENTS

First I would like to thank my parents for their help and support over the years. Their encouragement helped push me to continue my education.

I would also like to thank Dr. James Breakall for providing me the opportunity to work with him. As an advisor he helped me learn a great deal of information about how antennas work, both theoretically and in actual real world applications.

Finally I would like to thank Dr. Mike Sulzer and everyone at the Arecibo Observatory for their help in the refinement of the HF Heating Facility design. I would also like to thank them for the opportunity to work on such an interesting and complex project.

Chapter 1

Background

1.1 General Background

The Arecibo Observatory conducts research in several fields of science. These fields include Radio Astronomy, Radar Astronomy, and Atmospheric Science. Radio Astronomy involves studying the natural radio energy emitted by galaxies, erupting stars, clouds of gas, pulsars, and quasars. It uses receiving antennas to locate and study the energy emissions from these far off objects. Radar Astronomy studies objects in our solar system such as asteroids, planets, moons, and comets. It involves sending energy from the 1000 foot reflector to the object under study and collecting the reflected energy. This information is processed to determine information such as composition, size, shape, rotation, surface roughness, and the path of the object under study. The third area of research, and the area of most interest to this paper, is Atmospheric Science. Atmospheric Science is the study of the gases surrounding the Earth [1]. One way of studying the atmosphere is through HF heating.

1.2 Atmospheric Heating

Atmospheric heating involves observing the response of ionospheric plasma to HF excitation. When an electromagnetic wave passes through a partially ionized medium some of the energy of the wave is lost. If there is enough power density it will disturb the

plasma properties. The observation of this affect can help tell a lot of information about the plasma and the neutral upper atmosphere. The geographic location of Arecibo makes it an ideal place to study plasmas because it has a relatively calm atmosphere compared to polar or equatorial locations. Figure 1-1 is a graphic taken from the original proposal that summarizes the intended uses for the HF facility. The following sections explain the intended used in more detail [7].

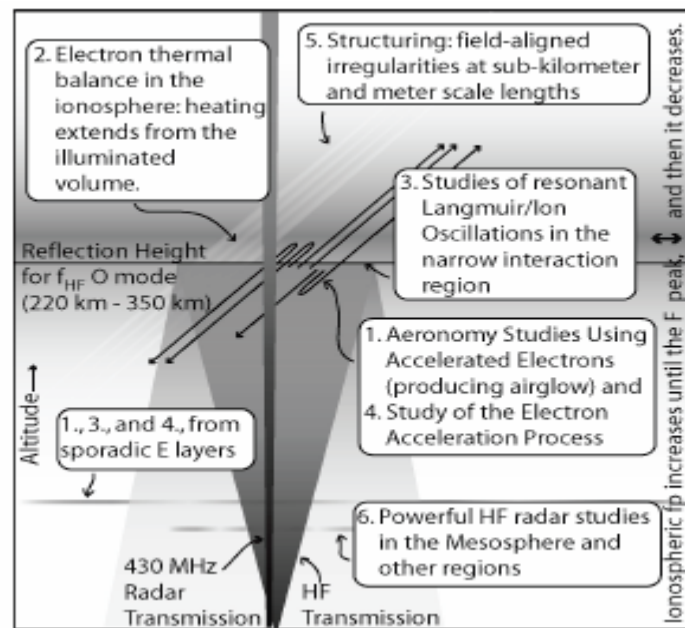


Figure 1-1: Proposed HF Facility Uses

1.2.1 Aeronomy

Aeronomy is a study of the upper regions of the atmosphere. As part of this study a facility is required that will provide enough power density to create accelerated

electrons. The accelerated electrons create several affects that are important to study to better understand these regions of the atmosphere. One affect is that it can produce a phenomenon called airglow. Airglow is a side affect of the electron acceleration process that produces a visible glow when atoms are excited by the electrons. The threshold at which this occurs is at 80 MW of power. Creating and studying this phenomenon, along with the other affects of the HF facility can yield new information on the ionosphere.

1.2.2 Electron Thermal Balance in Ionosphere

By using different power levels at the HF facility it is possible to calculate electron gas heating and cooling rates. This will be done through monitoring the HF-induced temperature changes. There is still much to be understood about atom and ion-atom exchange rates. Right now uncertainty in the exchange rate is still around 50%. Using the HF facility to heat the atmosphere, the ion and electron temperature growth and decay curves can be analyzed and modeled. This will be done via radar and optical methods.

1.2.3 Resonant Langmuir/Ion Oscillations Study

HF heating experiments have shown that the HF heating increases these resonant instabilities in the plasma. This facility will provide a means of accentuating these Langmuir/ion oscillations for detailed study.

1.2.4 Electron Acceleration Process Study

The physical process that accelerates electrons to suprathermal energies through the HF waves is not well understood. Current observations from after the facility has been on for 50 ms or more do not match theoretical predictions. Arecibo hopes to combine the HF induced acceleration of electrons with its advanced radar to better understand the physical processes at work.

1.2.5 Structuring of the Ionospheric Plasma at Sub-Kilometer and Meter Scale Lengths

Heating experiments have shown that irregularities in the atmosphere can disturb communication and navigation systems. The difference between naturally occurring disturbances and the HF-induced disturbances are not well understood. It is known that HF-induced irregularity amplitudes saturate quickly and do not exceed 1%. Naturally occurring irregularities saturate at higher amplitudes of tens of percent. It is not known how the new facility will compare to naturally occurring phenomena, but it is hoped that a better understanding of the plasma physics involved will occur. The relatively stable mid-latitude ionosphere above Arecibo will also allow the plasma to stay within the beam longer and allow more observation and excitation time.

1.2.6 HF Radar Studies

The facility will also be able to be used as an HF radar to look at the mesosphere, turbopause, and lower thermosphere. Using the HF radar while using the 430 MHz radar will add greater detail to measurements and will better define the process of HF observation. It could also image HF induced irregularities excited in the F-region above Arecibo, along with other possible radar applications.

1.3 The Need for a New HF Heating Facility

Two previous attempts were made to have an HF facility at the Arecibo Observatory. Both installations are no longer in use due to damage from two different sources: time and nature.

The first HF facility was a log periodic antenna suspended from the upper platform. It was driven with a 100 kW source and had a frequency range of 3 to 10 MHz. This antenna was put in place for heating campaigns then stored away next to one of the support towers. This design eventually started arcing and there was corona formation that caused this iteration of the HF facility to fall out of use [5].

The second iteration of the HF facility at Arecibo was located off-site. It was a pyramidal log-periodic array with 32 elements. The frequency range of the array was 3 to 8 MHz and had a gain of 23 dBi. The input power was 600 kW [6]. This facility was hit by Hurricane Georges in September 1998. It was not rebuilt due to government restrictions on land use [7].

1.4 Current Design

1.4.1 Previous Cross-Dipole Study

A prior study was done on the feasibility of using a cross dipole array with a mesh subreflector. There would be three cross dipoles at each frequency. The subreflector would be suspended under the platform and was modeled based on the how a circus net of similar size would hang if suspended from three points. This study focused on two separate arrays at 5.1 MHz and 8.175 MHz. It did not study interactions between arrays and was a best case scenario examination of the feasibility of this plan. The results are found in a thesis written by William Glessner [2].

1.4.2 Current Array Study

The previous design was deemed acceptable. The gain of 22.0 dBi at 5.1 MHz and 25.65 dBi at 8.175 MHz was acceptable. There are no concerns for the near field, and the cross polarization rejection was above 27 dB. The next iteration of the project is concerned with refining the design and studying the interactions between the arrays. The other question that has to be answered is how will the arrays be designed? Will there be 3 towers and the two arrays will be stacked? Will there be 6 towers? What are the benefits of each design and which one makes the most sense? The last questions that have to be answered concern the subreflector. Can the size of the subreflector be reduced while maintaining previous performance of the system? The following chapters provide the final design specification along with the performance as predicted by FEKO [10].

Chapter 2

Theoretical Background

There are many methods used to solve electromagnetics problems. Method of Moments, Finite Element Method, and Finite Difference Time Domain are a few of the more well known methods. Method of Moments is an integral based electromagnetics numerical method. It is based in the frequency domain. The finite element method is another frequency based method, but it is differential equation based. Finite difference time domain is another popular method. It is differential equation based and in the time domain. The FEKO code is based on method of moments and will be the focus of this section

2.1 Method of Moments

Although a commercial code such as FEKO is very complicated to write, this section will give a basic introduction to the method of moments numerical method. The idea is to break up the problem space into smaller parts. From there the current distribution is approximated by a basis function. Either Pocklington's integral or Hallen's integral (or some other method) is used as the basis for the calculation of the current density. The current on each segment is assumed to be an unknown constant that can be solved for based on the basis function. The electric fields on the object under analysis are known already whether they are caused by source of the antenna, or the

scattered fields off of other elements. From there the impedance matrix is solved based on the assumed current distribution. The current is then found from the impedance matrix and the known excitation. Most of the following explanation is taken from [8] unless otherwise noted.

Let's start with a generic form describing an antenna in the z-axis:

$$-\int I(z')K(z, z')dz' = E_z^i(z) \quad 2.1$$

$K(z, z')$ in Eq. 2.1 is an integral equation that depends on the method chosen [8]. Examples include Pocklington's Integral Equation and Hallen's Integral Equation [9]. If the equation is rewritten as follows:

$$-\int_{-L/2}^{L/2} I(z')K(z, z')dz' = E_z^i(z) \quad 2.2$$

$I(z')$ in eq. 2.2 can be approximated by:

$$I(z') = \sum_{n=1}^N I_n F_n(z') \quad 2.3$$

I_n in eq. 2.3 is an unknown expansion coefficient. F_n is a basis function that governs the current distribution. It can be implemented in several ways. It can be a triangular distribution over a segment or it can be a pulse function [9]. For simplicity an orthogonal pulse function will be used:

$$F_n(z') = \begin{cases} 1 & \text{for } z' \text{ in } \Delta z_n \\ 0 & \text{otherwise} \end{cases} \quad 2.4$$

Substitute eq. 2.3 into Eq. 2.2:

$$-\int_{-L/2}^{L/2} \sum_{n=1}^N I_n F_n(z') K(z_m, z') dz' \approx E_z^i(z_m) \quad 2.5$$

Eq. 2.5 is approximately equal to the right side of the equations because the current distribution is now being approximated. The ‘m’ subscript refers to the fact that the integral equation is only being enforced at segment m. This is because a weighting function has been applied to simplify the equations. The next section will discuss weighting functions in more detail. Rearranging Eq. 2.5 yields:

$$-\sum_{n=1}^N I_n \int_{\Delta z_n} K(z_m, z') dz' \approx E_z^i(z_m) \quad 2.6$$

Let:

$$f(z_m, z_n) = -\int_{\Delta z_n} K(z_m, z') dz' \quad 2.7$$

Substituting eq. 2.7 into Eq. 2.6:

$$\sum_{n=1}^N I_n f(z_m, z_n) \approx E_z^i(z_m) \quad 2.8$$

Eq. 2.8 can be rewritten in the following form:

$$\sum_{n=1}^N Z_{mn} I_n = V_m \quad m = 1, 2, 3, \dots, N \quad 2.9$$

$$V_m = E_z^i(z_m)$$

$$Z_{mn} = f(z_m, z_n)$$

Eq. 2.9 can be rewritten in matrix form as:

$$[Z_{mn}] [I_n] = [V_m] \quad 2.10$$

It is not obvious why Z_{mn} is equal to $f(z_m, z_n)$ without looking at one of the integral equations that govern the current distribution. The general form of the Pocklington Integral is given below:

$$-\frac{1}{j\omega\epsilon_0} \int_{-L/2}^{L/2} I(z') \left[\frac{\partial^2 \psi(z, z')}{\partial z'^2} + \beta^2 \psi(z, z') \right] dz' = E_z^i(z) \quad \mathbf{2.11}$$

Where the free space greens function given by:

$$\psi(z, z') = \frac{e^{-j\beta R}}{4\pi R} \quad \mathbf{2.12}$$

$$R = \sqrt{(z - z')^2 + a^2} \quad \mathbf{2.13}$$

'a' in Eq. **2.13** is the radius of the wire.

Part of the assumption made is that the current on each segment is an unknown constant that has to be solved for. This constant is governed by the basis function. In this case it is a constant value. If a triangular basis function was used the triangular distribution would have to be accounted for. Since it is a constant value for this example, it can be taken out from under the integral in Eq. **2.11**. This leaves us with an equation similar in form to eq. **2.7**.

2.1.1 Weighting Functions

A very important step in MoM formulations is applying the weighting functions. Most of this material is taken from [9]. Since method of moments only enforces boundary conditions at discrete points, the space in between may not satisfy boundary conditions. In order to improve the results and reduce the deviation between the discrete points a weighting function is used. The weight application is a scalar operation. If 'g' is

the basis function, ‘w’ is the weighting function, and ‘s’ is the surface of the structure being analyzed then:

$$\langle w, g \rangle = \iint_s w^* g \, ds \quad \mathbf{2.14}$$

A mathematical representation of the weighting function is:

$$\sum_{n=1}^N a_n \langle w_m, F(g_n) \rangle = \langle w_m, h \rangle \quad m = 1, 2, \dots, N \quad \mathbf{2.15}$$

The weighting functions are also linearly independent so that the N equations produced are linearly independent. Galerkin’s method is to let the basis function equal the weighting function. Proper choice of weighting functions can reduce the number of integrations necessary. It will remove the integration in Eq. **2.14** . A Dirac delta weighting function accomplishes this task:

$$[w_m] = [\delta(p - p_m)] = [\delta(p - p_1), \delta(p - p_2), \dots] \quad \mathbf{2.16}$$

The Dirac delta function reduces eq. **2.15** to:

$$h|_{p=p_m} = \sum_{n=1}^N a_n F(g_n) |_{p=p_m} \quad m = 1, 2, \dots, N \quad \mathbf{2.17}$$

Eq. **2.17** is the same form as eq. **2.9**. Applying the weight to Eq. **2.9** allows the Pocklington integral equation to be solved on a segment by segment basis. It also removes some of the anomalies in boundary conditions introduced by looking at the structure one point at a time.

Chapter 3

Project Design

3.1 Software Modeling

Several different software packages were used to model the HF facility. The platform was modeled using GNEC 1.4. The Gregorian dome, the dish, and the dipoles were modeled using FEKO 5.2. The preliminary design was performed by William Glessner and the original files can be found in his thesis [2]. The preliminary design did not include both arrays at the same time and therefore did not evaluate the effects of the passive array on the active array. The original cassegrain subreflector was remodeled using CADFEKO 5.3 and imported into the EDITFEKO file. Method of Moments was used to evaluate the model and look at VSWR, gain pattern, and near field effects.

The FEKO code for the array operating at 5.1 MHz is found in Appendix A. The FEKO code for the active array operating at 8.175 MHz can be found in Appendix B. Both files contain port loads that allow the passive array source to be either closed or open. They were included in the same file with one set commented out with a ‘**’ symbol before the lines in order to reduce the number of appendices included in this document.

3.2 Antenna Specifications

The goal of this project was to meet the original specifications given below:

Operating Frequency

5.1 MHz

8.175 MHz

2:1 VSWR Bandwidth

100 KHz (+/- 50 KHz from center operating frequency)

Polarization

LHC or RHC with the ability to switch between

Input Power

600kW peak power

In addition to these requirements the new design would also:

Meet the results given by a single array when both are present:

8.175 MHz

Gain 25 dBi

VSWR bandwidth

5.1 MHz

Gain 22 dBi

VSWR bandwidth

Reduce the size of the cassegrain reflector

3.3 Phased Dipole Array Model

The original feed design for the HF facility looked at both frequency arrays separately and optimized the locations without the second array being present [2]. The height above the dish, the distance between dipoles and the orientation of the dipoles with respect to each other were all optimized for each array at its specific frequency

When the time came to move the design forward and look at both arrays together two designs were put forth. One design proposed that only three towers would be used, and therefore each tower would have two sets of dipoles on it. Figure 3-1 shows an initial model of the design with two sets of crossed dipoles on one tower.

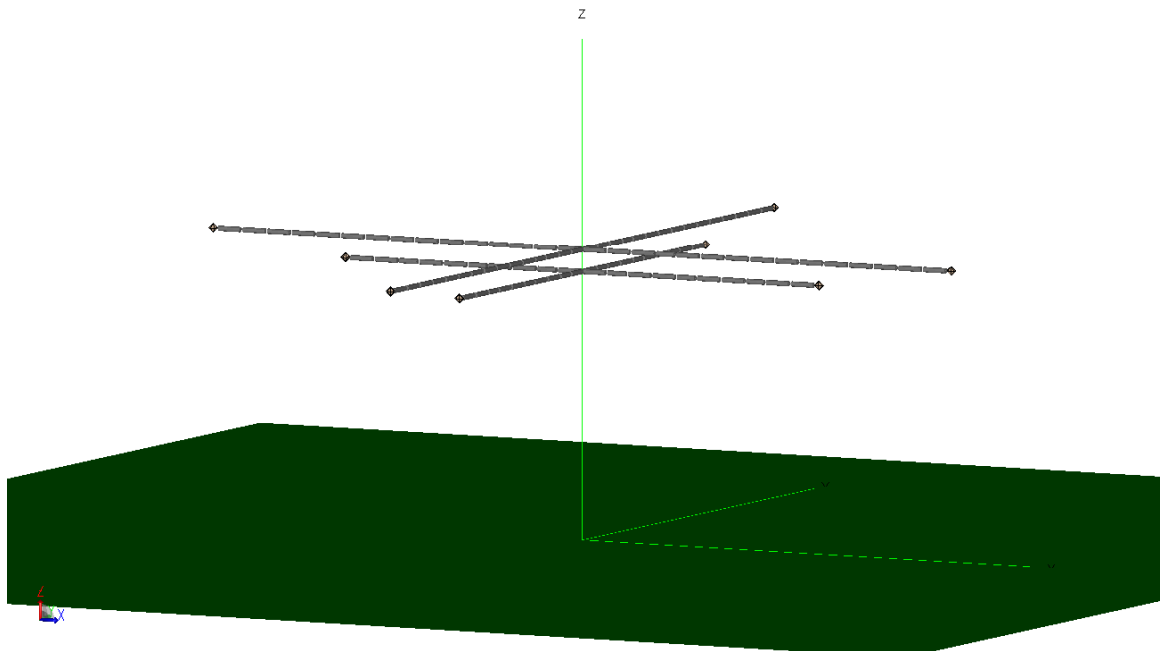


Figure 3-1: Proposed dual frequency tower design

The dual frequency tower design proved too difficult to conceptualize due to the complexity of the balun and the issue of how to efficiently switch between frequencies. Part of the balun's job is to choke off currents that would flow back down the input cable and resonate, affecting the radiation characteristics of the antenna. One type of balun is called a bazooka balun. The design of this type of balun calls for a tube that is $\lambda/4$ in length near the feed point of the antenna. A bazooka balun design for this application

would call for some kind of switch or filter to be designed that would allow the dual frequency operation. Since no off the shelf and well tested design met this criteria a six tower design was decided upon due to its less complex nature.

Figure 3-2 shows the initial state of the design once both arrays were imported into the same file. The elements of the arrays clearly overlap with detrimental affects to the VSWR even though both arrays are at different heights above the dish.

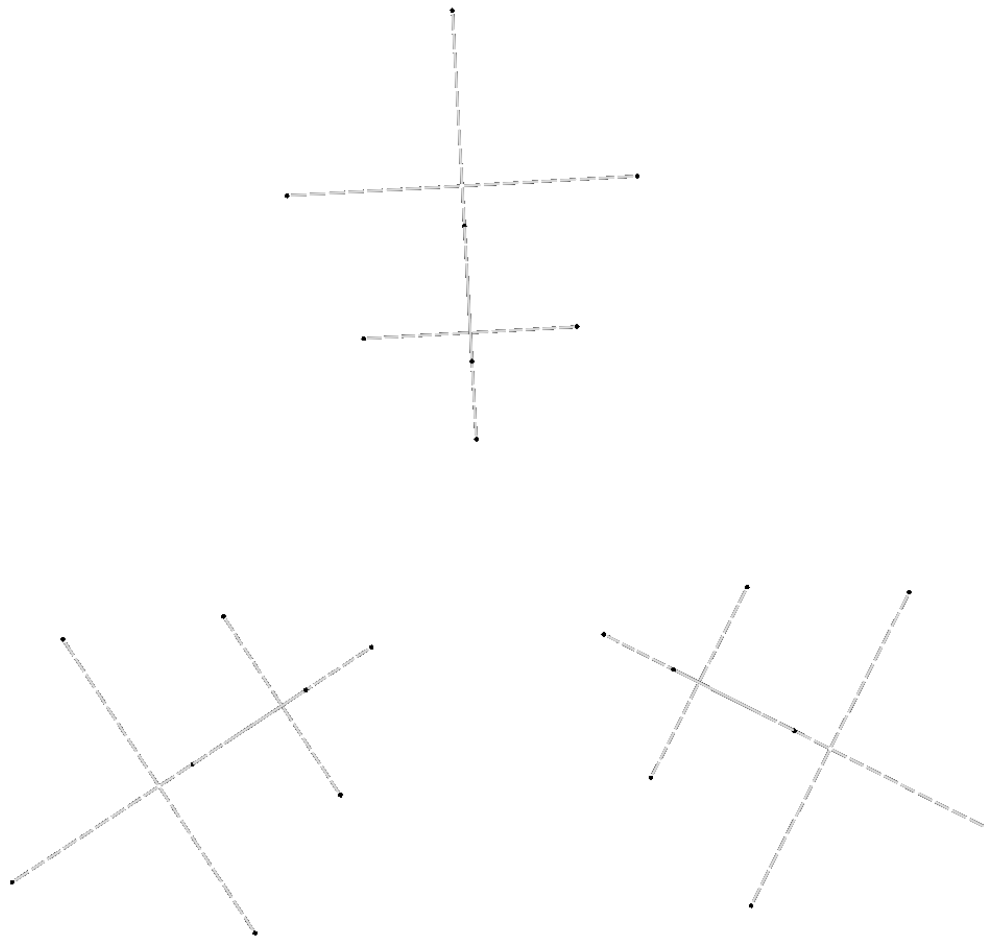


Figure 3-2: Six tower array design before rotation

To reduce the interaction of both arrays the 8.175 MHz array was rotated 60° from its original orientation. Figure **3-3** shows the new orientation of the feed antennas. The new orientation not only reduced the amount of antenna interaction, it also slightly improved the overall response of the antenna compared to Figure **3-2** .

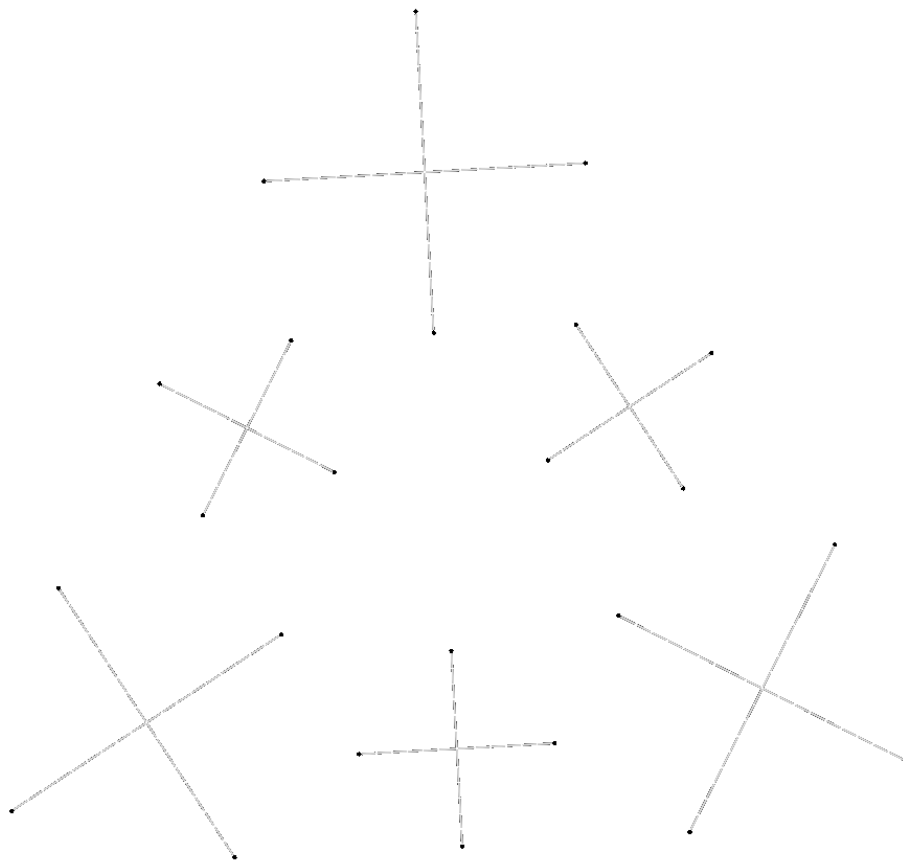


Figure **3-3**: Six tower array design after rotation

3.4 Subreflector Modeling

There were two embodiments of the cassegrain subreflector. The original one was modeled by Mr Glessner. Subsequent examination of the original design revealed that the subreflector could be reduced in size and cost without having a great impact on the performance of the facility

3.4.1 The Original Cassegrain Model

The original idea for the subreflector was a metallic net that would hang below the platform. The net creates a less costly solution to the problem of how to reflect the energy back onto the dish from the fed dipoles. A solid reflector of the same size would be prohibitively large and difficult to put in place without affecting the other instruments already in place at the Arecibo facility.

For modeling purposes the net is assumed to take a catenary shape due to a combination of suspension cables and gravity. Figure 3-4 shows the original design for the cassegrain subreflector. In order to minimize construction cost of the net and to lighten the weight associated with it, the hole spacing was set at the maximum distance that would still allow illumination at the smaller wavelength from the 8.175 MHz array. 5 foot openings are proposed for the net, with corresponds to $\lambda/24$ openings at 8.175 MHz. The original cassegrain model was optimized for height at each frequency separately so that the same reflector could be used for both arrays. It will be moved vertically up and down to the correct height for the array in use.

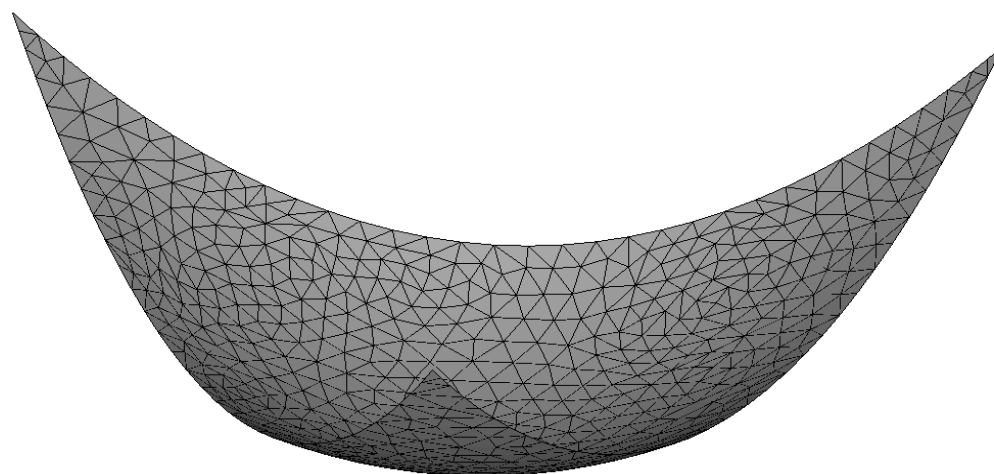


Figure 3-4: The original cassegrain subreflector design

A cassegrain shape can be approximated by a parabola. Figure 3-4 was designed from a parabola cut down into a triangular footprint using FEKO. The subreflector shown in the figure is broken up into triangular pieces by FEKO in order to model it. This creates a solid surface for the purposes of modeling and simulation. A mesh of wires in the same shape would require too many wires and therefore too much memory to reasonably model in FEKO. This is especially true in the testing phases while tweaking the design. Waiting a week for results of minor changes is not a reasonable use of time. In addition, the weight bearing characteristics of the net have to be designed by a mechanical engineer. Researching cable strength, diameter, and placement of the cables within the subreflector net is a task in itself. Mr. Glessner verified using Multilevel Fast Multipole Method (MLFMM) in FEKO that a surface cut up into a triangular mesh and a surface made of wires with 5 foot openings act the same at the frequencies of operation [2]. He used MLFMM because the number of segments used for the grid was too large for regular MOM to reasonably handle. His study compared the effects of a square, flat wire grid with openings of ten, six, five or four feet to a field pattern from a solid reflector. He verified that 5 openings or smaller will adequately approximate a solid reflector at 8.175 MHz. Since 5.1 MHz frequency corresponds to a larger wavelength the 5 foot openings will approximate a solid surface at this frequency as well.

3.4.2 The Refined Cassegrain Model

One goal of the model revision was to cut down on the size of the cassegrain if possible. A large custom metal net requires a lot of time, money, and manpower to

construct. Trimming off excess material became a priority to try to reduce the overall cost of the system. Figure 3-5 shows the current distribution at 5.1 MHz on the subreflector. It can be seen from the picture that the current is concentrated in the center of the mesh, and that the corners of the triangle have much less current on them.

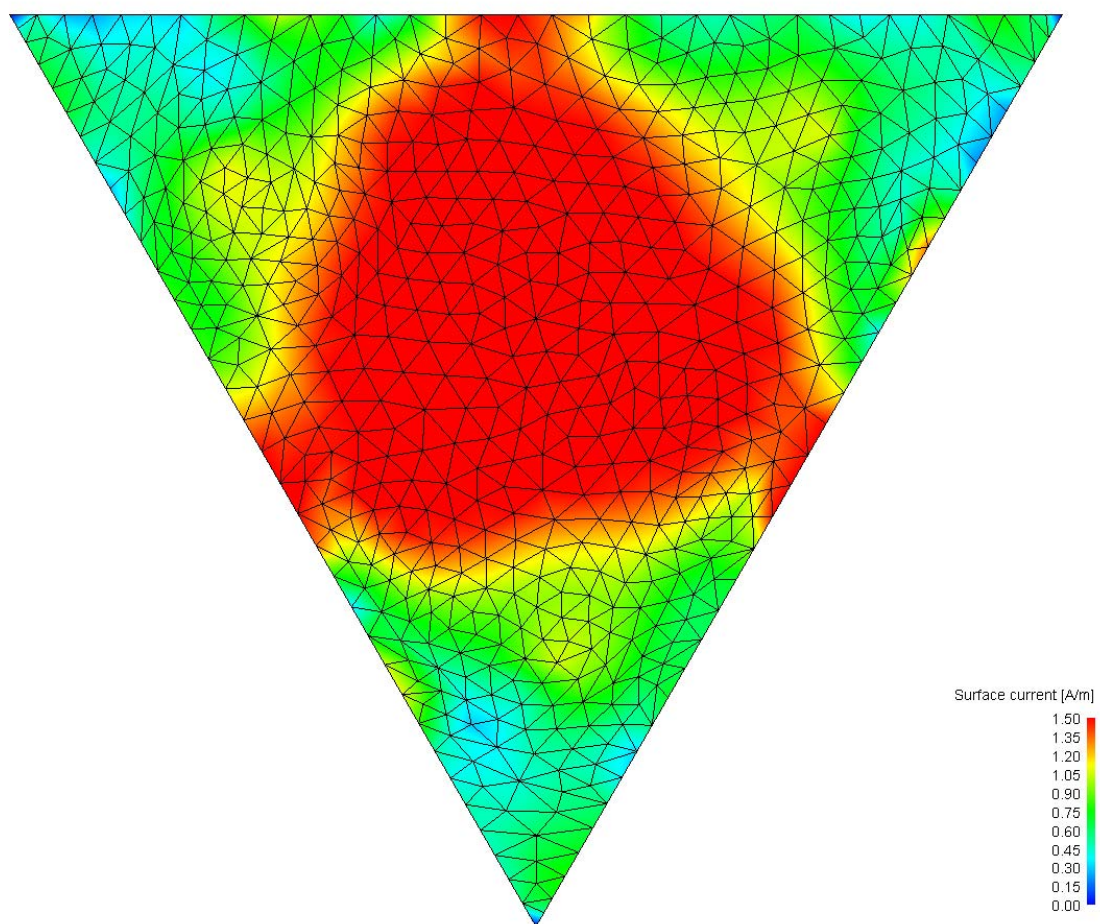


Figure 3-5: Surface Currents at 5.1 MHz on Subreflector Mesh

With the current distribution of Figure 3-5 in mind, the tips of the triangle were removed to create a hexagonal footprint. The same concept applies to this array as the previous array. The openings will be 5 feet across, and this array will move vertically up and down for the optimum illumination of each array. Figure 3-6 shows the new

subreflector at the same zoom level as the original subreflector in Figure 3-5 . The current distribution and other data will be discussed in chapter 4.

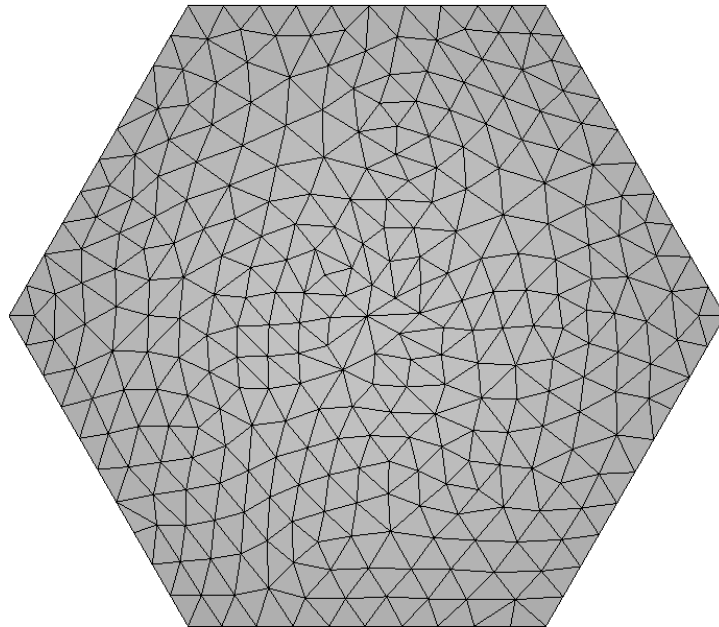


Figure 3-6: Cut Down Cassegrain Subreflector

3.5 Source Modeling

3.5.1 Single Array Design

When a half wave dipole is fed by a source, one half of the dipole is out of phase with the other half by 180° . Normally FEKO can handle this situation using one source. The HF Facility design called for two dipole antennas perpendicular to each other, with one fed 90° out of phase from the other dipole. In order to obtain this phasing in FEKO, each half of the dipole is fed with a separate source. This translates to a total of four sources for one crossed dipole. The phasing for the sources, going counterclockwise, would then be 0° , 90° , 180° , 270° with each arm fed 180° out of phase with the arm across from itself. Figure 3-7 illustrates this phase scheme on a single crossed dipole. Sources 1 and 3 are 180° out of phase with each other. Sources 2 and 4 are 180° out of phase with each other, and 90° out of phase with sources 1 and 3.

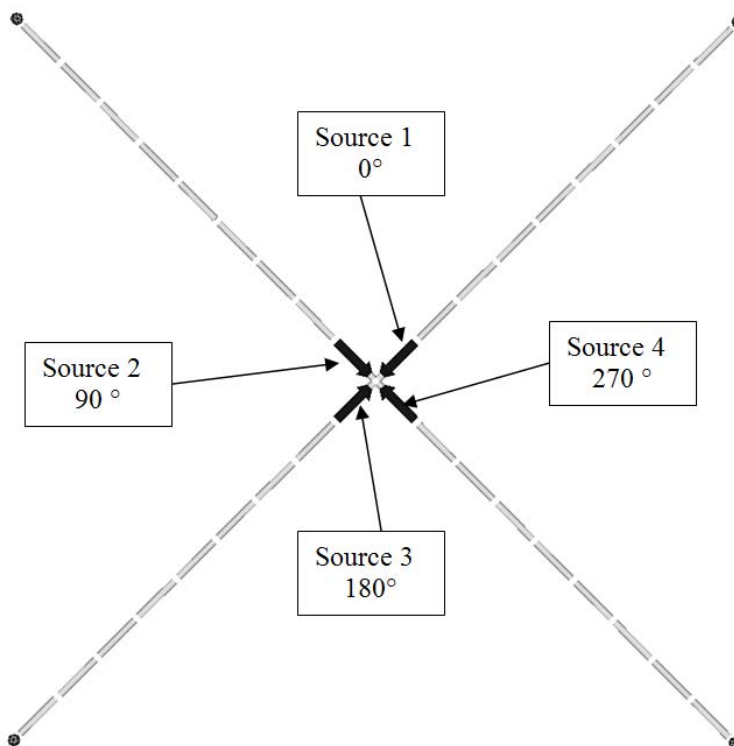


Figure 3-7: Single Crossed Dipole with Sources and Phase Labeled

Extending this to an array of three crossed dipoles at each frequency, twelve sources are needed. In addition to phasing between the arms of the individual dipoles, the dipole towers need to be phased with respect to each other. The phases of the towers are offset by the physical rotation between towers. This means that if there were 4 towers rotated 90° from each other that the phase of the towers would be offset by 90° . In the case of the three tower array, if tower 1 is designated as being positioned at 0° and offset some distance from the center of the circle, the second tower will be rotate 120° from the first tower. The third tower will then be offset 120° from the second tower to make them all at equal angle spacing from the next tower. Figure 3-8 shows a top view of the towers as they appear in the final design. The figure only shows one of the two arrays to

simplify the figure. Towers 1, 2, and 3 are equidistance from the center and they are 120° from the nearest tower. Table **3-1** shows the phasing of the sources at the towers.

Sources 1, 5, and 9 are the first sources on towers 1, 2, and 3 respectively. The table also shows that sources 1, 5, and 9 are 120° out of phase, which is expected since the towers are physically offset by 120° .

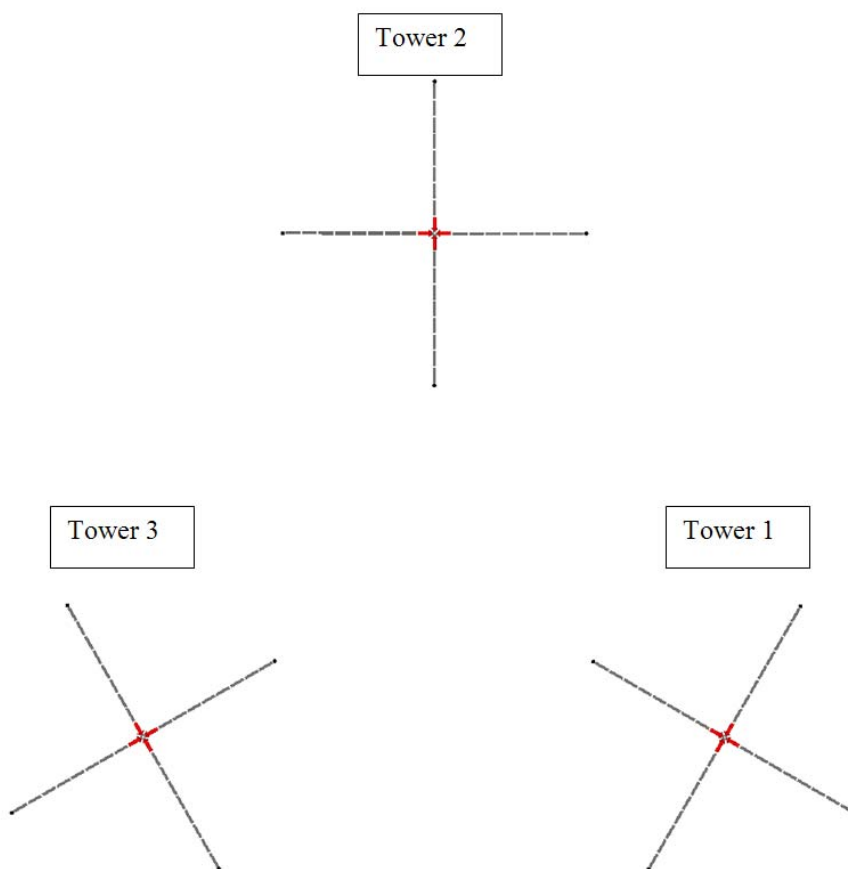


Figure **3-8**: Top View of the Three Tower Array

Table 3-1: Array Phasing

Tower1		Tower 2		Tower3	
Source Number	Phase	Source Number	Phase	Source Number	Phase
1	0°	5	120°	9	240°
2	90°	6	210°	10	330°
3	180°	7	300°	11	420°
4	270°	8	390°	12	510°

3.5.2 Dual Array Design

Adding both arrays to the design does not change the phasing of the system.

Since the two arrays will not be active at the same time, the 5.1 MHz array and the 8.175 MHz array share the same phasing. Figure 3-3 shows how the two arrays will be placed with respect to each other.

One aspect that did change in adding both arrays into the model was what to do with the feed points of the passive array. The feed point could be an open, or it could be a short depending on the final lengths of the transmission line running from the transmitter to the towers. With this in mind, the model was run twice at each frequency. One set of runs had a load of $10 \times 10^{10} \Omega$ at the feed point of the passive load to simulate an open at the feed point. The other set of runs replaced the feed point with a wire to simulate a closed circuit at the feed point.

3.6 Size and Dimensions

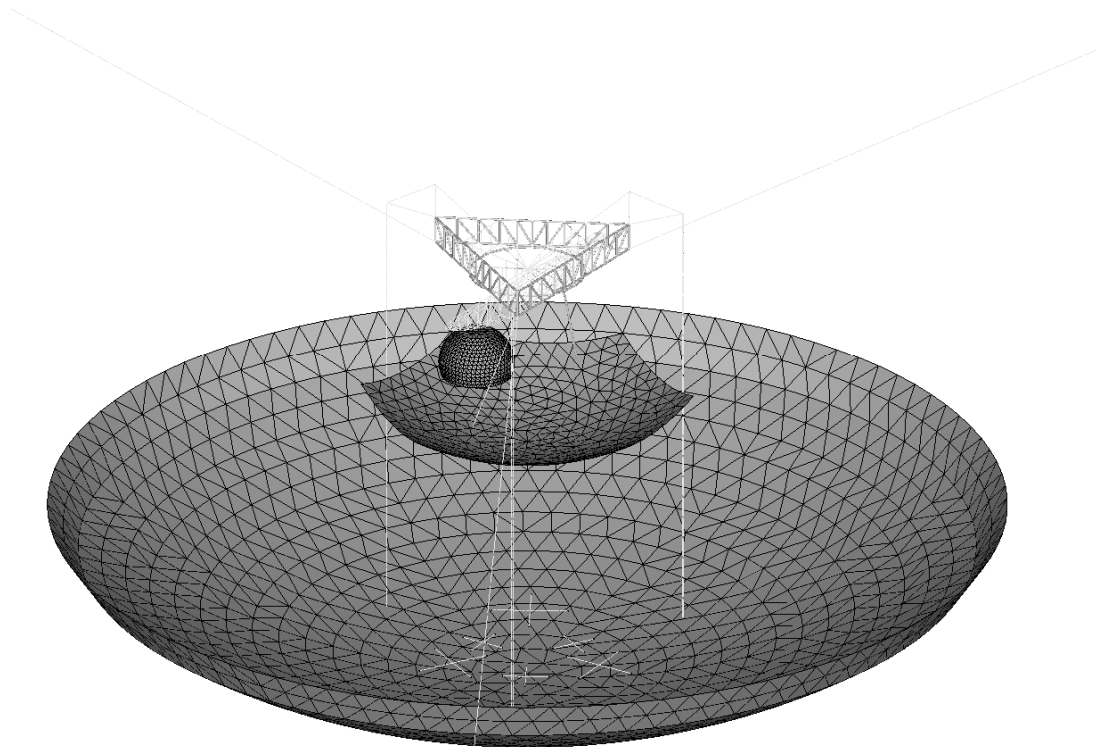


Figure 3-9: FEKO Model of the HF Facility at Arecibo

Figure 3-9 is a view of the proposed HF Facility at Arecibo. The lower dish, the upper triangular platform, and the Gregorian dome are already in place. The dipoles at the bottom of the dish and the hexagonal screen below the Gregorian dome are the proposed additions to the site. The hexagonal screen is modeled using triangles in the picture, but the actual subreflector will be a net similar to a metal fence with 5 foot holes.

The table on the next page displays the dimensions of various parts of the model. The table contains a figure number that references a picture of the actual part. It also contains a letter that refers to a labeled dimension on the figure, along with a description

and the actual length. The final lengths for the dipoles were 0.43λ at 5.1 MHz and 0.42λ at 8.175 MHz.

Table 3-2: Antenna Dimensions

Figure Number	Label	Description	Dimension (Feet)
Figure 3-10	A	Diameter of end spheres	12 inches
Figure 3-10	B	Diameter of antenna elements	4 inches
Figure 3-11	C	Length of 5.1 MHz dipole	83.7
Figure 3-11	D	Length of 8.175 MHz dipole	50.5
Figure 3-11	E	Array spacing for 5.1 MHz	162.3
Figure 3-11	F	Array spacing for 8.175 MHz	100.8
Figure 3-12	G	Height of 5.1 MHz antenna measured from bottom of dish	33.9
Figure 3-12	H	Height of 8.175 MHz antenna measured from bottom of dish	24.1
Figure 3-12	I	Height of subreflector from bottom of dish for 5.1 MHz	284
Figure 3-12	J	Height of subreflector from bottom of dish for 8.175 MHz	299
Figure 3-13	K	Length between two subreflector sides	320.7
Figure 3-13	L	Length between two subreflector corners	370.4
Figure 3-11	M	Distance from center of dish to 5.1 MHz tower	93.7
Figure 3-11	N	Distance from center of dish to 8.175 MHz tower	58.3
--	--	Subreflector focal depth	136
	--	Rotation angle of array	63.2°

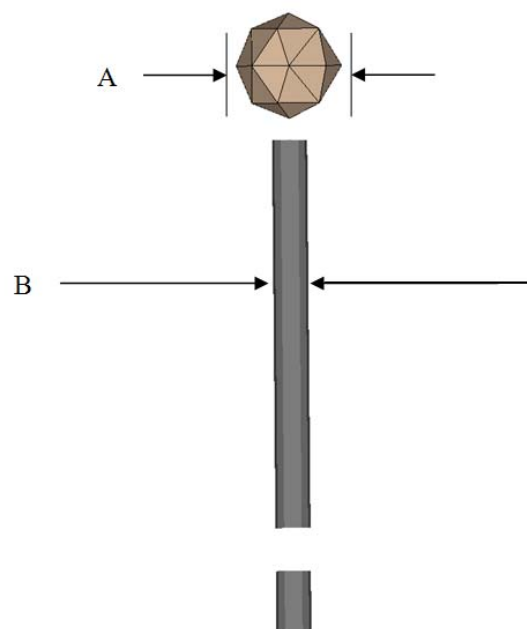


Figure 3-10: Dipole Ends with Balls

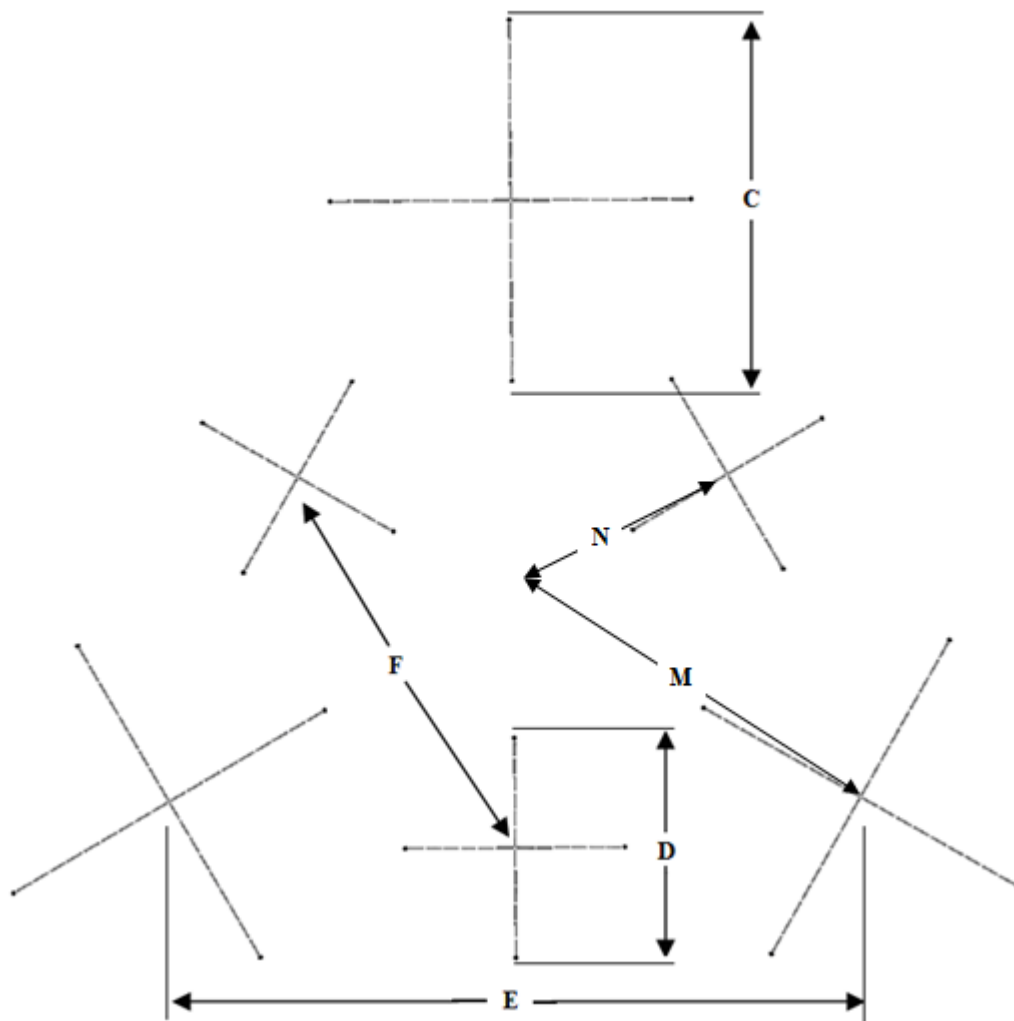


Figure 3-11: 5.1 MHz and 8.175 MHz arrays

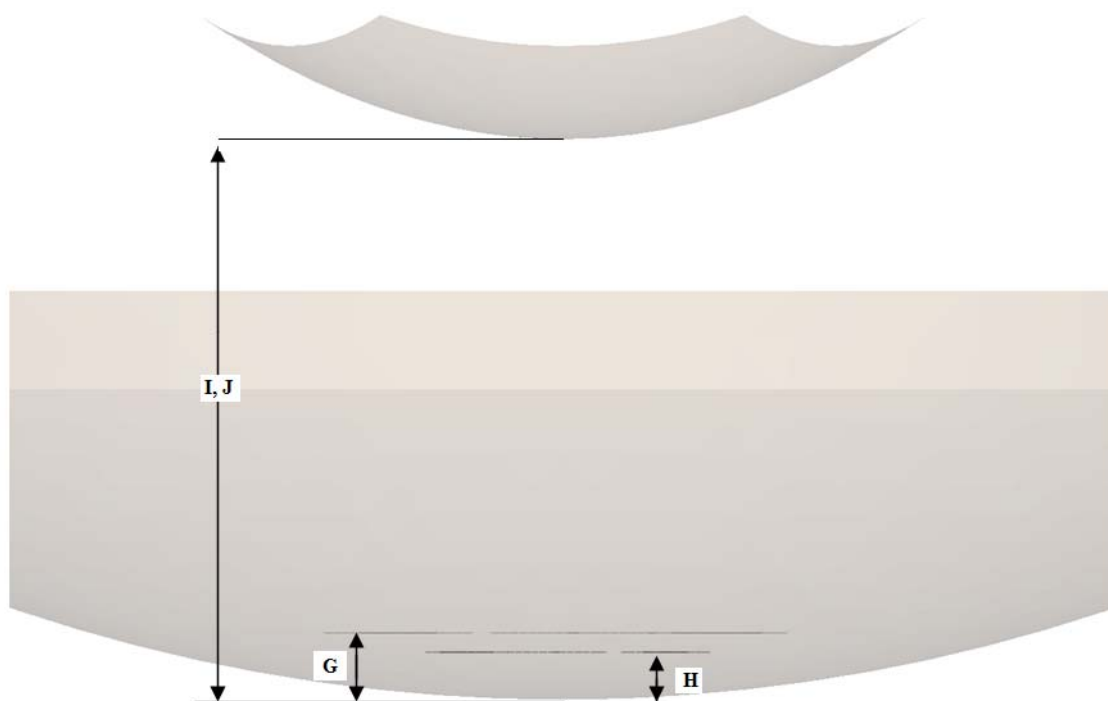


Figure 3-12: Side View of Dish (transparent), Dipole Arrays and Subreflector

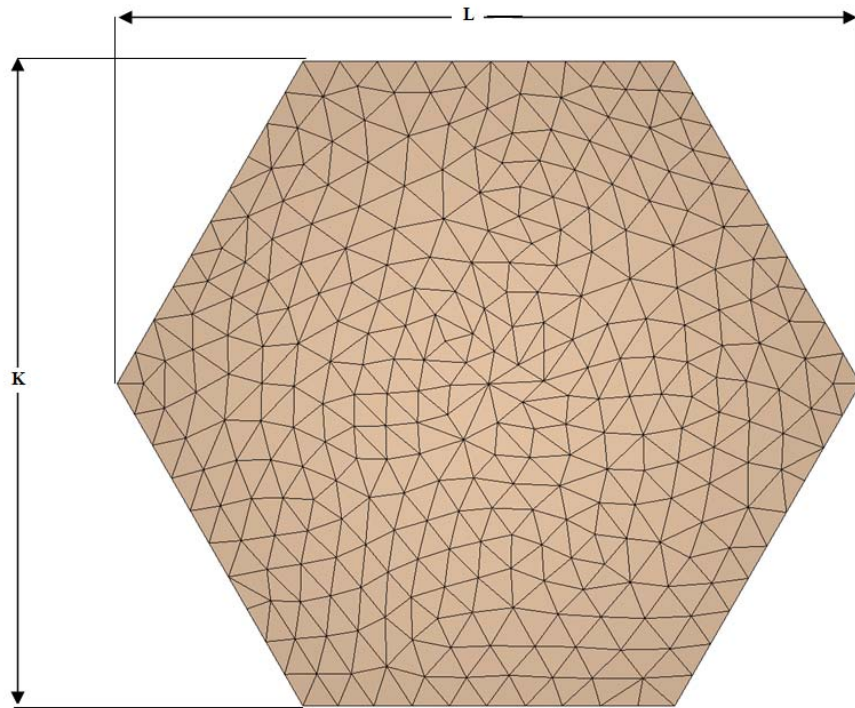


Figure 3-13: Top view of subreflector

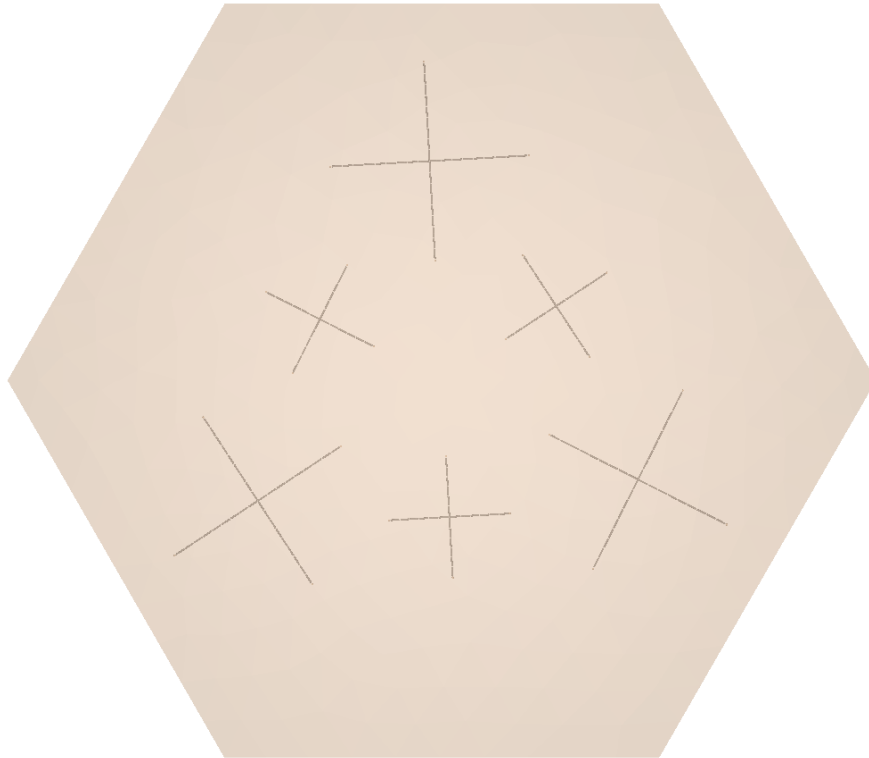


Figure 3-14: Transparent Subreflector with Dipole Arrays Underneath

3.7 Additional Facility Components

The other components of the heating facility have not changed since the study by Mr. Glessner, but have been included in this study for completeness [2].

3.7.1 Transmitters

Six 100 kW transmitters will be used in the facility. One transmitter will drive a single dipole on a tower. This means there will be two transmitters per tower, for a total

of six transmitters per array. The total power used will be 600 kW for the operation of one array. The two arrays will each need six transmitters, but since they won't be operated at the same time the transmitters will be used for both arrays. A scheme for switching between arrays is still under development as of the time of writing this document.

3.7.2 Transmission Lines

High quality copper transmission lines will be used in this design. A total of twelve transmission lines will be run from the transmitter location to the tower locations. Due to the size and thickness of the cable it was decided that it was easier to run twelve separate lines instead of trying to move the cable and switch arrays on the tower end.

3.7.3 AC Power Transmission and Switching

A turbine at the HF heating facility will power the transmitters. A high power and voltage system is being designed for the new HF facility.

Chapter 4

Array Modeling Results

The active arrays were modeled along with their passive counterparts to make sure there were no issues arising from the additional metal near the active array. The passive arrays were modeled with both open and closed feed points. It is not yet known if the passive arrays will be open or closed at the feed points so both possibilities were considered in case a problem arose. The active arrays were swept across a 200 kHz bandwidth around the center frequency. The results for impedance, VSWR, gain, and near field values for various locations are examined for the arrays. The cut down cassegrain was also used for these runs.

4.1 Impedance and VSWR

Part of evaluating the antenna design is looking at how efficiently the antenna system will radiate energy. Ideally all the power input to the antenna will radiate due to a perfect impedance match between the source and the load of the antenna. One way of examining this property is to look at the VSWR. One embodiment of VSWR uses the reflection coefficient Γ . The reflection coefficient is given in Eq. 4.1 [3]. The reflection coefficient is the ratio of the reflected voltage wave to the incident voltage wave.

$$\Gamma_L = \frac{Z_L - Z_o}{Z_L + Z_o} = \frac{V^-}{V^+} \quad 4.1$$

Where, Z_L = Antenna impedance
 Z_0 = Characteristic impedance
 V^- = Amplitude of reflected voltage wave
 V^+ = Amplitude of incident voltage wave

A perfect match between the load impedance and the source impedance results in an SWR of 1. This means that all the energy is transmitted to the antenna for radiation. Eq. 4.2 is the equation for VSWR based on the reflection coefficient. When there is a less than perfect match some of the voltage wave is reflected back into the source by the load. In this case the VSWR measures the amount of interference between the incident and reflected waves. When the SWR is infinite it means that the reflected wave is equal in amplitude to the incident wave, but traveling back into the source. The actual value will be somewhere in between full reflection and full transmission of the incident wave. It indicates how efficiently the system is working and how much power is being lost. Energy reflected back into the source is energy not radiated by the antenna

$$VSWR = \frac{1 + |\Gamma_L|}{1 - |\Gamma_L|} \quad 4.2$$

4.1.1 Single Array Results at 5.1 MHz

The following results are taken directly from William Glessner's thesis [2]. Figure 4-1 is the input impedance of the 5.1 MHz array without the 8.175 MHz array present. Figure 4-2 is the input reactance of the 5.1 MHz array. Figure 4-3 is the VSWR of the 5.1 MHz array.

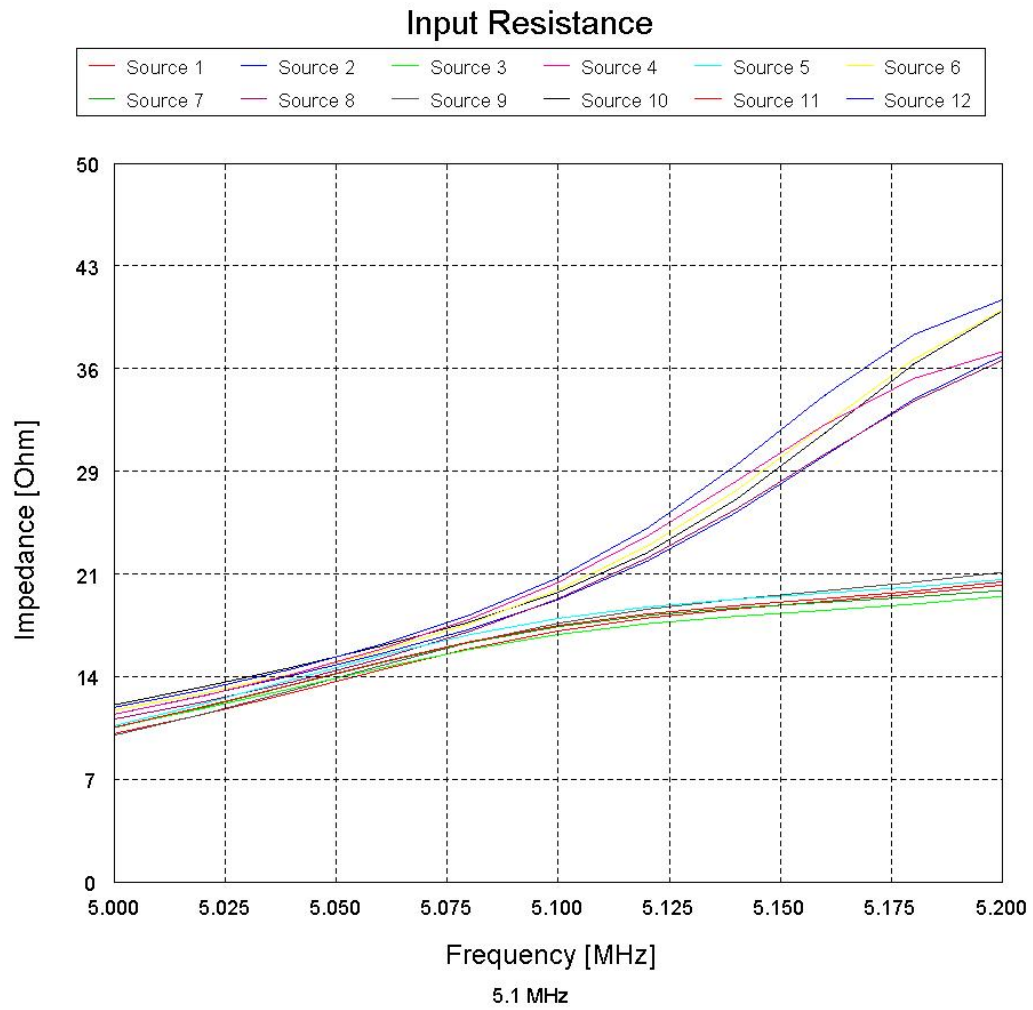


Figure 4-1: Input Resistance for 5.1 MHz Array Alone

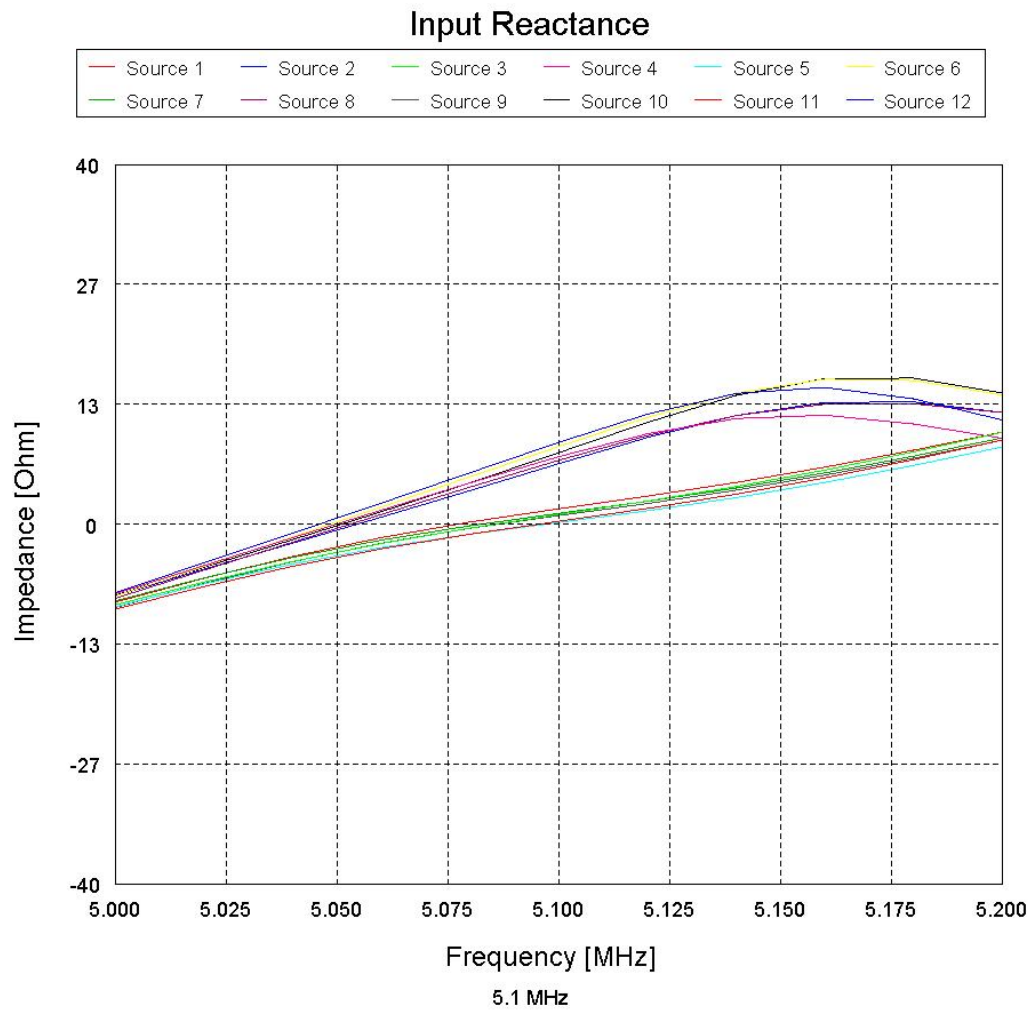


Figure 4-2: Input Reactance for 5.1 MHz Array Alone

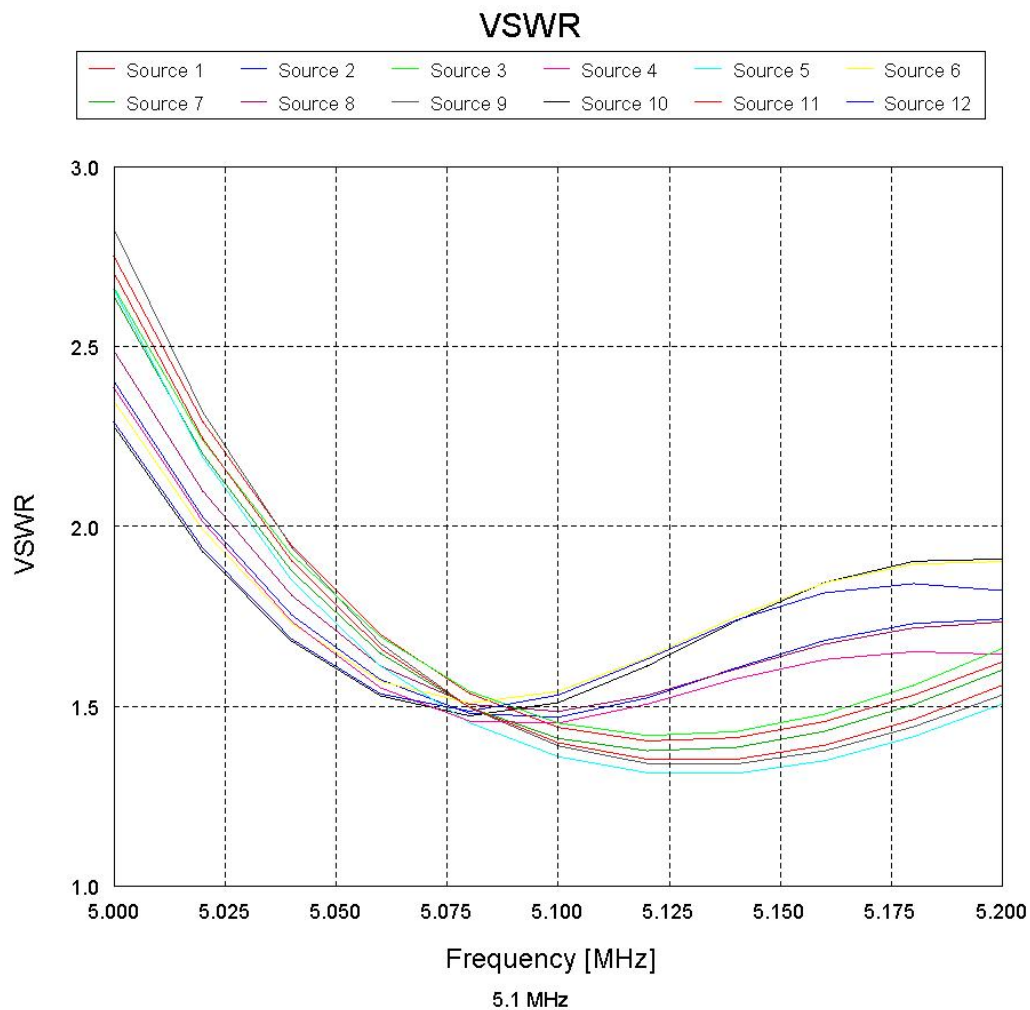


Figure 4-3: VSWR for 5.1 MHz Array Alone

4.1.2 5.1 MHz Array with 8.175 MHz Array Shorted

FEKO was used to analyze the input impedance, reactance, and VSWR. In order to model the crossed dipole geometry, each antenna element was modeled with its own source. As a result the reference impedance for the VSWR calculation was 25Ω . The actual antenna will have a 50Ω impedance. Antenna resonance occurs when the

reactance of the antenna is zero. Complementary sources were modeled with the same line color. The complementary sources are the ones on opposite arms of a single dipole that will add together to create one 50Ω source.

Figure 4-4 shows the input resistance for the 5.1 MHz array operating while the 8.175 MHz array is shorted at the feed point. Figure 4-5 is a plot of the input reactance and shows that resonance occurs between 5.04 and 5.08 MHz.

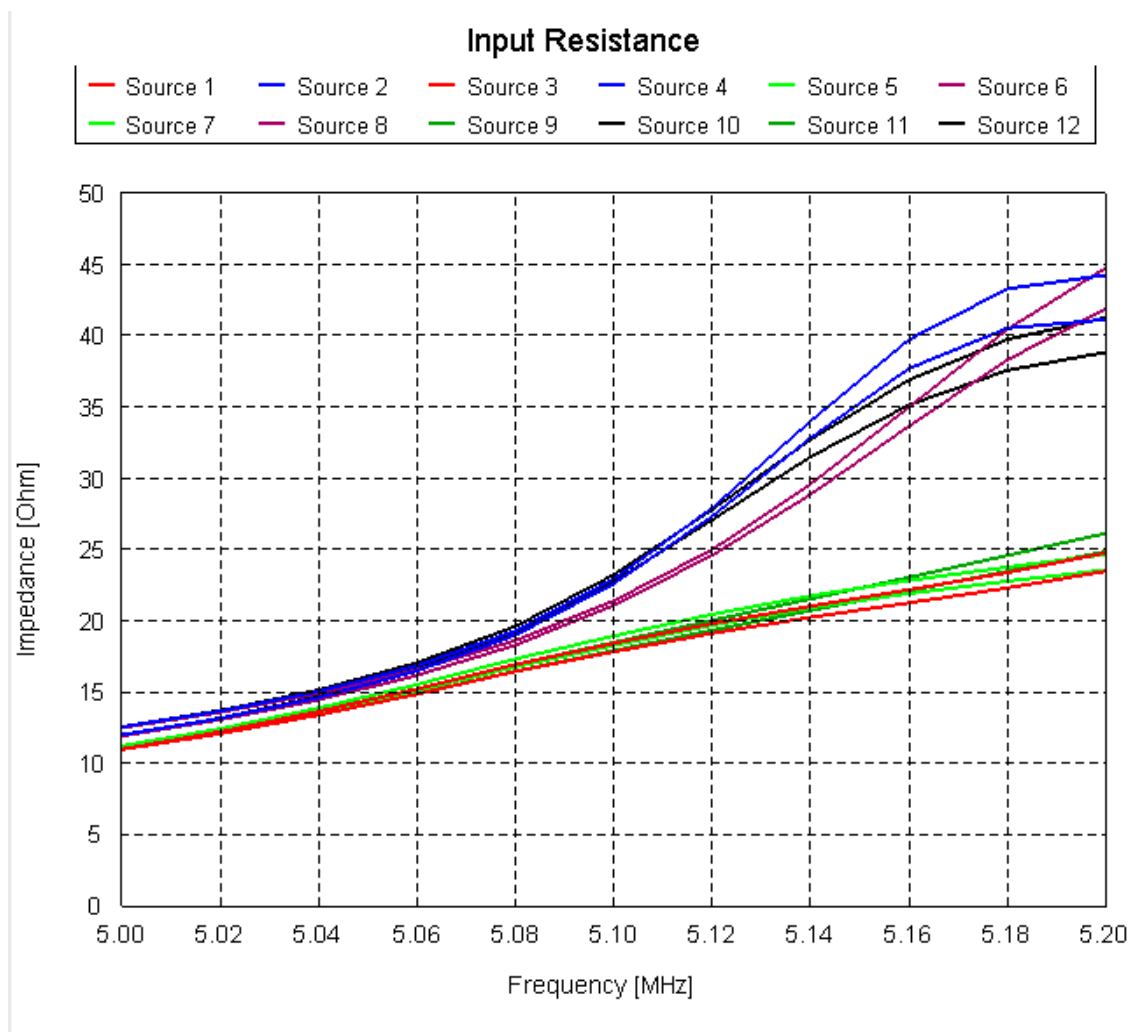


Figure 4-4: Input Resistance at 5.1 MHz with 8.175 MHz Array shorted

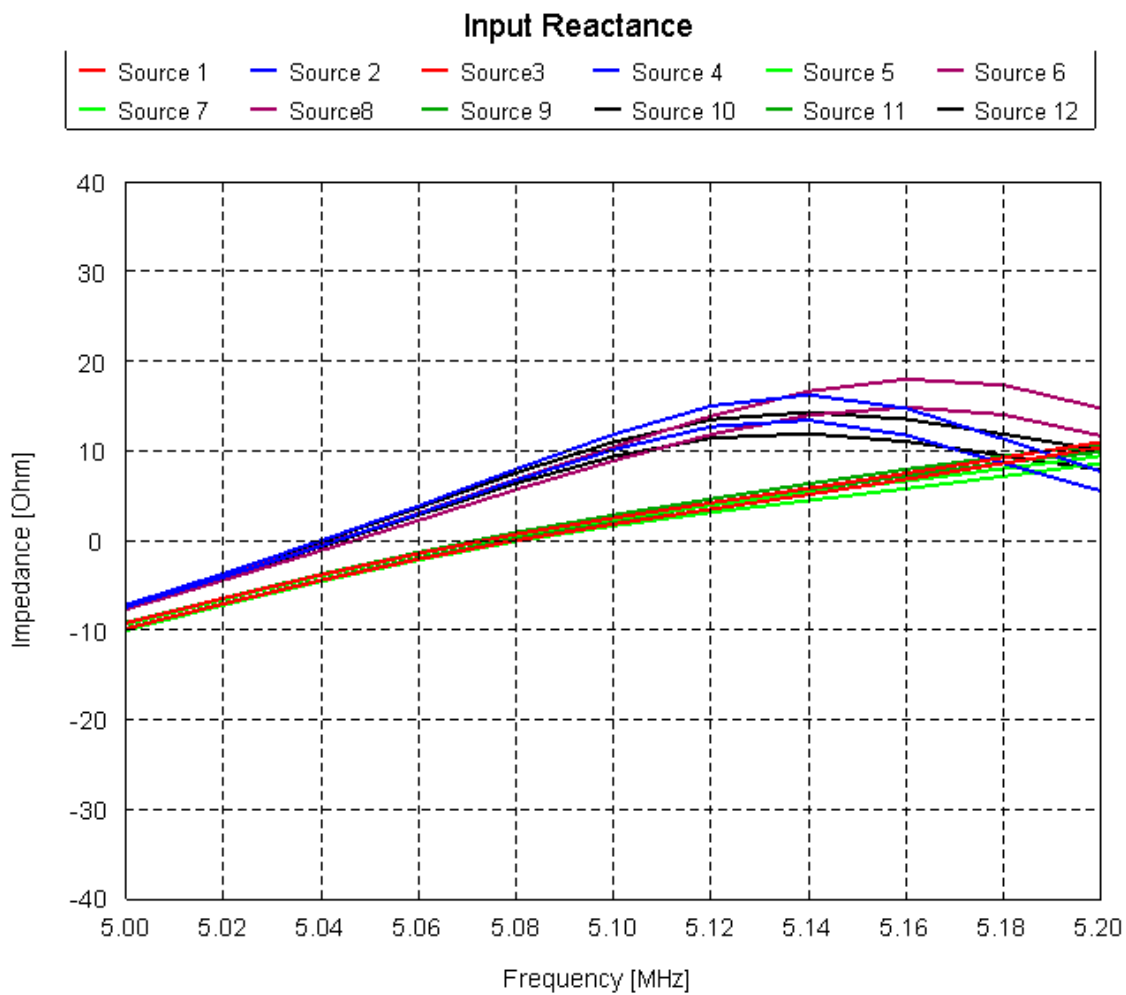


Figure 4-5: Input Reactance at 5.1 MHz with 8.175 MHz array shorted

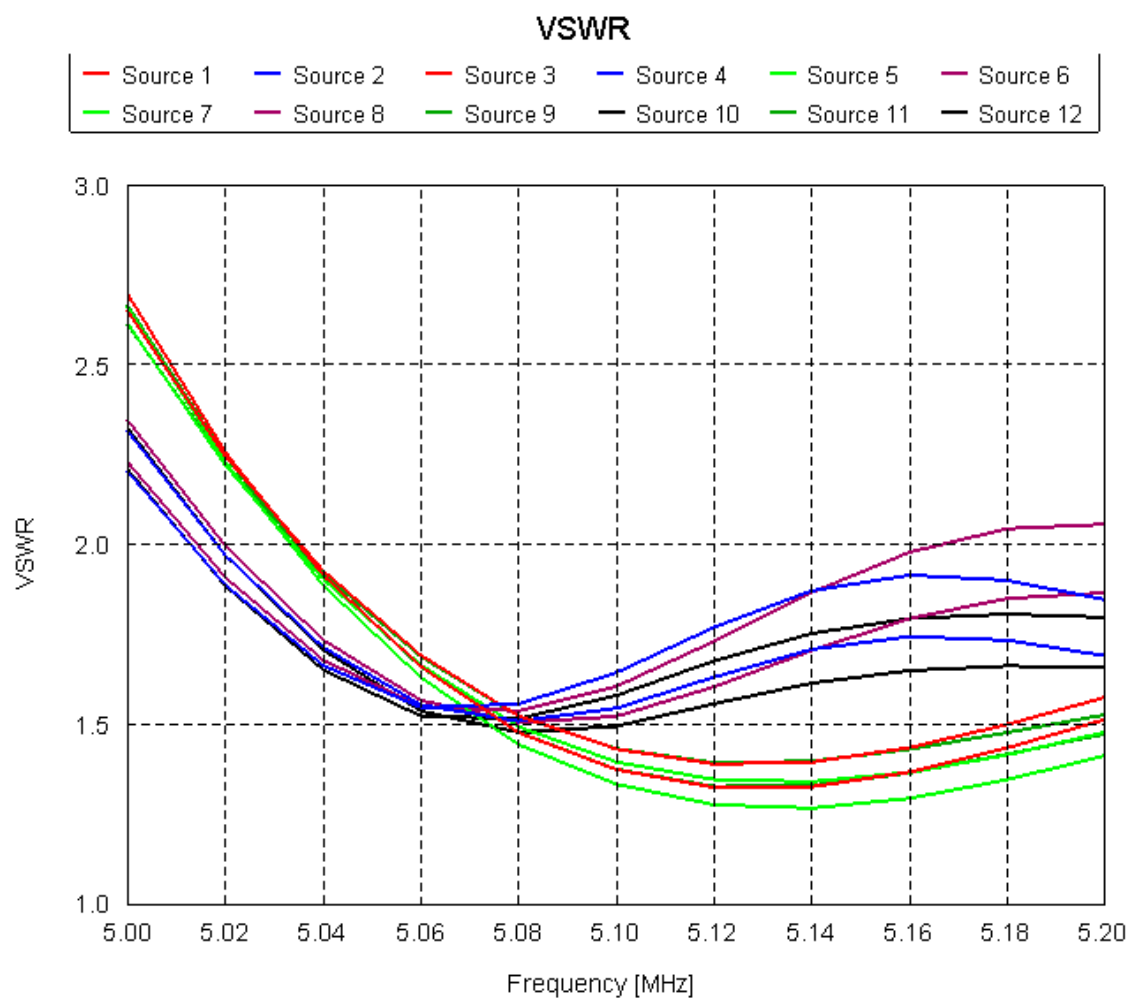


Figure 4-6: VSWR at 5.1 MHz with 8.175 MHz array shorted

Figure 4-6 is the VSWR of the 5.1 MHz array with the 8.175 MHz array shorted. It is interesting to note that the VSWR on the sources facing the center all have the VSWR increase after 5.08 MHz. The other sources perpendicular to the center of the dish continue to slope down, eventually increasing after about 5.13 MHz. Looking at the 100 kHz band from 5.05 to 5.15 MHz the highest SWR is 1.93:1 at 5.15 MHz.

4.1.3 5.1 MHz Array with 8.175 MHz Array Open

Figure 4-7 shows the input resistance at 5.1 MHz. The 8.175 MHz array has a $10 \times 10^{10} \Omega$ resistor at the source to simulate an open circuit. Figure 4-8 shows the input reactance for this configuration. It also shows that the system is resonant between 5.04 and 5.08 MHz.

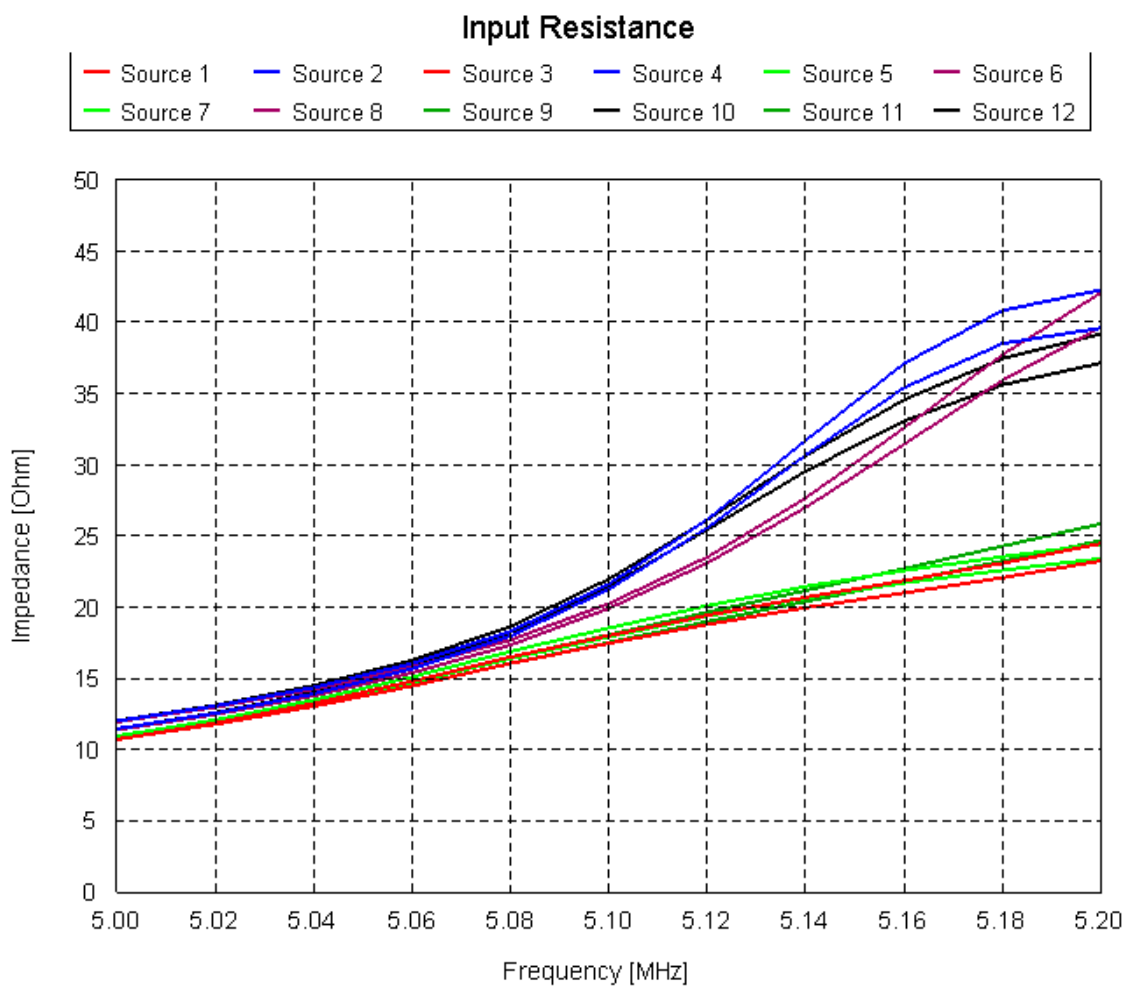


Figure 4-7: Input Resistance at 5.1 MHz with the 8.175 MHz Array Open

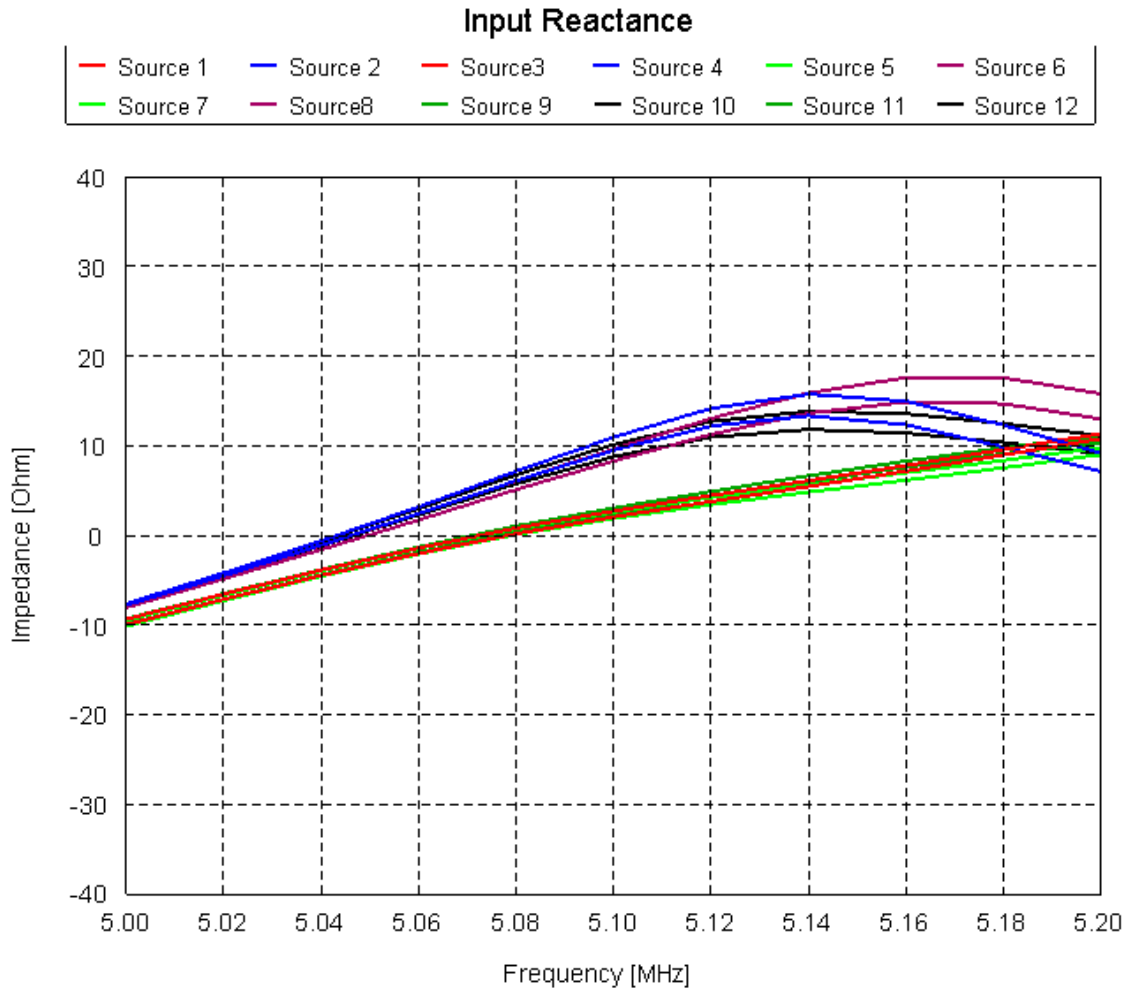


Figure 4-8: Input Reactance at 5.1 MHz with the 8.175 MHz array open

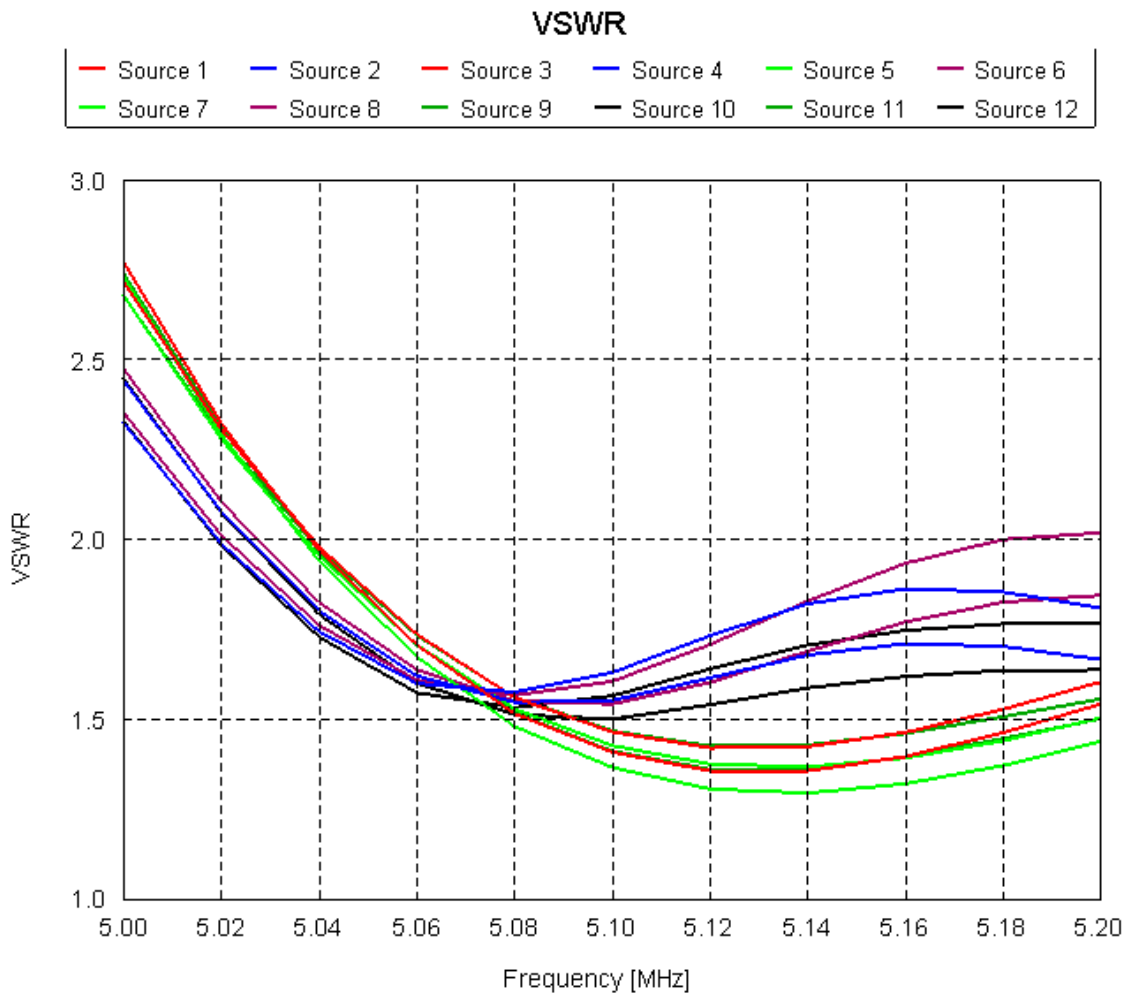


Figure 4-9: VSWR at 5.1 MHz with 8.175 MHz Array Open

Figure 4-9 shows the VSWR of the 5.1 MHz array with the 8.175 MHz array open. The sources facing the center increase in VSWR after 5.08 MHz. In the 100 kHz band from 5.05 to 5.15 MHz the worst VSWR is 1.88:1 and it occurs at 5.15 MHz.

4.1.4 Single Array Results at 8.175 MHz

The following results are taken directly from William Glessner's thesis [2].

Figure 4-10 is the input impedance of the 8.175 MHz array without the 5.1 MHz array present. Figure 4-11 is the input reactance of the 8.175 MHz array. Figure 4-12 is the VSWR of the 8.175 MHz array.

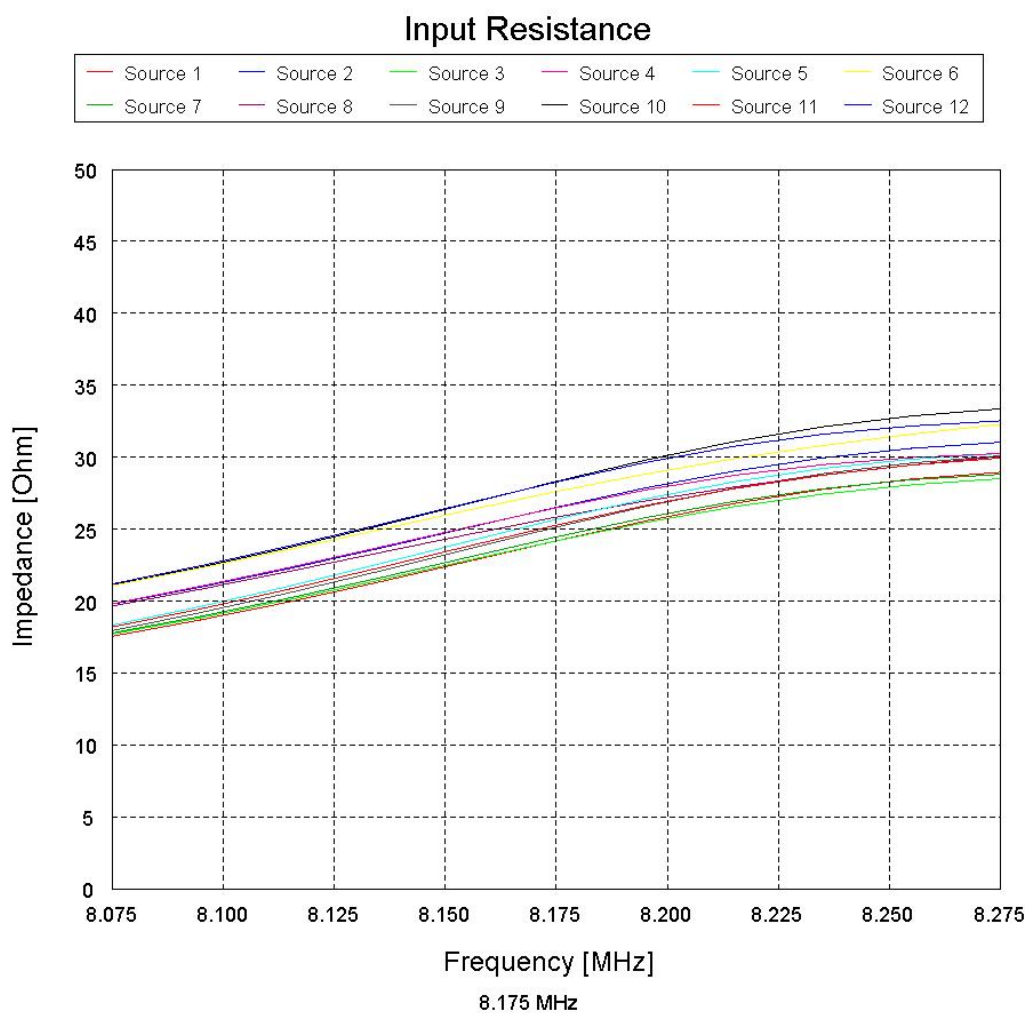


Figure 4-10: Input Resistance for 8.175 MHz Array Alone

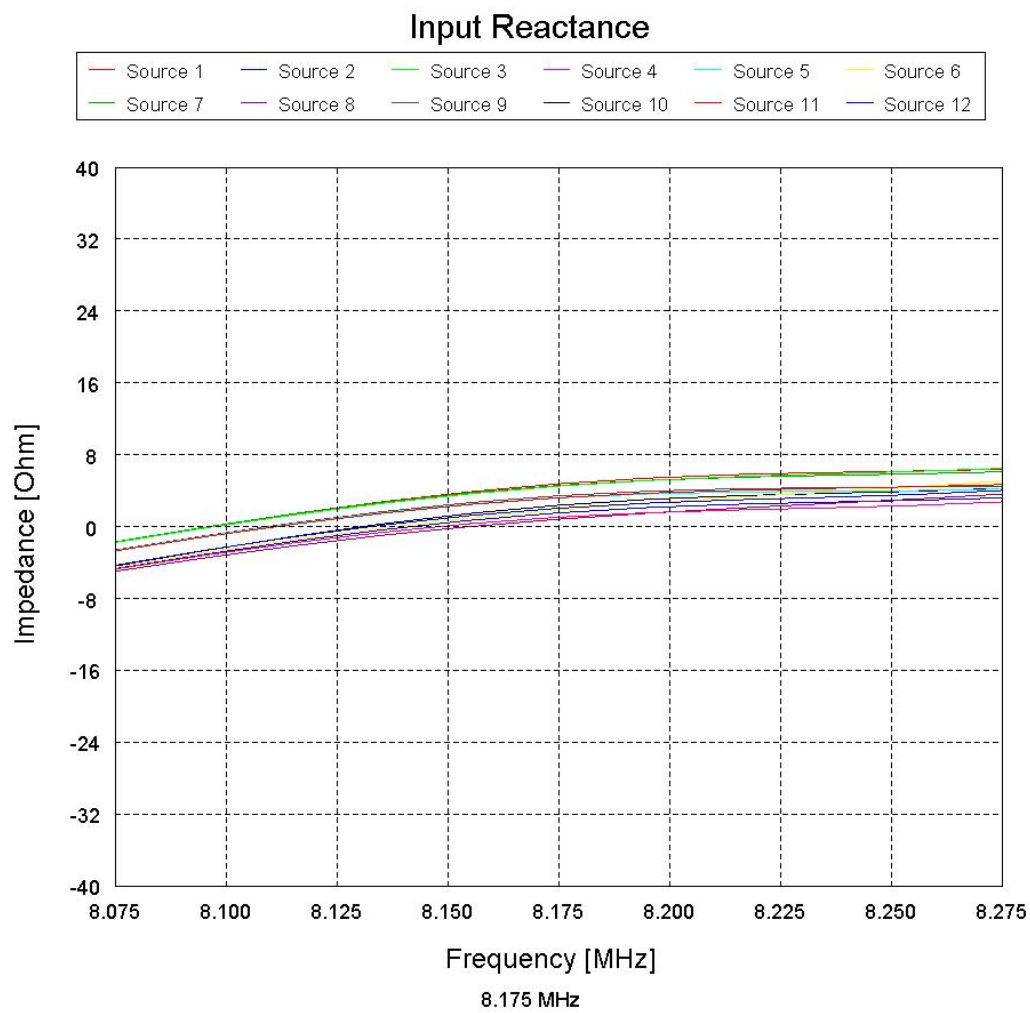


Figure 4-11: Input Reactance for 8.175 MHz Array Alone

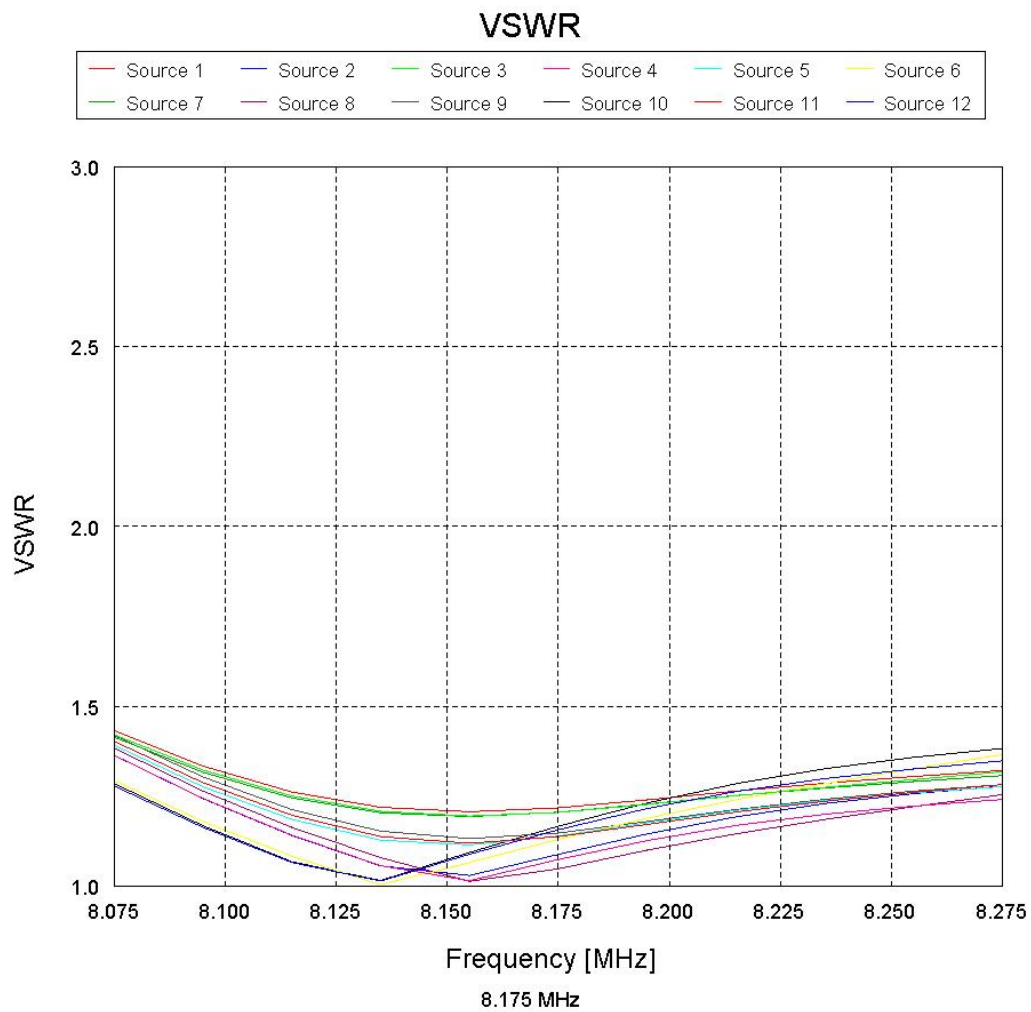


Figure 4-12: VSWR for 8.175 MHz Array Alone

4.1.5 8.175 MHz Array with 5.1 MHz Array Shorted

Figure 4-13 shows the input resistance at 8.175 MHz with the 5.1 MHz array shorted. Figure 4-14 is the reactance of the 8.175 MHz array. The reactance graph shows that resonance occurs between 8.125 and 8.15 MHz.

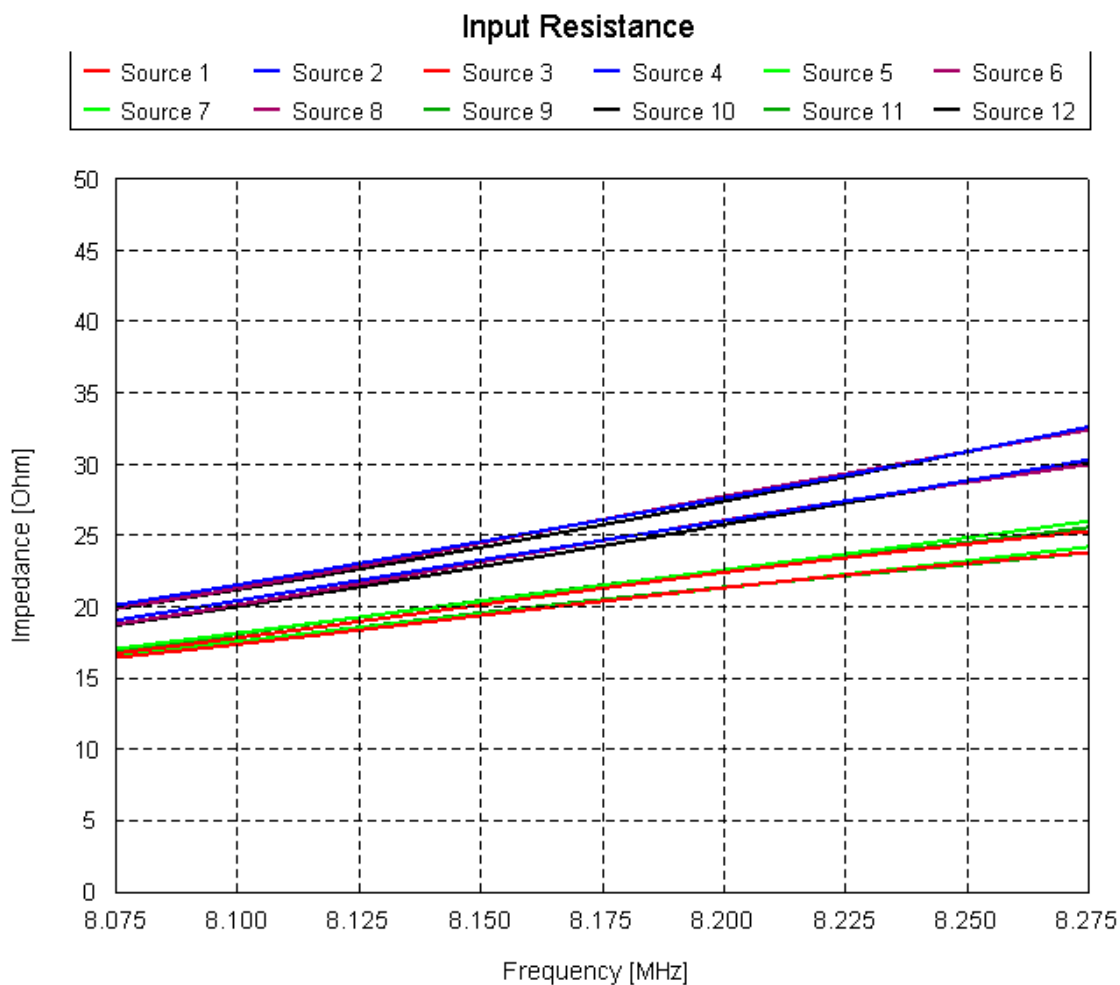


Figure 4-13: Input Resistance at 8.175 MHz with the 5.1 MHz Array Shorted

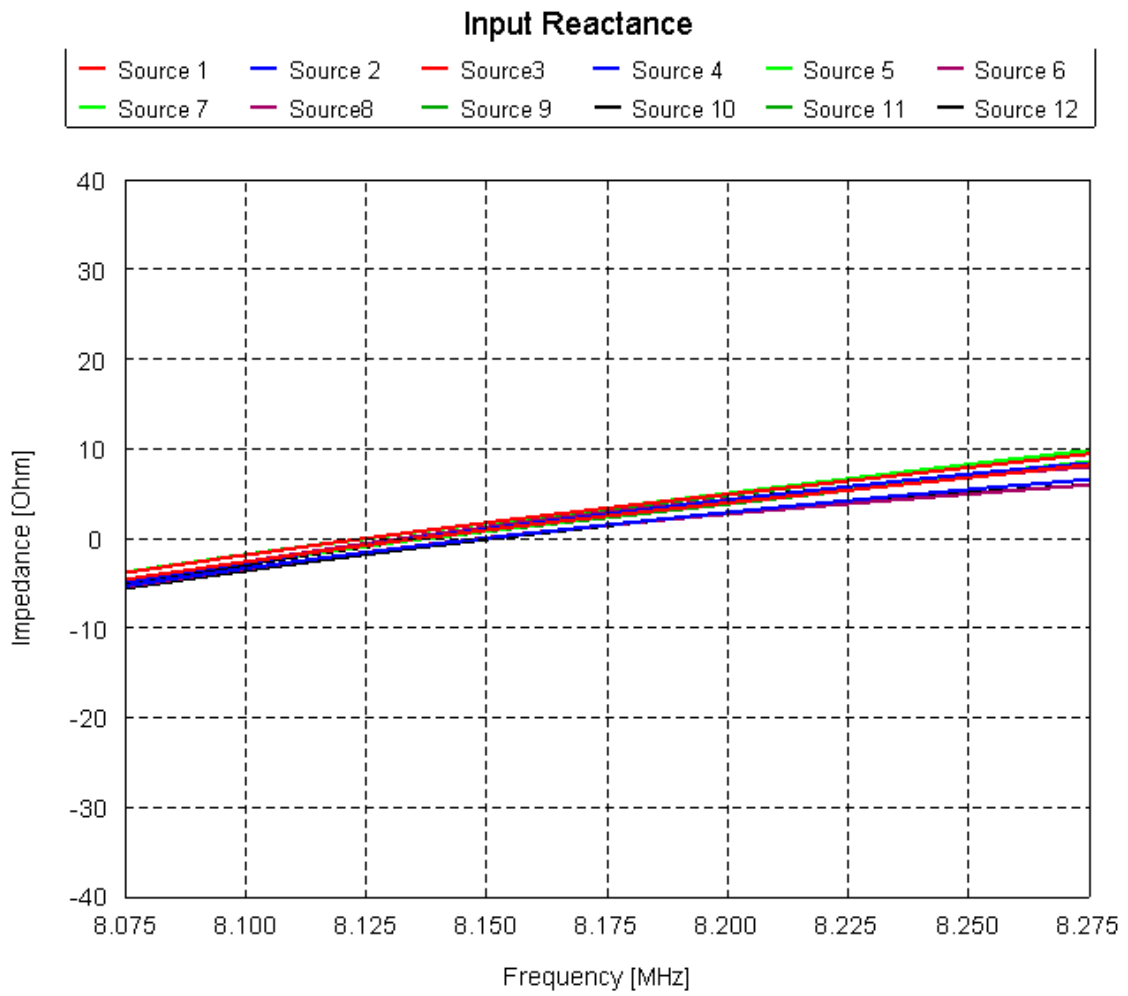


Figure 4-14: Input Reactance at 8.175 MHz with 5.1 MHz Array Shorted

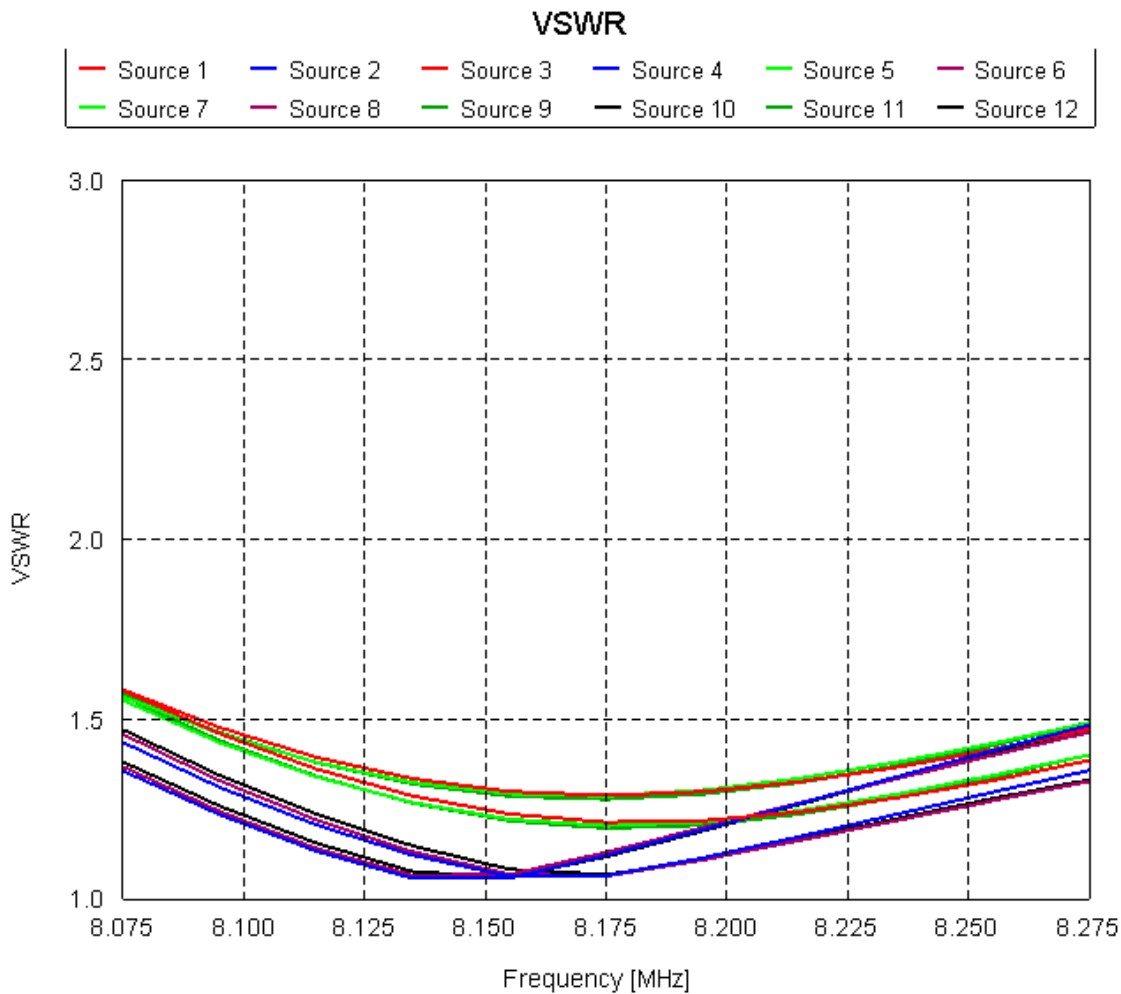


Figure 4-15: VSWR at 8.175 MHz with 5.1 MHz Array Shorted

Figure 4-15 shows the VSWR at 8.175 MHz with the 5.1 MHz array shorted. The 100 kHz bandwidth from 8.125 to 8.225 MHz is all below 1.5:1. The worse VSWR is 1.37:1 and it occurs at 8.125 MHz.

4.1.6 8.175 MHz Array with 5.1 MHz Array Open

Figure 4-16 is a graph of the input resistance to the 8.175 MHz array when the 5.1 MHz array has a $10 \times 10^{10} \Omega$ resistor at the feed point creating an open circuit. Figure 4-17 is the input reactance at 8.175 MHz. From the reactance graph resonance occurs between 8.125 and 8.157 MHz

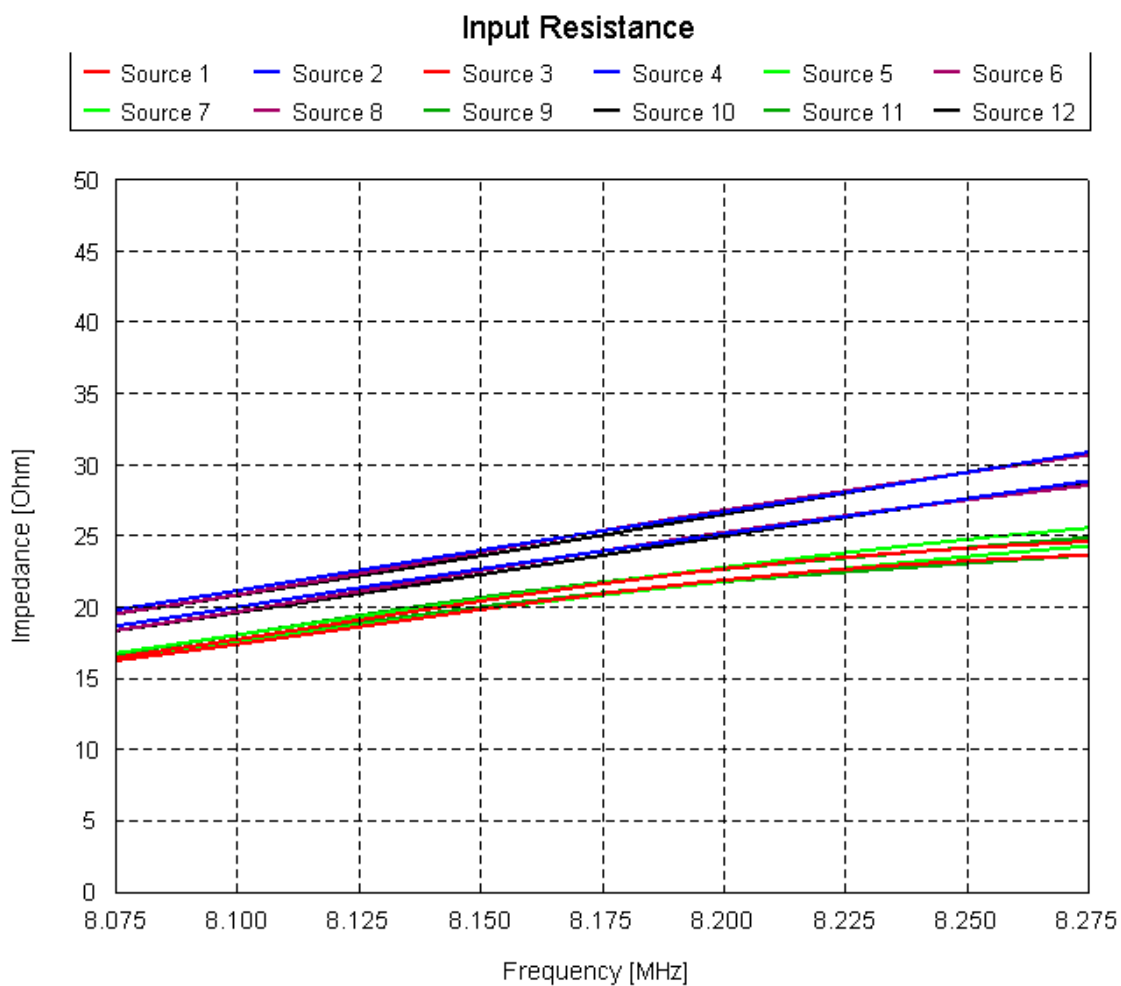


Figure 4-16: Input Resistance at 8.175 MHz with the 5.1 MHz Array Open

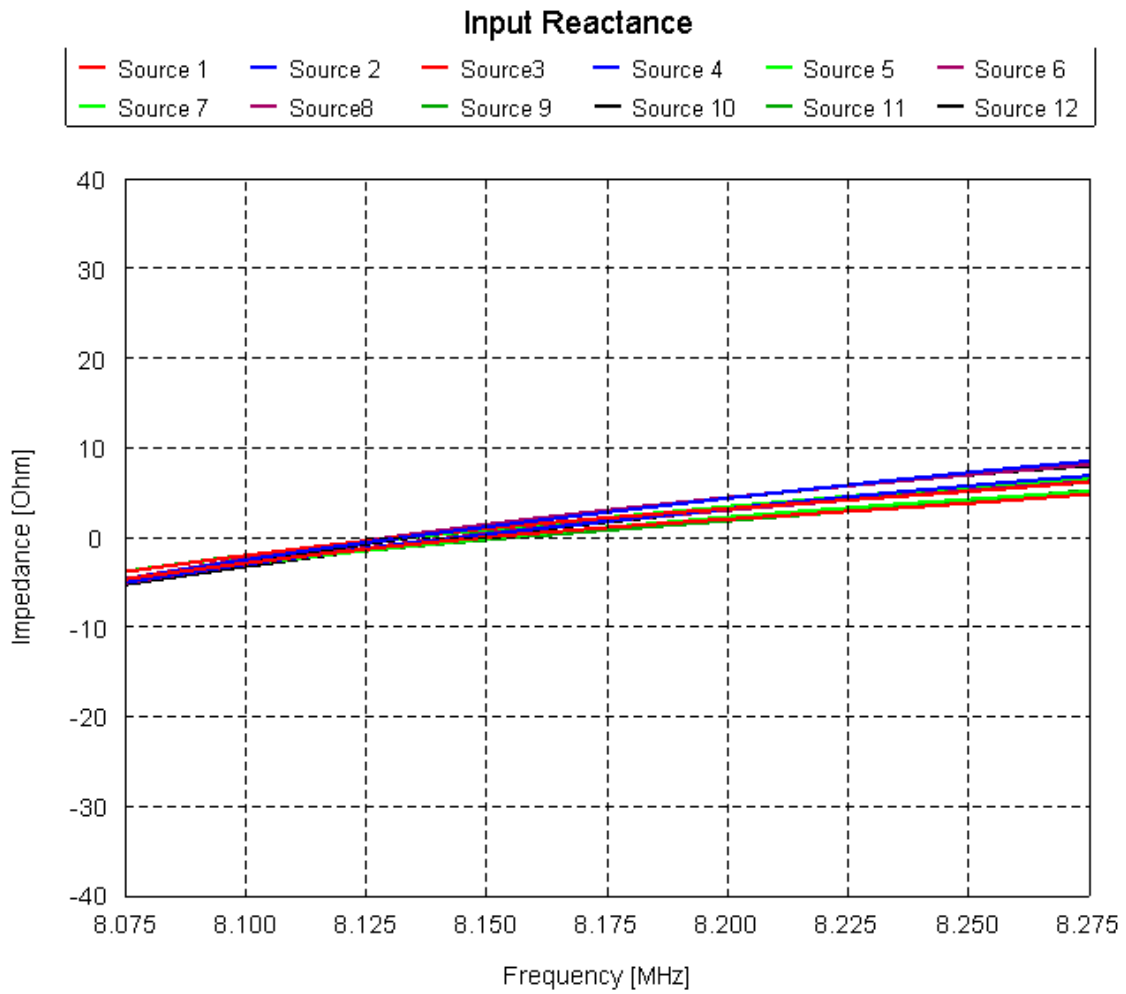


Figure 4-17: Input Reactance at 8.175 MHz with 5.1 MHz array open

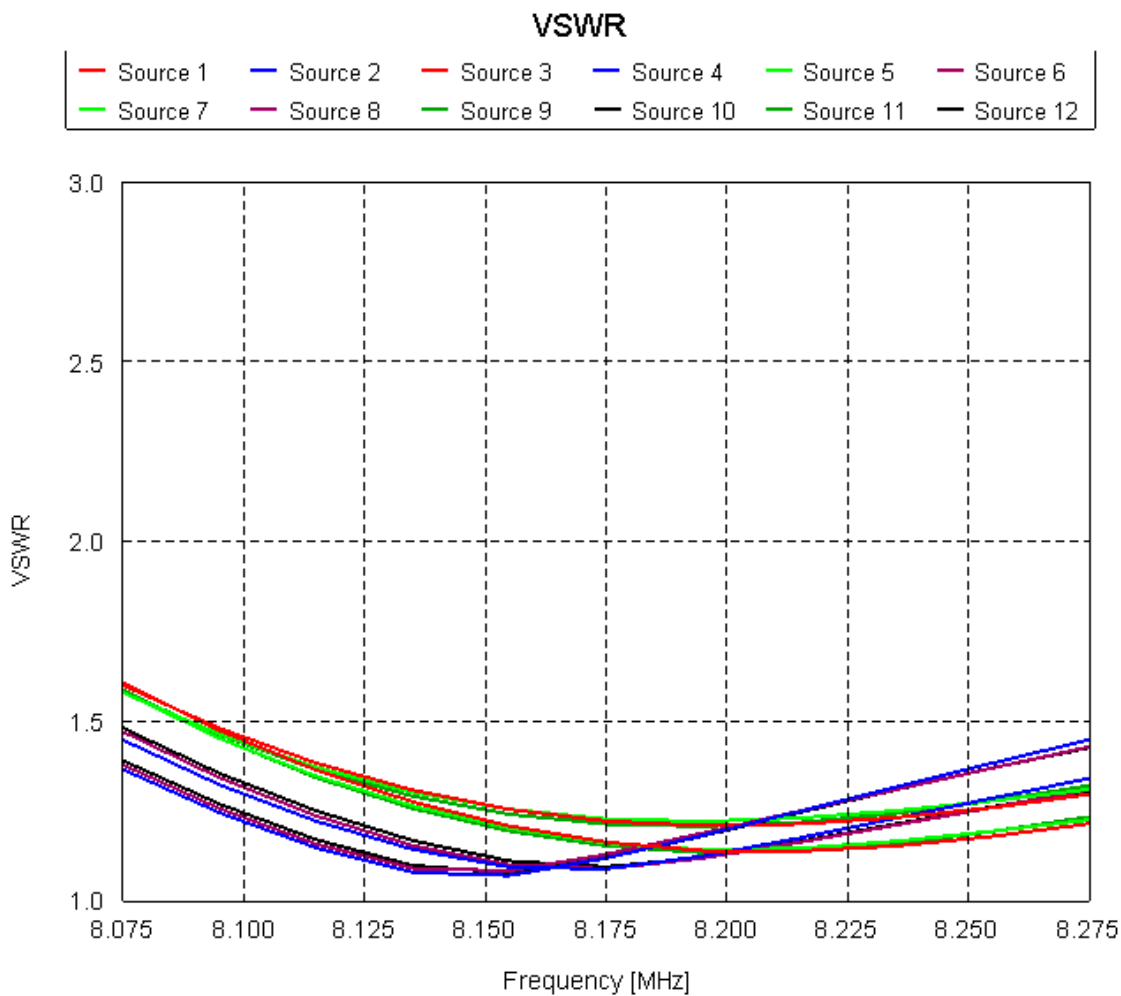


Figure 4-18: VSWR at 8.175 MHz with 5.1 MHz open

Figure 4-18 shows that the VSWR is under 1.5:1 for the whole band. Looking at the 100 kHz band from 8.125 to 8.225 MHz the worst VSWR of 1.35:1 occurs at 8.125 MHz.

4.2 Far Field Results

The gain of the HF facility was examined using FEKO. The FEKO model only contained the dipole towers, the subreflector, the reflector dish, the upper platform and the Gregorian dome. The foliage, buildings, anchor towers, and mountains were left out of the model and could have a minor affect on the actual gain of the antenna. The next section contains far field graphs that vary with angle. The XY plane can be considered the ground, with the Z-axis being the height of the objects off of the XY plane. The bottom center of the dish is the point (0, 0, 0). Spherical coordinates are used in the far field graphs. Figure **4-19** shows the entire FEKO model with the axis labeled for reference.

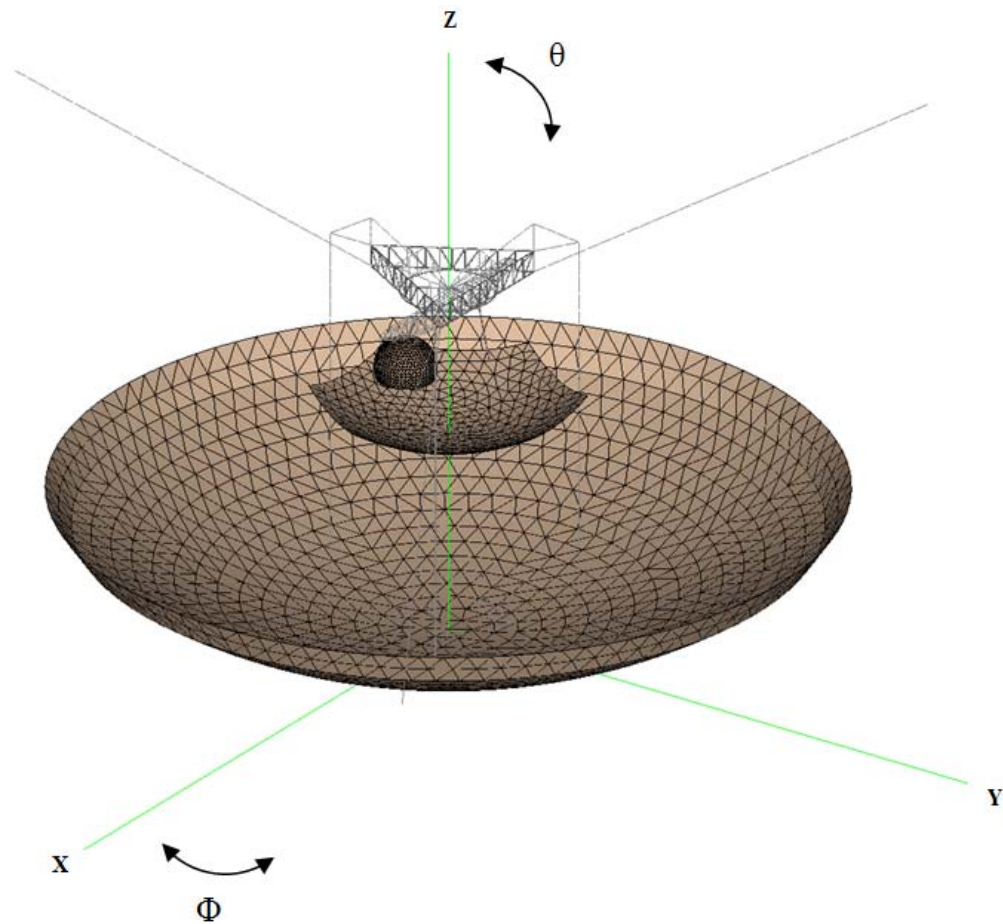


Figure 4-19: HF Facility Design with Coordinate Axis

4.2.1 Far Field 5.1 MHz Array with 8.175 MHz Array Shorted and Open

Figure 4-20 compares the gain in the $\phi = 0^\circ$ and the $\phi = 90^\circ$ planes. The maximum gain in both planes is 22.16 dBi. The figure shows that the main lobes are comparable in both planes, but the side lobes are not identical. This is due to the fact that the feed array is symmetric at 120° apart, not 90° apart. The graph has 10 divisions with 4 dB per division. The range of the graph is -17 to 23 dB. The Results for the passive

array having an open and shorted feed point were nearly identical so both were not included.

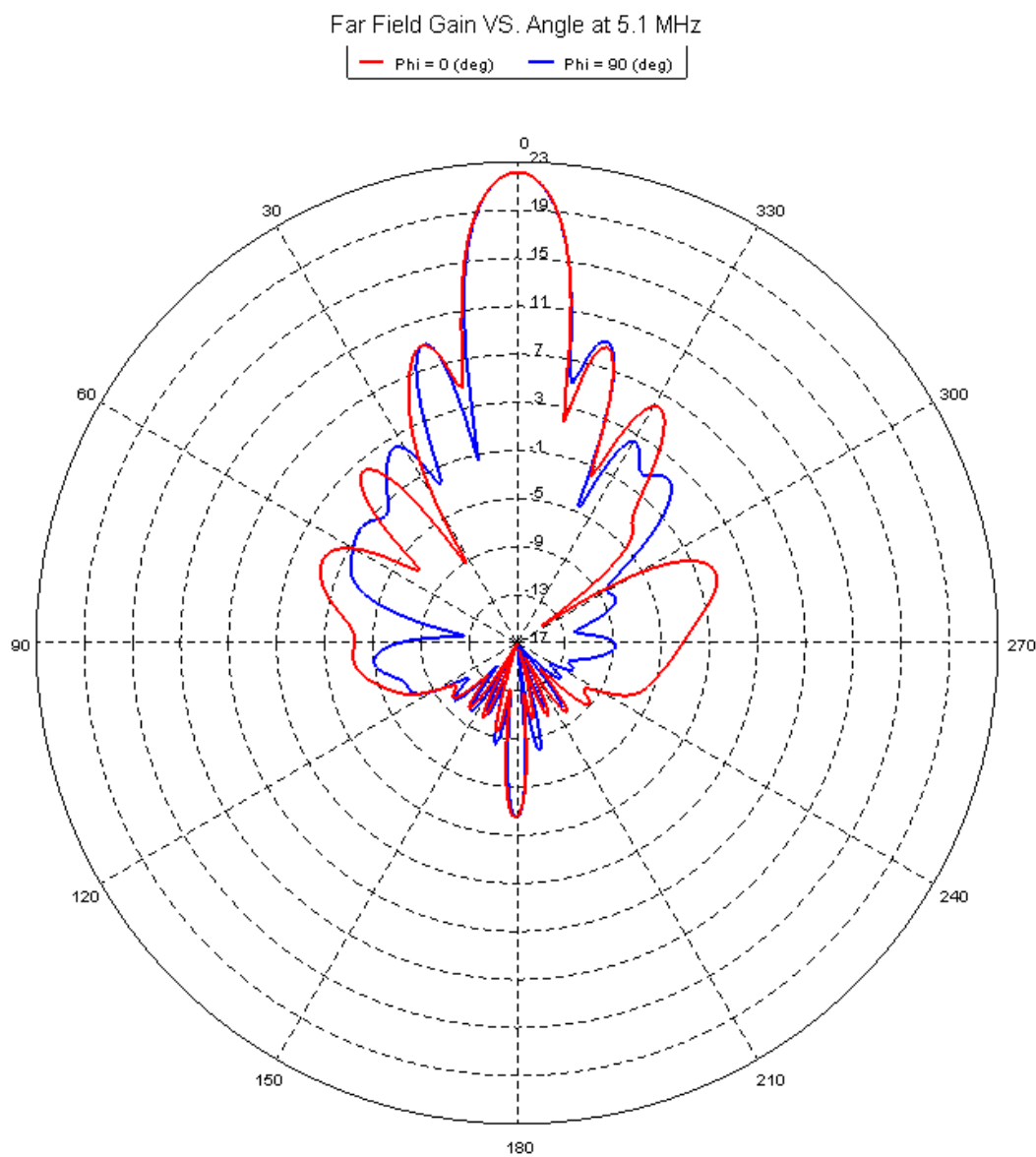


Figure 4-20: Comparison of the Far Field Gain at $\Phi = 0^\circ$ and $\Phi = 90^\circ$ at 5.1 MHz

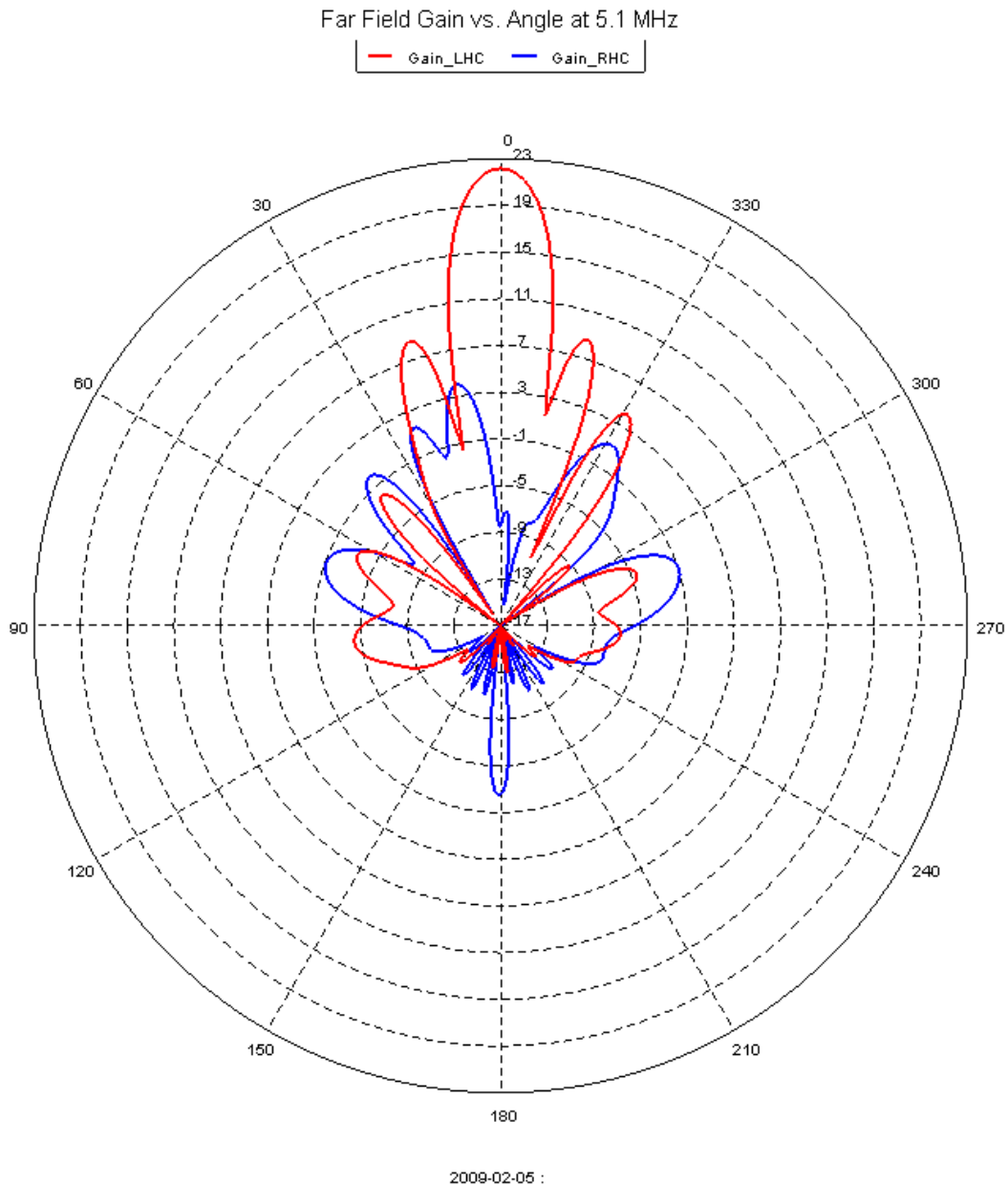


Figure 4-21: Comparison of the LHC and RHC Gain Patterns at 5.1 MHz

Figure 4-21 compares the Right Hand Circular (RHC) polarization rejection. The RHC polarization is graphed against the LHC polarization. The cross polarization rejection is above 27.0 dB relative to the maximum throughout the main beam.

4.2.2 Far Field 8.175 MHz Array with 5.1 MHz Array Shorted

Figure 4-22 graphs the far field gain vs. angle for both $\Phi = 0^\circ$ and the $\Phi = 90^\circ$. The scale is from -14 to 26 dBi with 10 divisions at 4 dB per division. The graph shows that the main beams overlap almost exactly. The gain is 25.46 dBi in both planes. The pattern is not exactly symmetric due to the symmetry of the model lying at 120° intervals, not 90° intervals.

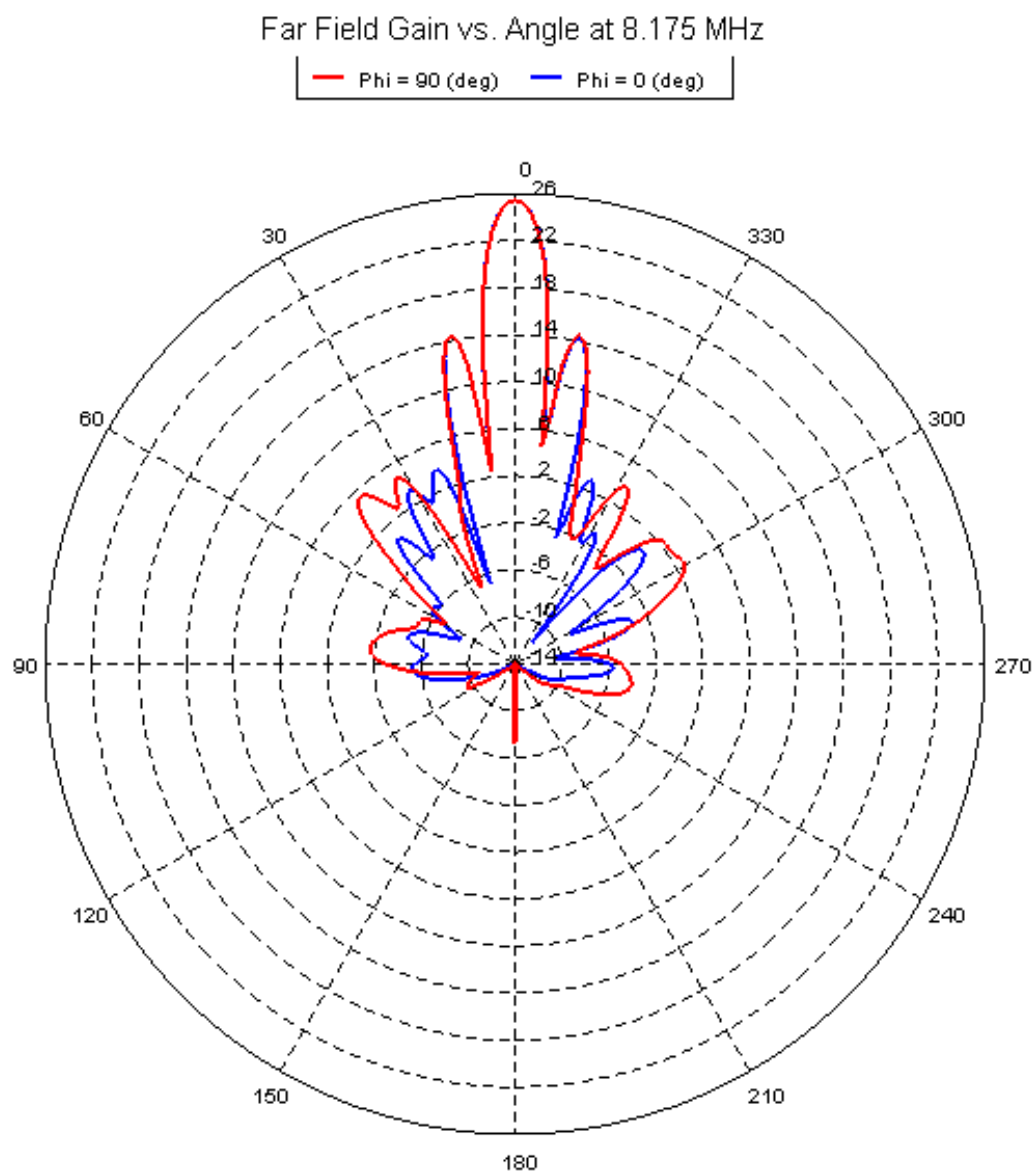


Figure 4-22: Comparison of the Far Field Gain at $\Phi = 0^\circ$ and $\Phi = 90^\circ$ at 8.175 MHz

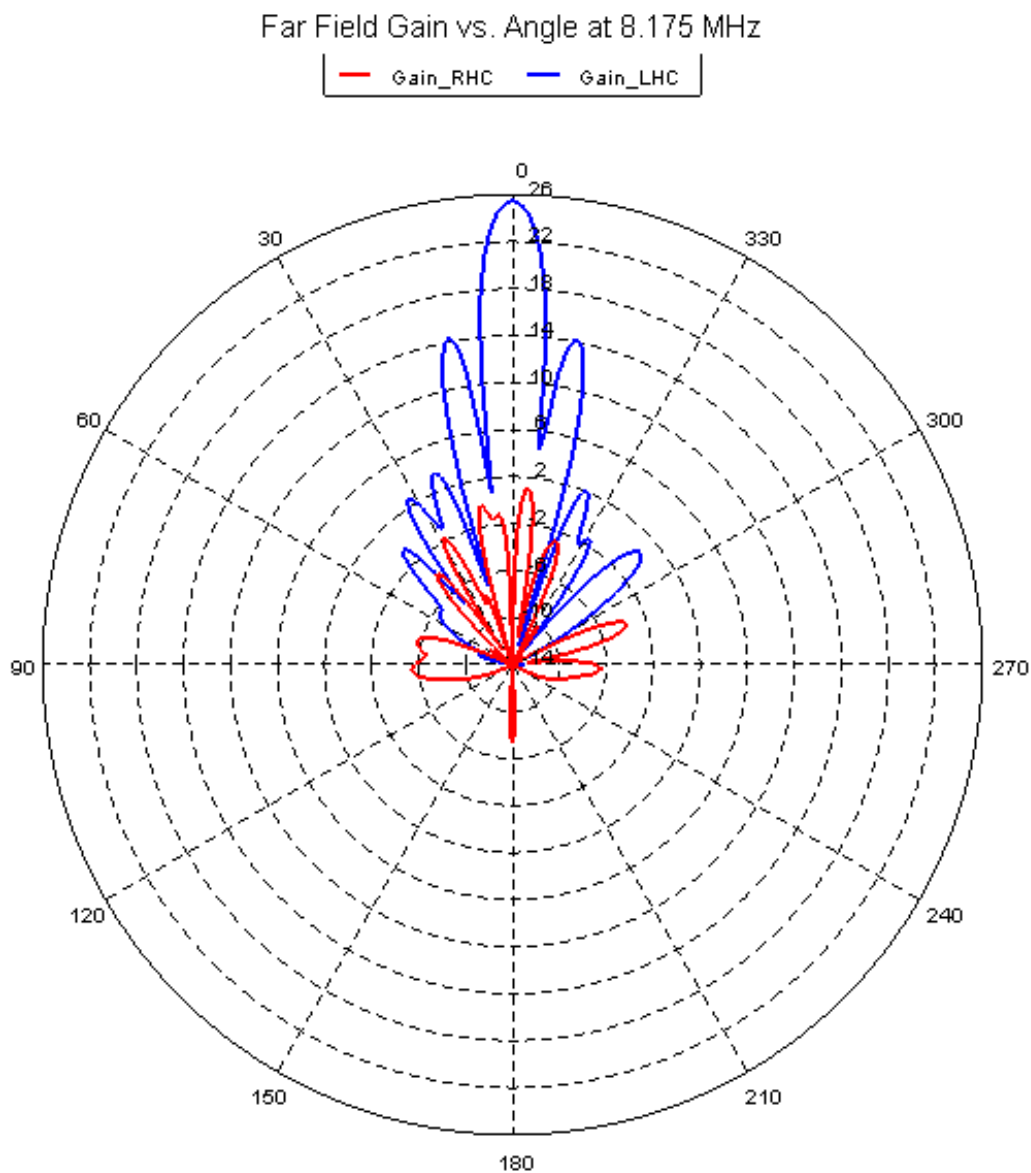


Figure 4-23: Comparison of the LHC and RHC Gain Patterns at 8.175 MHz

Figure 4-23 compares the Right Hand Circular (RHC) polarization rejection. The RHC polarization is graphed against the LHC polarization. The cross polarization rejection is above 27.0 dB relative to the maximum throughout the main beam.

4.2.3 Far Field 8.175 MHz Array with 5.1 MHz Array Open

The far field patterns at 8.175 MHz with the passive array having an open at the feed point were very similar to the pattern when the passive array had a closed circuit at the feed point. There was some difference in the side lobe levels, and the main lobe gain was 25.39 dBi. This is a loss of only 0.05 dB. Figure 4-24 is a graph of the far field gain vs. angle for both $\Phi = 0^\circ$ and the $\Phi = 90^\circ$. The scale is from -14 to 26 dBi with 10 divisions at 4 dB per division. The graph shows that the main beams overlap almost exactly

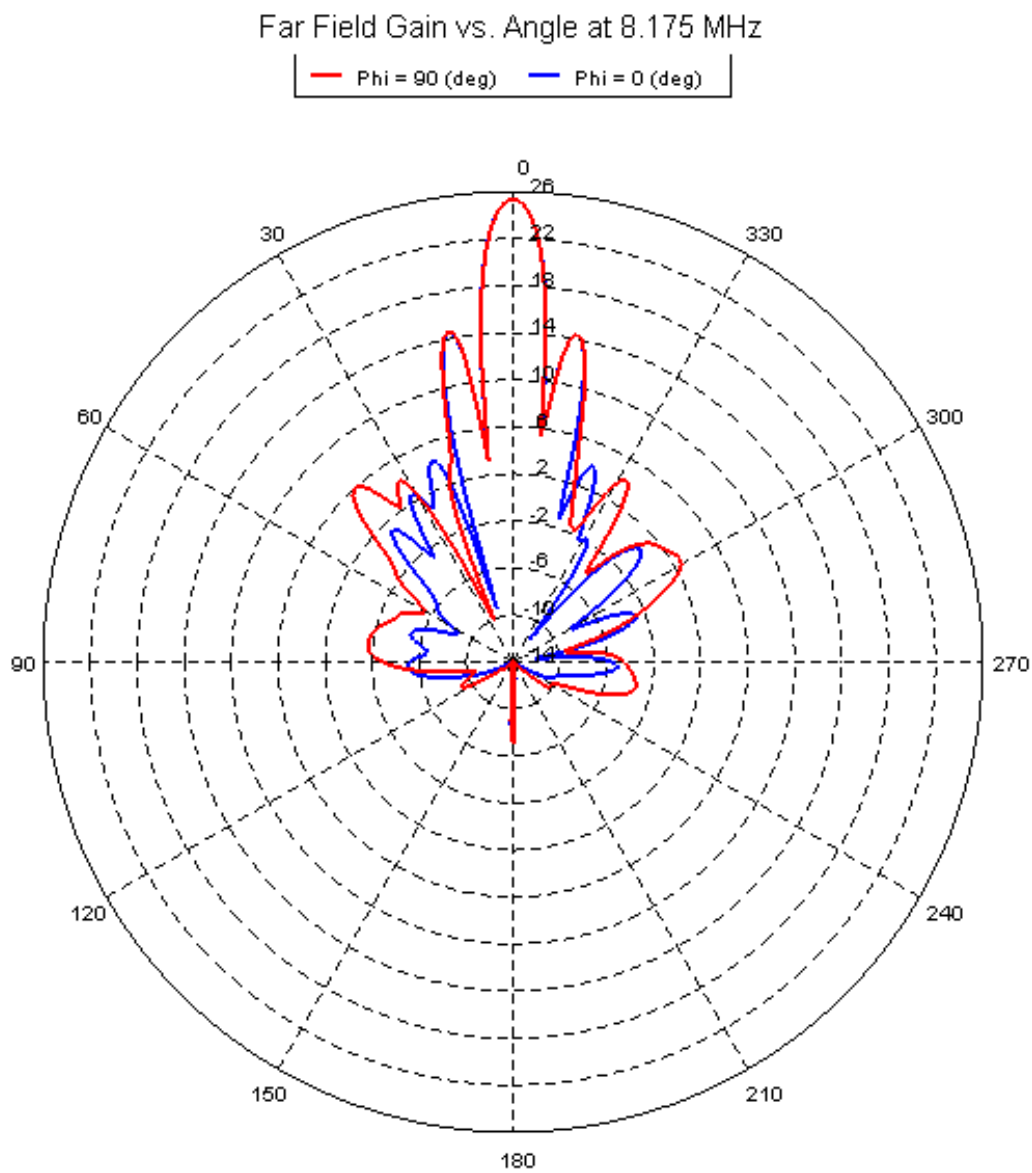


Figure 4-24: Comparison of the Far Field Gain at $\Phi = 0^\circ$ and $\Phi = 90^\circ$ at 8.175 MHz

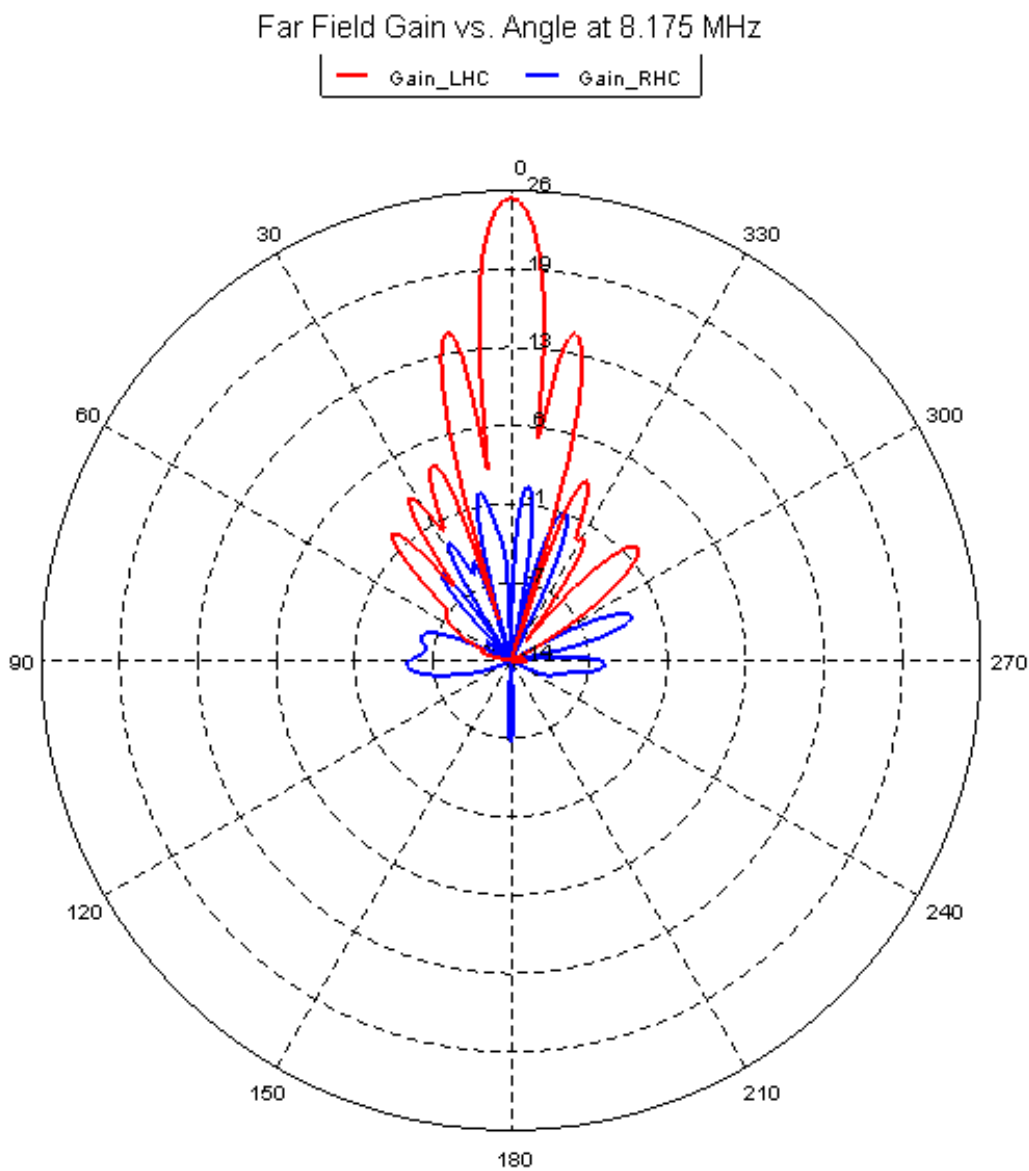


Figure 4-25: Comparison of the LHC and RHC Gain Patterns at 8.175 MHz

Figure 4-25 compares the Right Hand Circular (RHC) polarization rejection. The RHC polarization is graphed against the LHC polarization. The cross polarization rejection is above 27.0 dB relative to the maximum throughout the main beam.

4.3 Near Field Levels

Part of the design study was concerned with the field levels on the antenna. Since the peak power of the antenna system is 600 kW there is some potential for arcing due to the high field levels. The electric breakdown of air occurs at 3 MV/m, but a safety factor of ten was imposed for this study. As a result all field levels should be below 300 kV/m. Since a lot of power will be going through the dipoles, the dipole tips are of particular concern. The design incorporated metal spheres on the tips of the antenna to reduce the field levels there. Various locations around the HF facility were examined. These locations include the active array tips, the passive array tips, and the subreflector edges. The symmetry of the model reduces the number of field locations that have to be studied. Some of the figures contain gaps between parts where there is a high field level. The gaps are an artifact of the model and the high field should be ignored.

4.3.1 Near Field Levels at 5.1 MHz with 8.175 MHz Shorted

Figure 4-26 is a graph of the near field on the tip of the 5.1 MHz active array. The maximum field level in the graph is 160 kV/m. No points around the dipole end reach a field level of 300 kV/m, and therefore there is no concern for arcing on the dipole ends. Figure 4-27 shows the near fields on the subreflector edge and Figure 4-28 displays the near field values on the passive 8.175 MHz array with the feeds Shorted. Neither figures shows field levels that are of any concern to this study.

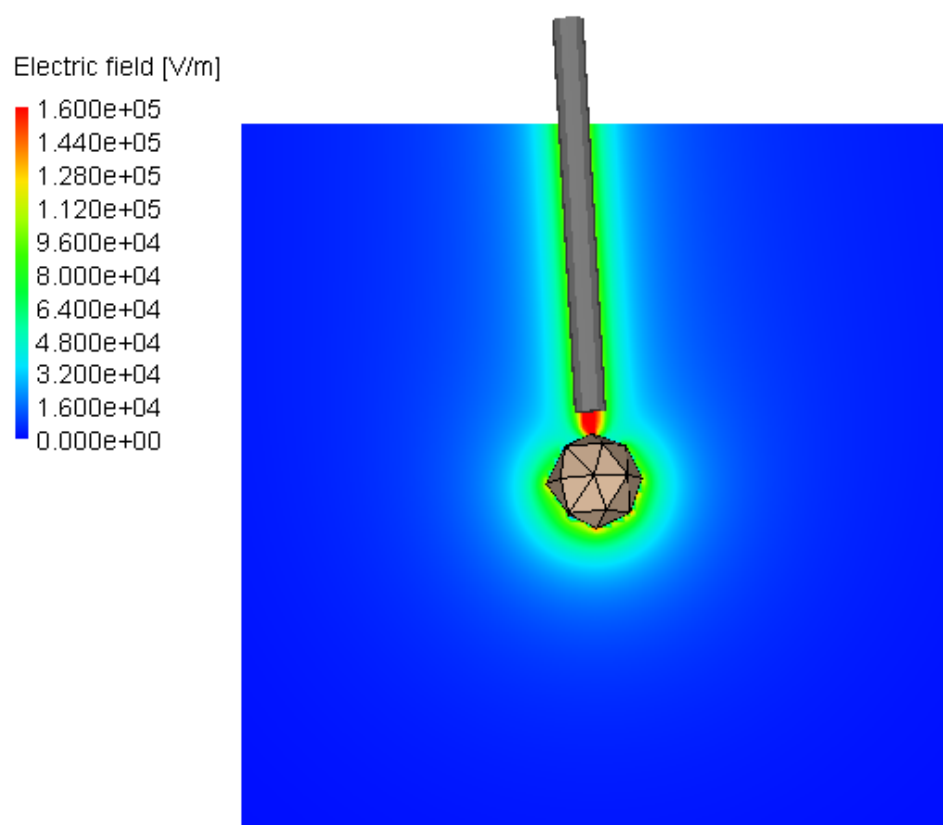


Figure 4-26: Near Field Plot of 5.1 MHz Active Dipole Tip

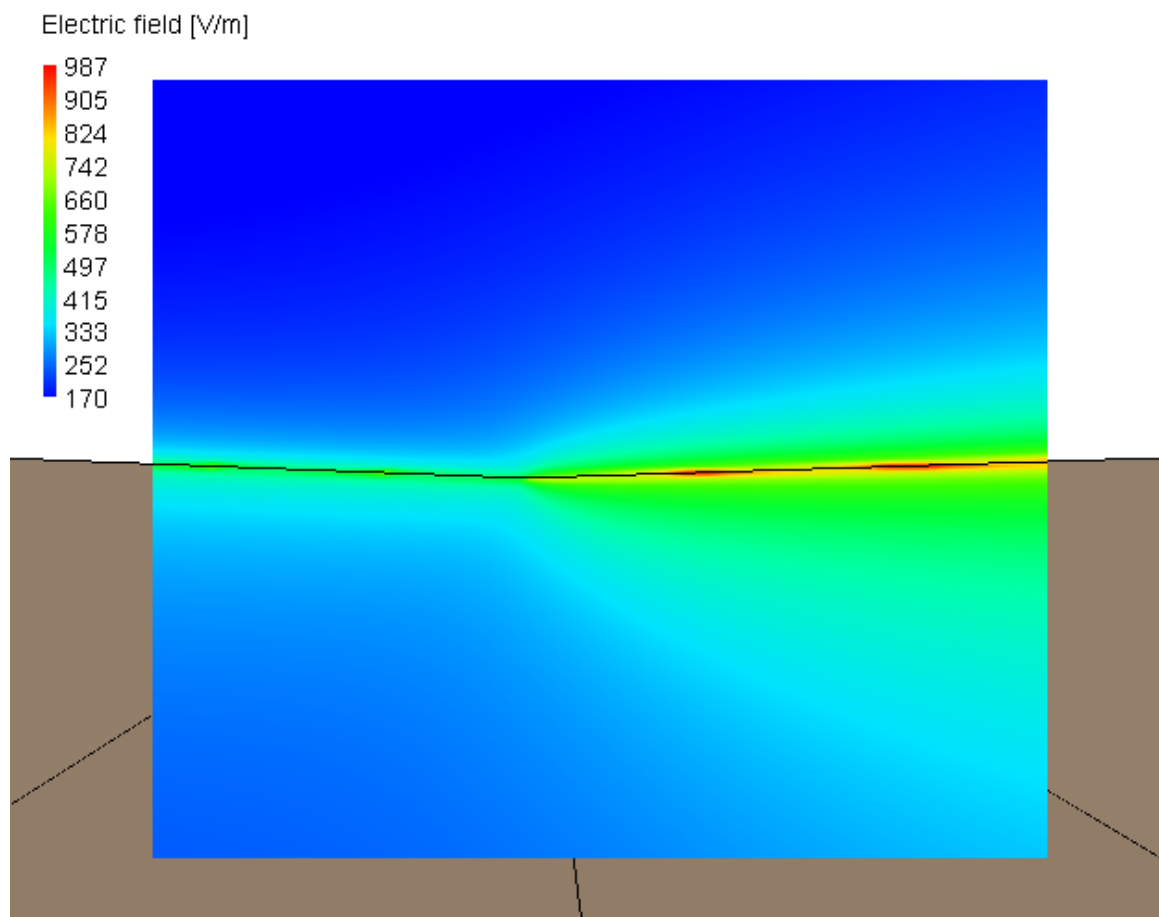


Figure 4-27: Near Field on Subreflector Edge with 5.1 MHz Active Array

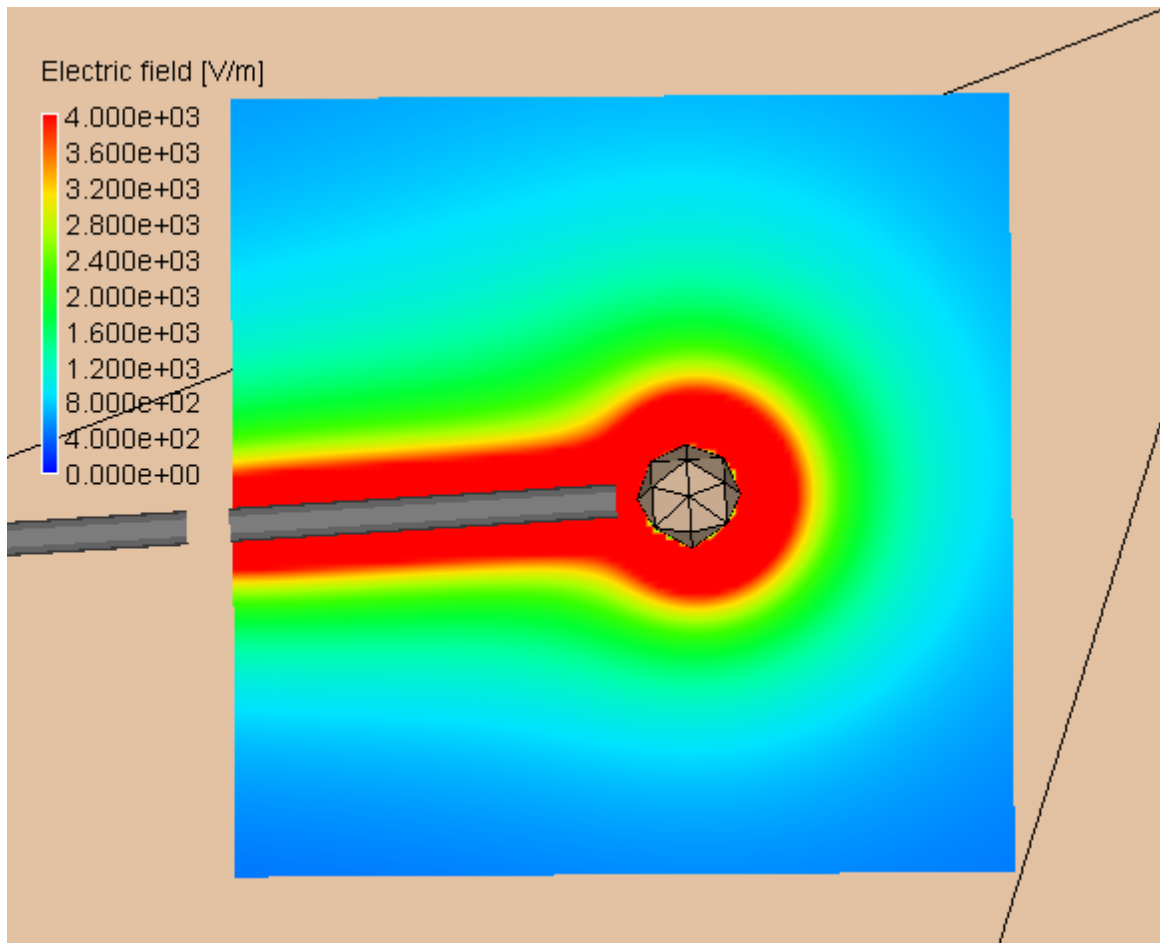


Figure 4-28: Near Field Levels on the passive 8.175 MHz Array (shorted)

4.3.2 Near Field Levels at 5.1 MHz with 8.175 MHz Open

Figure 4-29 is a graph of the near field on the tip of the 5.1 MHz active array. The maximum field level in the graph is 160 kV/m. No points around the dipole end reach a field level of 300 kV/m, and therefore there is no concern for arcing on the dipole ends. Figure 4-30 shows the near fields on the subreflector edge and Figure 4-31 displays

the near field values on the passive 8.175 MHz array with the feeds open (resistor).

Neither figures shows field levels that are of any concern to this study.

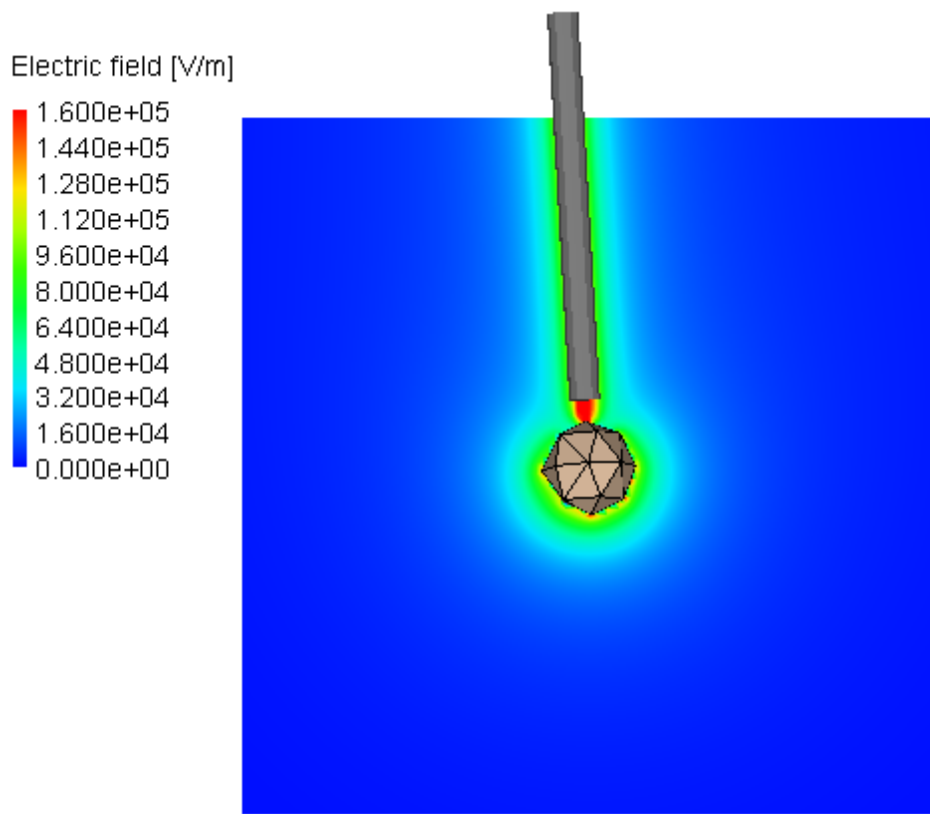


Figure 4-29: Near Field Levels on 5.1 MHz Active Array

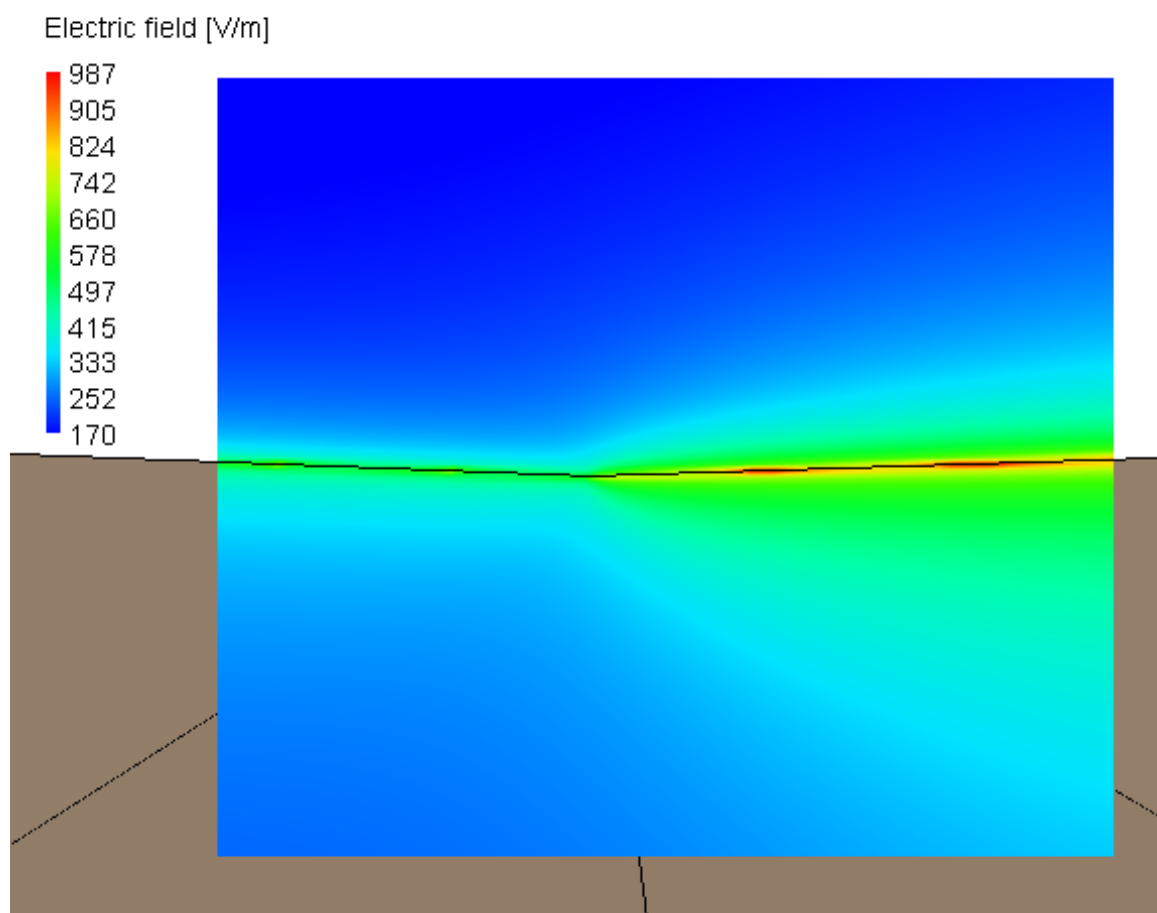


Figure 4-30: Near Field Levels on Subreflector Edge while 5.1 MHz Array Active

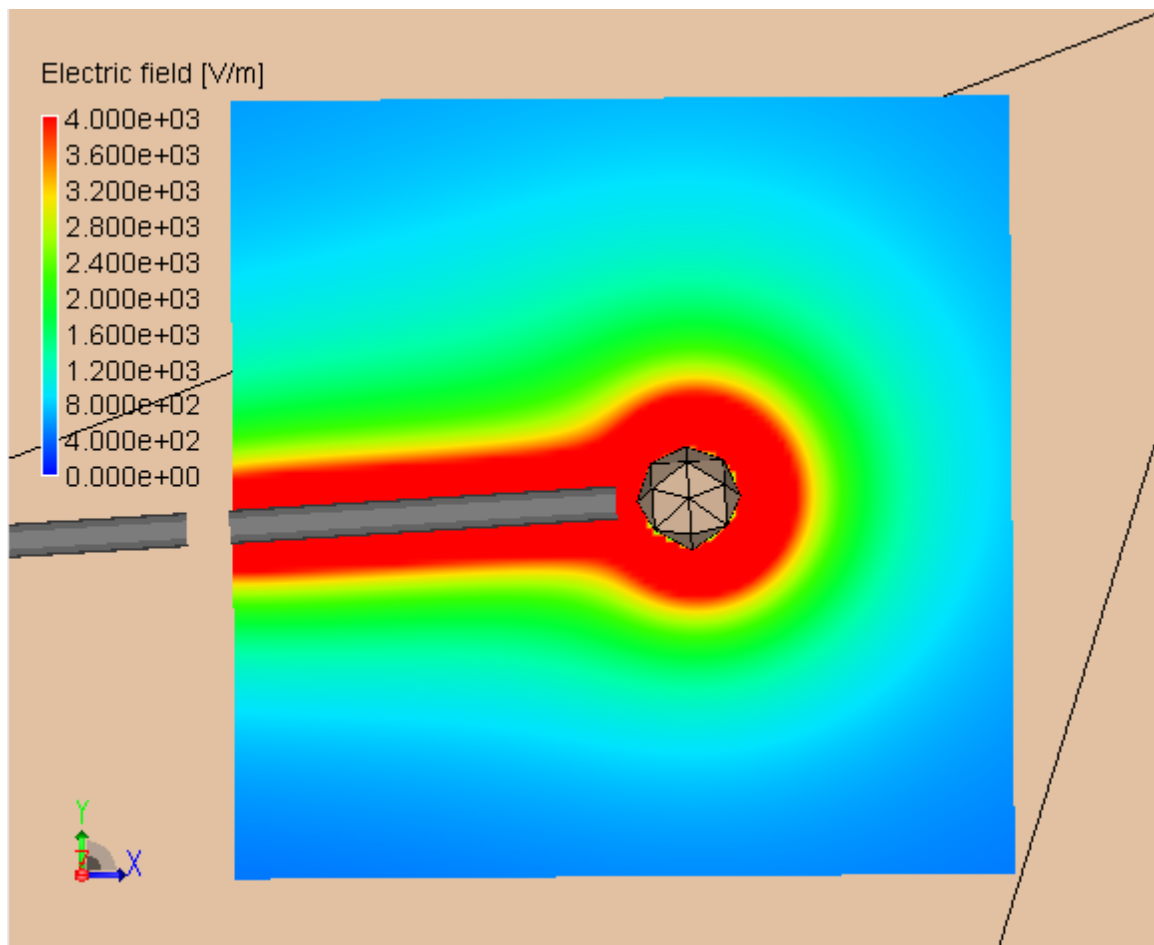


Figure 4-31: Near Field Levels on 8.175 MHz Passive Array (open)

4.3.3 Near Field Levels at 8.175 MHz with 5.1 MHz Shorted

Figure 4-32 is a graph of the near field on the tip of the 8.175 MHz active array. The maximum field level in the graph is 160 kV/m. No points around the dipole end reach a field level of 300 kV/m, and therefore there is no concern for arcing on the dipole ends. Figure 4-33 shows the near fields on the subreflector edge and Figure 4-34 displace

the near field values on the passive 5.1 MHz array with the feed shorted. Neither figures shows field levels that are of any concern to this study.

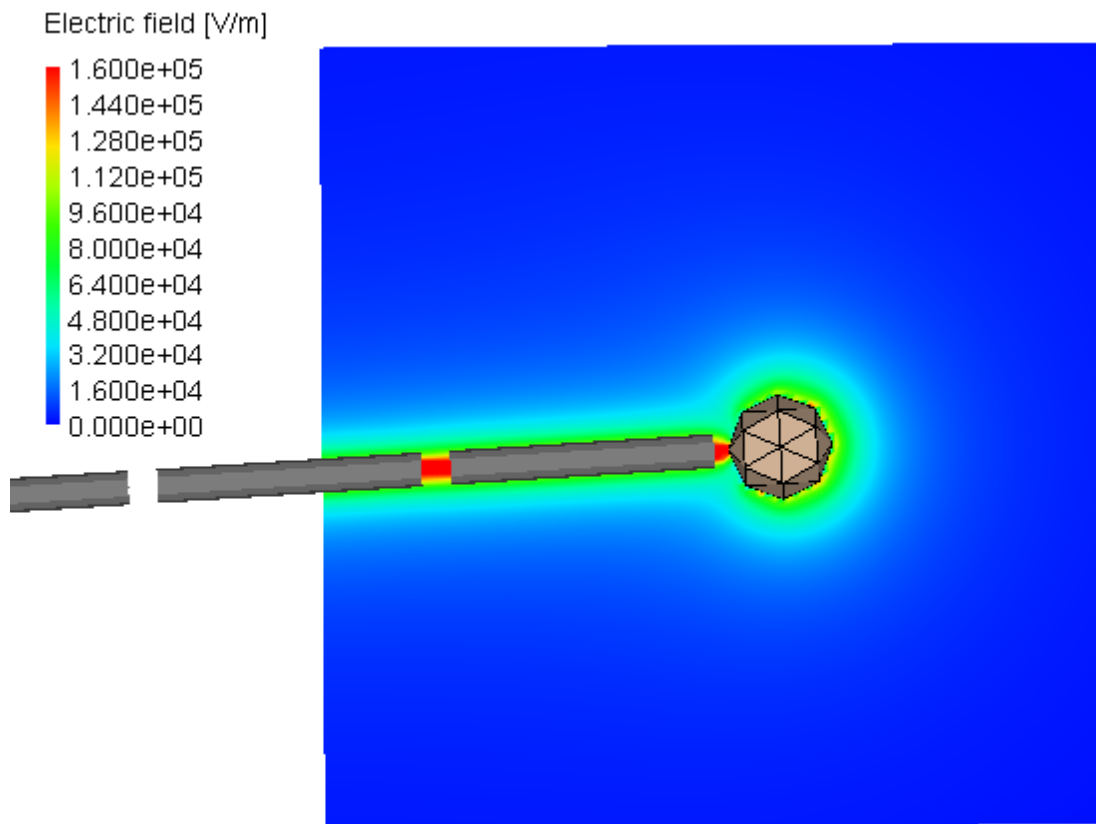


Figure 4-32: Near Fields on the 8.175 MHz Active Array

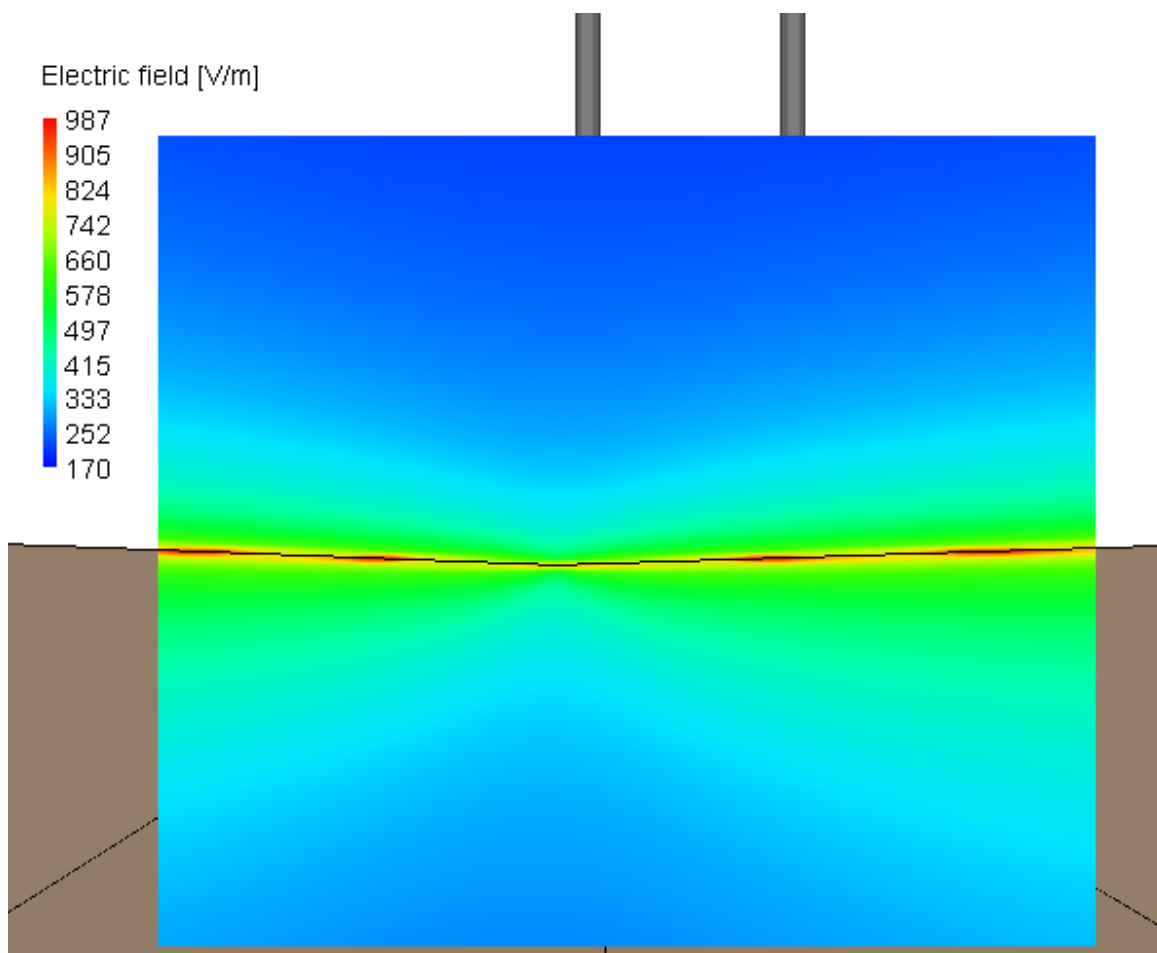


Figure 4-33: Near Field Levels on the Subreflector While 8.175 MHz Array Active

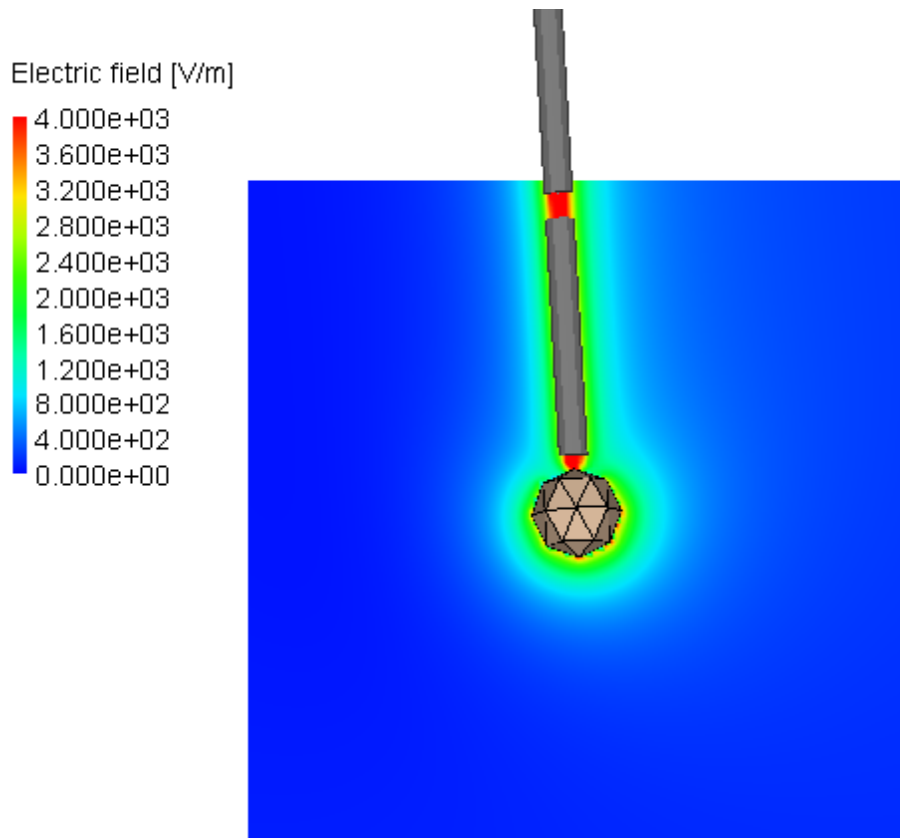


Figure 4-34: Near Field on 5.1 MHz Passive Array (shorted)

4.3.4 Near Field Levels at 8.175 MHz with 5.1 MHz Open

Figure 4-35 is a graph of the near field on the tip of the 8.175 MHz active array. The maximum field level in the graph is 160 kV/m. No points around the dipole end reach a field level of 300 kV/m, and therefore there is no concern for arcing on the dipole ends. Figure 4-36 shows the near fields on the subreflector edge and Figure 4-37 displays the near field values on the passive 5.1 MHz array with the feed open. Neither figures

shows field levels that are of any concern to this study. One interesting thing to note is that the field levels are slightly higher on the passive 5.1 MHz array with the open circuit than on the same array when it is shorted at the feed point.

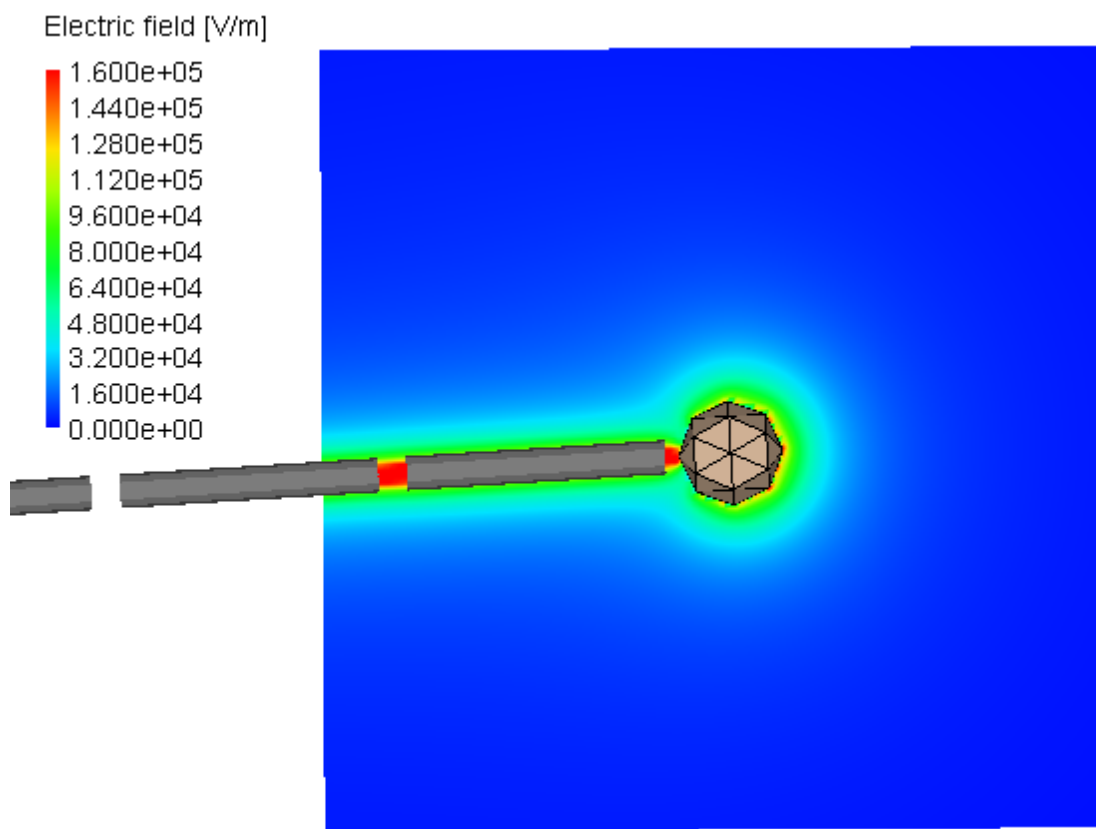


Figure 4-35: Near Fields on the 8.175 MHz Active Array

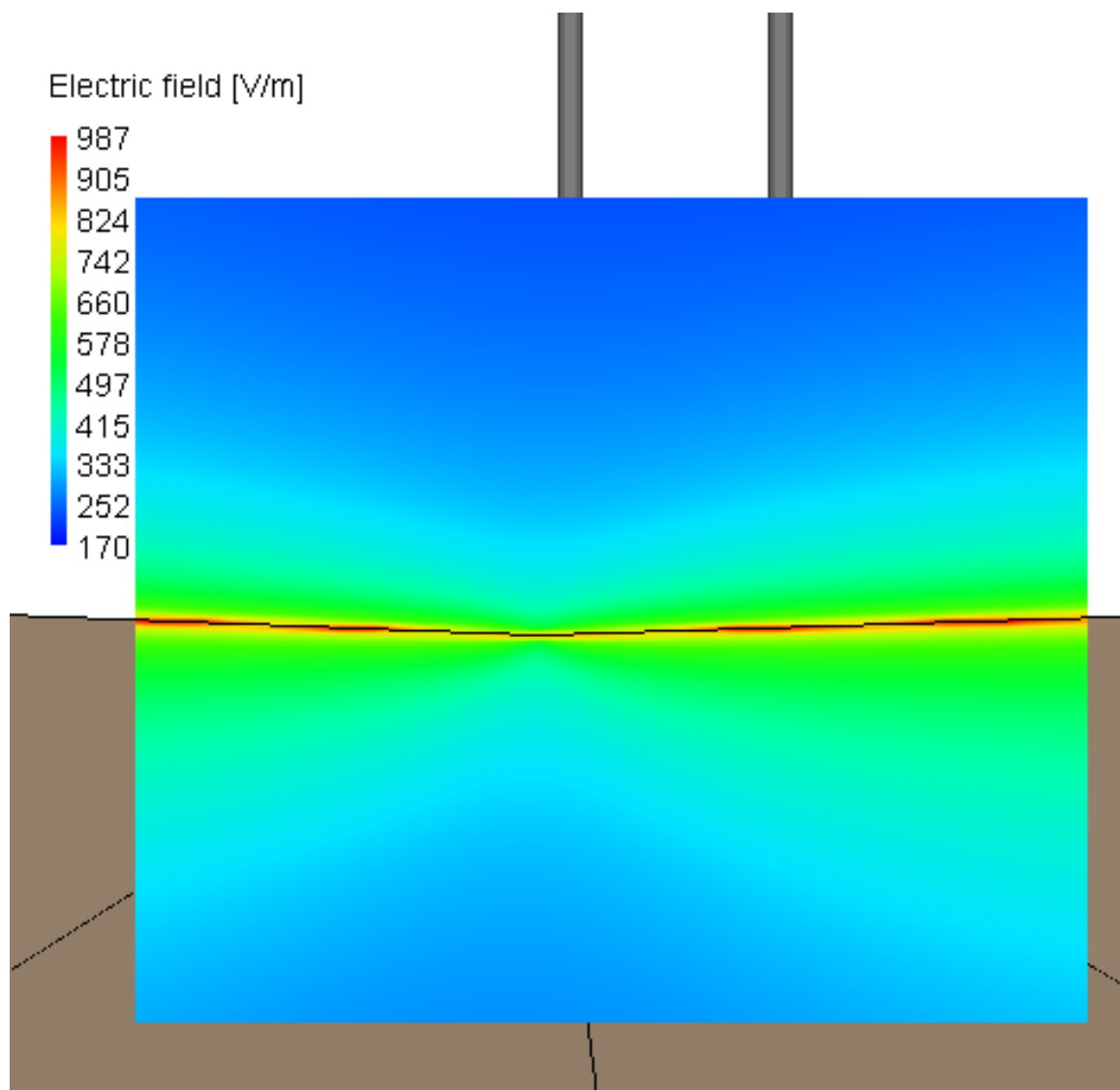


Figure 4-36: Near Fields on subreflector while 8.175 MHz Array Active

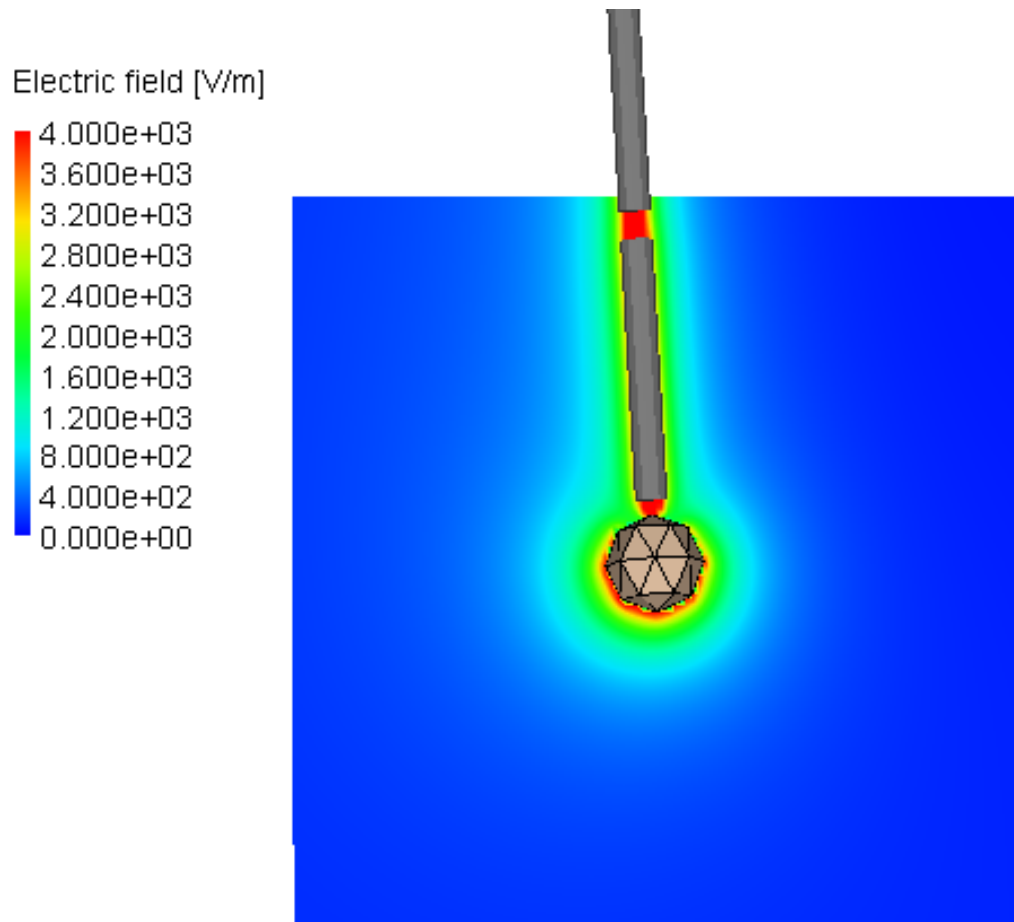


Figure 4-37: Near Fields on 5.1 MHz Passive Array (open)

4.4 Field Levels and Safety

The field levels analysis on the dipole ends and the subreflector was mainly concerned with the breakdown voltage of air. Another concern is for human beings in and around the observatory. IEEE has published safety standards that serve as guideline for evaluating human safety in areas where radio frequency electromagnetic fields are present [4].

The standards for IEEE separate the environments into two classes: controlled and uncontrolled environments. Controlled environments are areas where people are aware of their potential RF exposure. An uncontrolled environment is one in which people have no idea that they are being exposed to RF energy, and they have no control over their exposure. Three areas were examined, two areas that are considered controlled environments and one that is uncontrolled. The two controlled environments are the upper platform walkway and the Gregorian dome. The only people who have access to these areas are personnel that either work at Arecibo, or are authorized to be in these areas. The uncontrolled environment is the Visitors Center. People visiting the observatory do not need to be exposed to unnecessary RF energy. The allowable RF exposure level is much stricter for the uncontrolled environment than for the controlled environment. Table 4-1 presents the maximum permissible exposure levels for controlled and uncontrolled environments [4]. The variable ‘f’ in the calculations is the frequency in MHz.

Table 4-1: Table of Max. Permissible Exposure Levels for Controlled and Uncontrolled Environments

Environ Type	Freq. Range (MHz)	Electric Field Strength (E) (V/m)	Magnetic Field Strength (H) (A/m)	Power Density (S) (E-field), (H-field) (mW/cm²)	Averaging Time E ², or S (min)	Averaging Time H ² (min)
Cont	3 to 30	1842 / f	16.3 / f	(900 / f ²), (10000 / f ²)	6	6
Uncont	3 to 30	823.8 / f	16.3 / f	(180 / f ²), (10000 / f ²)	30	6

4.4.1 Field Levels at Gregorian Dome

Figure 4-38 shows the location of the near field slice on the Gregorian dome. The slice is located inside the dome at an area accessible to authorized personnel only.

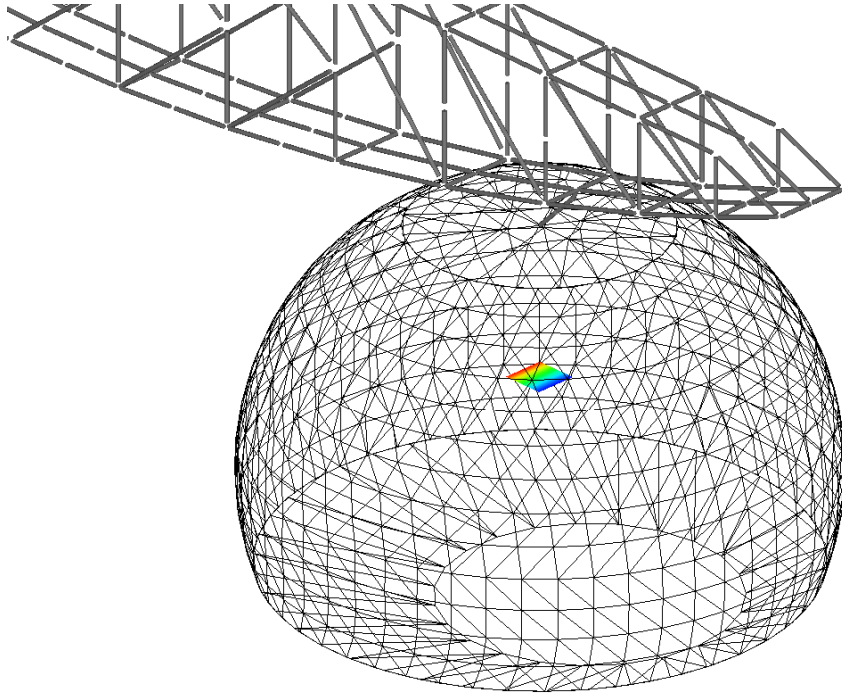


Figure 4-38: Transparent Model of Gregorian Dome Showing Near Field Slice Location

Figure 4-39 is the near field levels at 5.1 MHz inside the Gregorian dome. The highest field value is 10 V/m regardless of whether the passive array was open or closed. Figure 4-40 is the near field levels at 8.175 MHz. The highest field value is 110 V/m in the Gregorian Dome while the passive array is open at the feed point. The maximum field value is slightly lower when the passive array is closed at the feed point. The

highest field value in that case was 95 V/m. A figure was not included for this case because Figure 4-40 depicts the worse case and is therefore of more concern. Both figures are close up of views of Figure 4-38 with the dome removed.

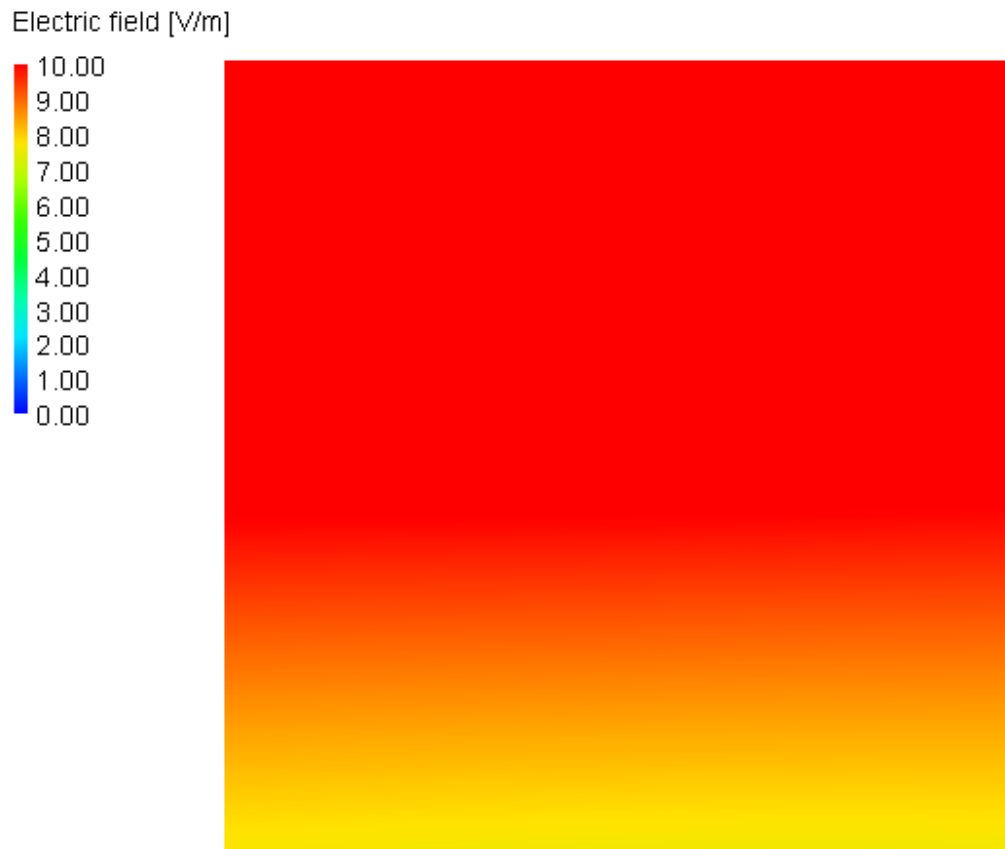


Figure 4-39: Near Field Values at 5.1 MHz in Gregorian Dome

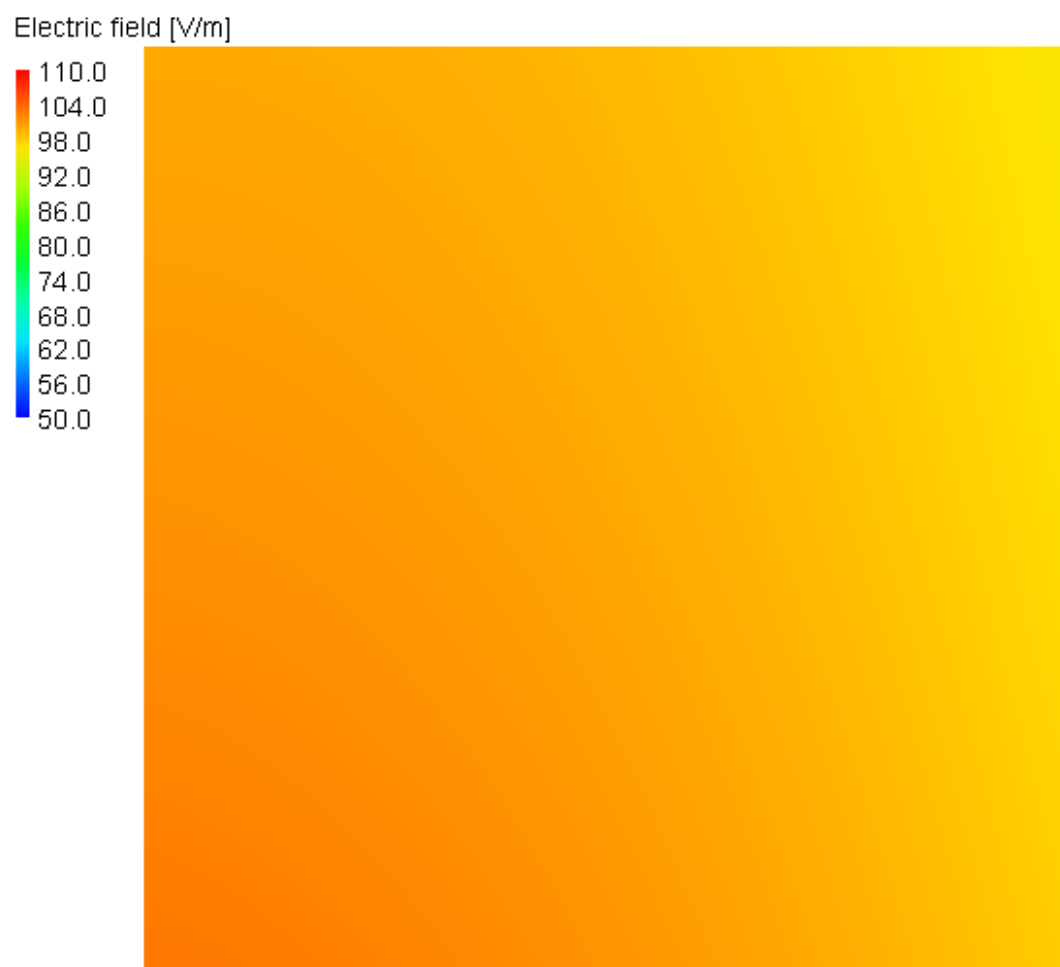


Figure 4-40: Near Field Values at 8.1 MHz in Gregorian Dome

4.4.2 Field Levels at Upper Platform

Figure 4-41 shows a side view of the upper platform. It shows the location of the near field on the upper platform.

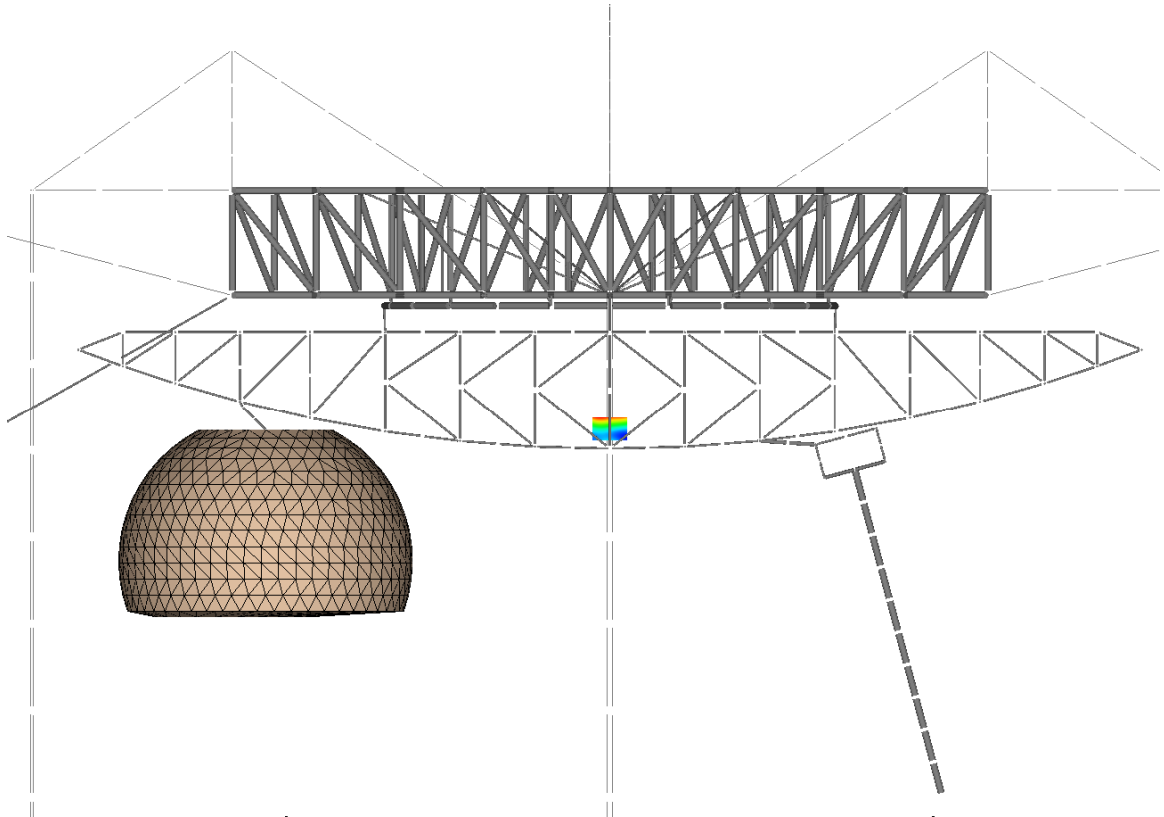


Figure 4-41: Side View of Upper Platform Showing Near Field Location

Figure 4-42 is a close-up of the field values on the platform at 5.1 MHz. The highest value for the electric field is 45 V/m regardless of the state of the feed point on the passive array. Figure 4-43 is the near field values on the upper platform at 8.175 MHz. The maximum value is 450V/m when the passive array has an open at the feed. When the passive feed is closed the maximum field value is 420 V/m.

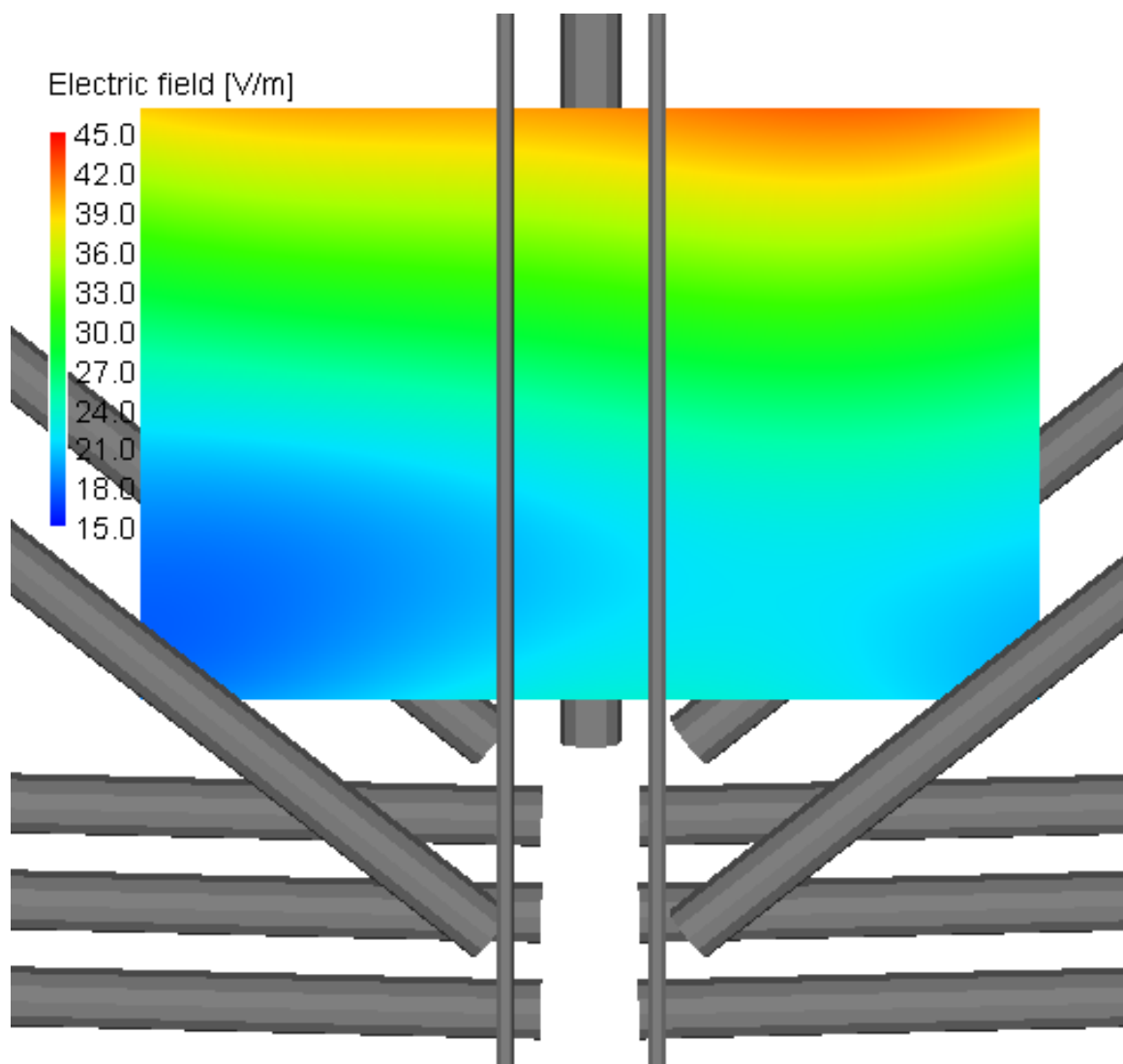


Figure 4-42: Near Field Values on Upper Platform at 5.1 MHz

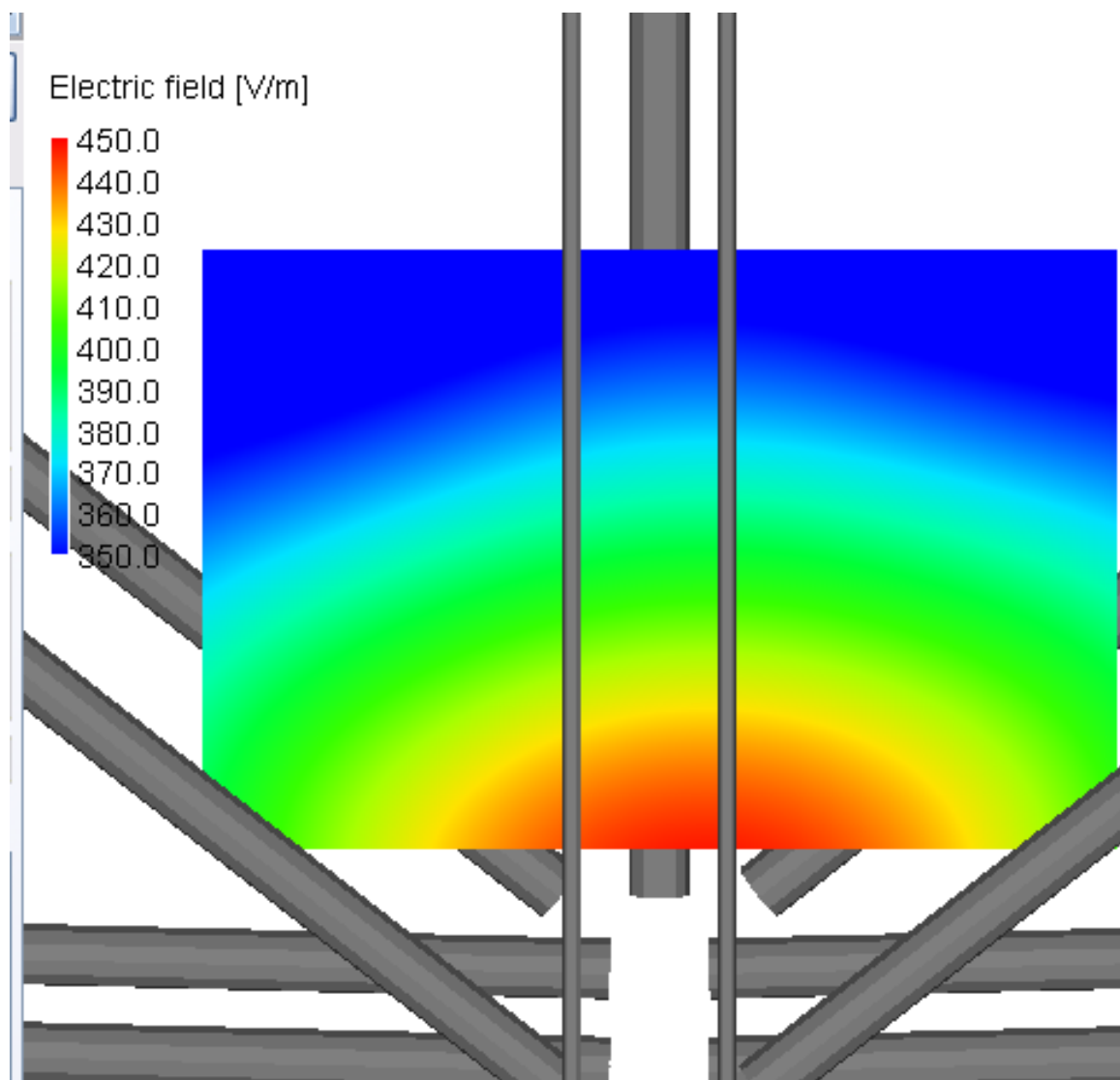


Figure 4-43: Near Field Values on Upper Platform at 8.175 MHz

4.4.3 Field Levels at Visitors Center

Figure 4-44 shows the field levels at the Visitors Center at 5.1 MHz. The highest field value was 13 V/m. Figure 4-45 displays the near field levels at the Visitors Center at 8.175 MHz. The highest field value is 15 V/m. The field values were the same at both

frequencies regardless of the state of the feed points of the passive arrays (i.e. open or shorted).

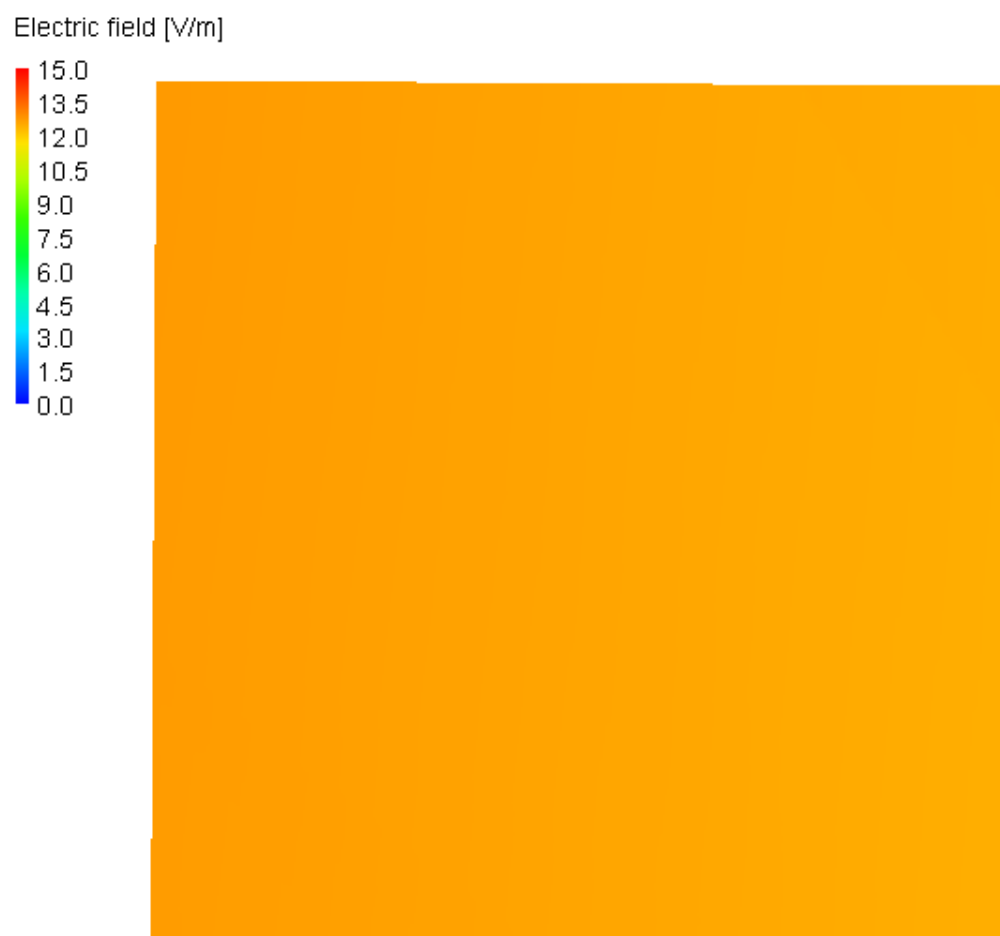


Figure 4-44: Near Field Levels at Visitors Center at 5.1 MHz

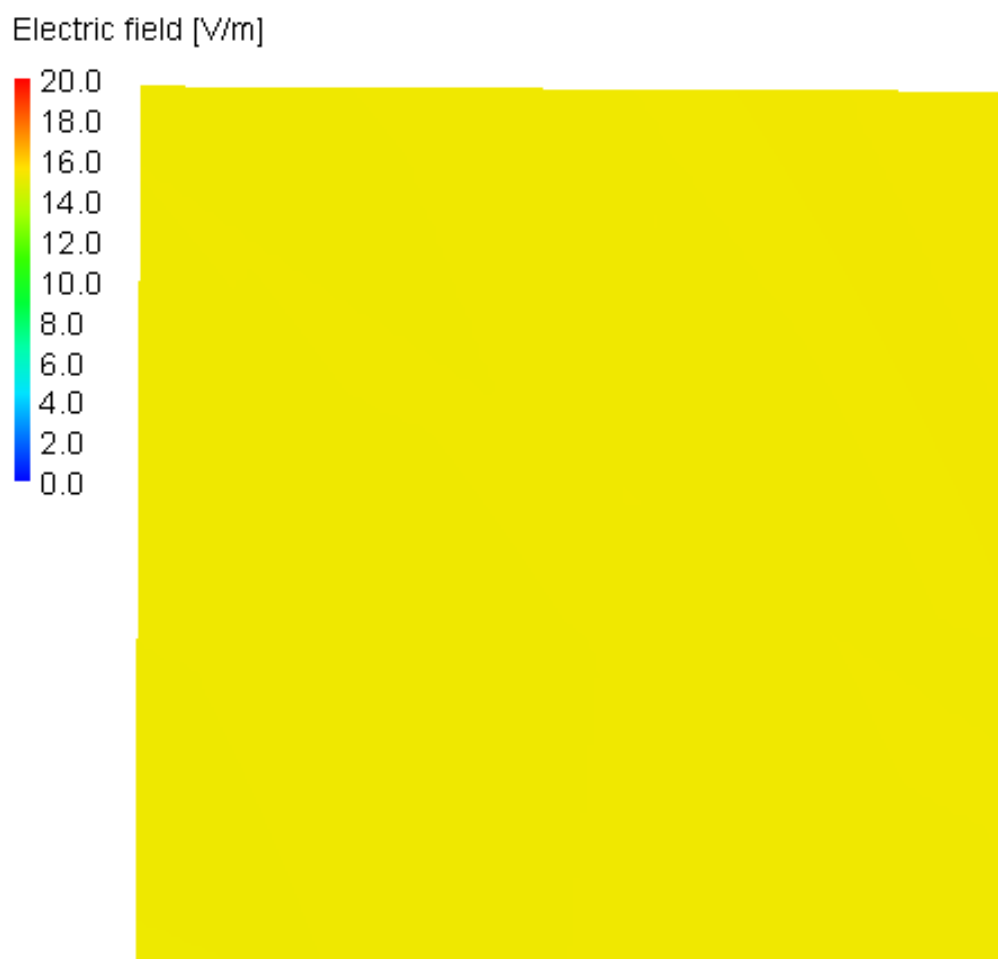


Figure 4-45: Near Field Levels at Visitors Center at 8.175 MHz

4.4.4 Field Level Summary

Since human safety is a concern for this study, the near field values need to be compared to the IEEE standards for Maximum Permissible Exposure Levels for controlled and uncontrolled environments. Table 4-2 compares the field levels calculated

in FEKO to the maximum permissible exposure levels calculated using the information from Table 4-1. The predicted field level in the Gregorian dome at 8.175 MHz exceeds the uncontrolled environment field level by about 10 V/m. Considering the Gregorian dome is on the platform suspended over the dish, it is safe to say it is a controlled environment. With that in mind there is no concern for field levels in the Gregorian dome. The upper platform walkway exceeds the maximum field level for a controlled environment by 225 V/m at 8.175 MHz. It is therefore recommended that the platform is evacuated while the 8.175 MHz array is in operation. It is possible that other areas on the upper platform exceed the maximum field value of 225.32 V/m by more than 225 V/m. This recommendation extends to the entire platform, including the Gregorian dome. Although the field levels in the dome appear to be safe, since the field levels on the platform walkway are so high it is not worth the risk. In addition the dome can move and rotate below the platform and it is possible that the location under study is a safe location, even though other locations are not considered safe by IEEE standards. The fields on the Visitors Center were well below the maximum exposure levels for both controlled and uncontrolled environments. This means there is no danger for civilians in Visitors Center while the facility is in operation.

Table 4-2: Comparison of FEKO Calculated Field Levels with Maximum Permissible Exposure Levels

Location	Frequency (MHz)	Electric Field Level FEKO (V/m)	Maximum Permissible Exposure Levels (V/m)	
			Controlled	Uncontrolled
Gregorian Dome	5.1	10	361.18	161.53
	8.175	110	225.32	100.77
Upper Platform Walkway	5.1	45	361.18	161.53
	8.175	450	225.32	100.77
Visitors Center	5.1	13	361.18	161.53
	8.175	15	225.32	100.77

Chapter 5

Conclusion

The new HF facility at Arecibo will replace functionality that was lost in the past. Prior facilities have been rendered unusable either by time or acts of nature. The new facility is being added to existing infrastructure (i.e. the observatory) which adds to the desirability. The control buildings and a portion of the infrastructure needed to build and maintain the proposed facility are already in place.

The proposed design will be fed by one of two arrays. Each array operates at a different frequency. One will operate at 5.1 MHz and the other array operates at 8.175 MHz. The facility will utilize the 305 m dish already in place along with a suspended metal mesh net that will work together to form a cassegrain system.

The facility was examined with both arrays present to look at any mutual coupling affects that may arise from having both arrays present. In addition, the feed point of the passive array was simulated with both a resistor to simulate an open circuit and a wire segment to simulate a closed circuit. Both arrays had a VSWR less than 2:1 over a 100 kHz bandwidth no matter what the state of the passive array's feed was. The gain at 5.1 MHz was 22.16 dBi. The arrays will be fed with 600 kW of power for an ERP of 98.6 MW at 5.1 MHz. At 8.175 MHz the maximum gain was 25.46 dBi when the passive array was closed at the feed point and 25.39 dBi when the feed on the passive array was open. This corresponds to an ERP of 210.9 MW and 207.6 MW respectively. The cross

polarization rejection was above 27 dB compared to the main beam at both frequencies. This means that the array can operate on either RHC or LHC polarization modes.

The near field values around the antenna were also examined for safety and the possibility of arcing. The antennas themselves did not present a risk for arcing because the field levels were below the safety value of 300 kV/m. The near field levels at several locations were also examined to see if there was any risk for exposure to radio frequency electromagnetic fields. The areas open to the public, such as the Visitor's Center, showed field levels that pose no threat to the public based on IEEE standards for Maximum Permissible Exposure Levels (MPEL). The controlled environments showed no areas of concern at 5.1 MHz, but at 8.175 MHz the upper platform walkway exceeded MPEL for controlled environments. This means that personnel should not be on the upper platform while the HF facility is in use.

The metallic cassegrain mesh reflector was also redesigned from previous embodiments as a triangular 'net'. Cutting off the corners to create a hexagon reduces the size, weight, and cost of creating this reflector. 5 foot holes were found to be adequate spacing to appear as a solid reflective surface at the frequencies of interest. 5 foot spacing corresponds to a little less than $\lambda/24$ holes at 8.175 MHz. The net will naturally take a parabolic shape due to gravity. Future mechanical work will focus on investigating how to build this shape in real life. It will look into weight and diameter of wires necessary to support the cassegrain's own weight, and how to tension the cables properly so that the proper shape is achieved.

Bibliography

- 1 Tony Acevedo, "Arecibo Observatory," [Online document] [cited 2009 Jan 13] Available HTTP: <http://www.naic.edu/index.htm>
- 2 William J. Glessner, "The New Arecibo HF Interactions Facility Cassegrain Antenna System Design", M.S. Thesis, The Pennsylvania State University, University Park, Pennsylvania, 2007.
- 3 Markus Zahn, "Electromagnetic Field Theory: a problem solving approach," Kreiger Publishing Company, Malabar, 2003.
- 4 IEEE Std C95.1, 1999 Edition, IEEE Standard for Safety Levels with Respect to Human Exposure to Radio Frequency Electromagnetic Fields, 3 kHz to 300 GHz, 1999
- 5 Ellwood E. Brem, "a High Power RF Transport System for the HF Interactions Facility at Arecibo, Puerto Rico", M.S. Thesis, The Pennsylvania State University, University Park, Pennsylvania, 2005.
- 6 Jon A. Arent, "Experimental Validation of the New Arecibo HF Interactions Facility Antenna", M.S. Thesis, The Pennsylvania State University, University Park, Pennsylvania, 2005.
- 7 M.P. Sulzer and S.A. Gonzalez, "Arecibo HF Facility Proposal" NSF Proposal, January 2007.
- 8 Warren L. Stutzman and Gary A. Thiele, "Antenna Theory and Design", Jon Wiley and Sons, Inc., New York, 1998.
- 9 Constantine A Balanis, "Antenna Theory Analysis and Design", Jon Wiley and Sons, Inc., New York, 1997.
- 10 FEKO, [Online document] Available HTTP: <http://www.feko.info/>
- 11 NEC, [Online document] Available HTTP: <http://www.nec2.org/>

Appendix A

FEKO Model Input File for Dual Array Design with 5.1 MHz Active

```
** Arcibo reflector as a casegrain system fed by crossed Dipoles
** Both Antenna Arrays Present (5.1 and 8.175 MHz)
** Active array 5.1 MHz
**
** Kyle Labowski
** Created: 9/29/2008
** Updated: 2/11/2009

** ----- **
** Variables **
** ----- **

** Scaling factor
#scaling = 0.3048          ** meters to feet

** Frequency and wavelength
#freq8MHz = 8.175e6        ** freq in Hertz
#lam8MHz = #c0/#freq8MHz  ** minimum wavelength for segmentation
#lam8MHz = #lam8MHz/#scaling ** scale the wavelength as desired

#freq5MHz = 5.1e6         ** freq in Hertz
#lam5MHz = #c0/#freq5MHz  ** minimum wavelength for segmentation
#lam5MHz = #lam5MHz/#scaling ** scale the wavelength as desired

** Dish variables
#Dr = 870                 ** Radius of the spherical reflector
```

```

#Rr = 300          ** Distance between sub-reflector and main dish
#Rr2 = 300        ** Radius of reflector for surface at dish focal point
#SRad = 145       ** Radius of sub-reflector area
#Rz = #Rr2+#Rr    ** Center of Reflector sphere (Rz > Dr/2 (435))

** Ground screen variables
#GSHgt = 50       ** Height of ground screen above main dish
#GSLen = 34.2     ** distance of tip from dish edge in x direction
#sang = ARCSIN(#SRad/#Rr2) ** angle from center of sub-reflector to edge off z axis
#sadeq = (#sang*180)/#pi ** angle in degrees
#adeq = 35        ** angle from center of main dish to edge off z axis
#ang = (#adeq*#pi)/180 ** angle in radians
#GSBasz = #Dr*(1-COS(#ang)) ** height from bot of main dish to bot of gnd screen
#GSTopz = #GSBasz + #GSHgt ** height from bot of main dish to top of gnd screen
#GSBasx = #Dr * SIN(#ang) ** lateral distance center to dish to bot of gnd screen
#GSTopx = #GSBasx + #GSLen ** lateral distance center to dish to top of gnd screen

** Point calculations for reflector
#Href = #Rr2*(1-COS(#sadeq*#pi/180)) ** Height of the reflector
#HdTop = #Href + #Rr ** Height of the top of the reflector

#yloc = -#SRad*COS(30*#pi/180) ** y-location of 2nd tie point of reflector
#xloc = -#SRad*SIN(30*#pi/180) ** x-location of 2nd tie point of reflector

** Antenna Variables 5.1 MHz
#Drv5MHz = 0.217*#lam5MHz ** half the length of a driven element
#Drspc5MHz = 0.1757*#lam5MHz ** distance from gnd (reflector) to driven
#Fd5Mhz = 0.0124*#lam5MHz ** Center of feed segment for each driven half
#aspace5MHz = 0.8414*#lam5MHz ** Array spacing

** Antenna Variables 8.175 MHz
#Drv8MHz = 0.214*#lam8MHz ** half the length of a driven element
#Drspc8MHz = 0.2*#lam8MHz ** distance from gnd (reflector) to driven
#Fd8Mhz = 0.0124*#lam8MHz ** Center of feed segment for each driven half
#aspace8MHz = 0.83814920*#lam8MHz ** Array spacing
#angshift = 63.19

```

```

#angshift8MHz = 3.19

** Subreflector Variables
#subscale = 1.106
** #subhght = 299    ** subreflector height for 8.175 MHz
#subhght = 284    ** subreflector height for 5.1 MHz

** Translation Variables
#shiftA8MHz =#aspace8MHz*TAN(#pi/6)
#shiftA5MHz =#aspace5MHz*TAN(#pi/6)

** Variables for defining the Gregorian housing
#GrX=30*3.28084      ** X location of Gregorian center
#GrY=0              ** Y Location of Gregorian Center
#GrZ=128*3.28084    ** Z Location of Gregorian Center
#GrRad=12.8016*3.28084  ** Radius of Gregorian Center
#GrTop=#GrZ+#GrRad  ** Top location of the Gregorian sphere
#GrSide=#GrX+#GrRad  ** Side location of the Gregorian sphere
#GrAngS=27          ** The angle to start the curve of sphere
#GrAng=110          ** The angle measured from Z axis to complete the sphere

** Variables for bottom cap of Gregorian sphere
#GrCpBas=#GrZ-#GrRad*cos((180-#GrAng)*#pi/180)  ** Height of base of the cap
#Cap_of_st=#GrCpBas-0.5*3.28084                ** Height of hole in cap offset value from cap edge
#GrB_rad=#GrX+#GrRad*sin((180-#GrAng)*#pi/180)  ** Radius for the base of the cap
#Gr_V_X=#GrX+3*3.28084                          ** X location of hole in the cap (vertex)
#Gr_V_rad=6.5532*3.28084                        ** Radius of the hole in the cap
#Gr_V_sid=#Gr_V_rad+#Gr_V_X                     ** Point for the radius with offset
#Gr_V_Y=#GrY+0                                  ** Y location of the Gregorian cap vertex hole

** Variables for top cap of the dome
#GrCp_top=#GrZ+#GrRad*cos((#GrAngS)*#pi/180)    ** Height of the flat top of the sphere Z
#GrCp_sid=#GrX+#GrRad*sin((#GrAngS)*#pi/180)    ** Radius of the cap of the dome top X
#GrCp_nor=#GrCp_top+1*3.28084                  ** Normal Position for the top cap
#inner=#GrX+0.3*#GrRad*sin((#GrAngS)*#pi/180)   ** X location for inner circle

```

```

** ----- **
** Segmentation parameters **
** ----- **
#seg_rad = 0.166667      ** segment radius
** #tri_len = #lam8MHz/4  ** triangle size for 8.175 MHz
** #seg_len = #lam8MHz/40 ** segmentation length for 8.175 MHz
#tri_len = #lam5MHz/6   ** triangle size for 5.1 MHz
#seg_len = #lam5MHz/40  ** segmentation length for 5.1 MHz

IP                      #seg_rad  #tri_len  #seg_len

** ----- **
** Define Points **
** ----- **
** Define dish points
** Define points for a quarter of the main dish
DP   D1                  0          0          #Dr
DP   D2                  0          0          0
DP   D3                  #Dr         0          #Dr

** Define ground screen points
DP   GS1                 0          0          #GSTopz
DP   GS2                 0          0          #GSBasz
DP   GS3                 #GSTopx   0          #GSTopz
DP   GS4                 #GSBasx   0          #GSBasz

** User defined points for the construction of the Gregorian sphere
DP   104                 #GrX     #GrY     #GrZ
DP   105                 #GrX     #GrY     #GrTop
DP   106                 #GrSide  #GrY     #GrZ

** User defined points for the construction of the Gregorian sphere cap
DP   111                 #GrX     #GrY     #GrCpBas  ** S1
DP   112                 #Gr_V_X  #Gr_V_Y  #Cap_of_st ** S2
DP   113                 #GrB_rad #GrY     #GrCpBas  ** S3
DP   114                 #Gr_V_sid #Gr_V_Y  #Cap_of_st ** S4

```

```

** User defined points for the construction of the Gregorian sphere top cap
DP  115                #GrX      #GrY      #GrCp_top    ** S1
DP  116                #GrX      #GrY      #GrCp_nor    ** S2
DP  117                #GrCp_sid #GrY      #GrCp_top    ** S3
DP  118                #inner    #GrY      #GrCp_top    ** S4

** Define a point to connect gregorian sphere to azimuth arm NEC file
DP  126                105        0          464

** Define antenna points for 5.1 MHz
** Define points for half driven element on x axis for 5.1 MHz
DP: DvX1_5MHz : : : : : #Drv5MHz : 0 : #Drspc5MHz
DP: DvX2_5MHz : : : : : #seg_len : 0 : #Drspc5MHz
DP: DvX3_5MHz : : : : : 0 : 0 : #Drspc5MHz

** Antenna ball points
DP: ball_5MHz : : : : : #Drv5MHz+0.5 : 0 : #Drspc5MHz
DP: ball2_5MHz : : : : : #Drv5MHz+0.5 : 0.5 : #Drspc5MHz

** Define antenna points for 8.175 MHz
** Define points for half driven element on x axis for 8.175 MHz
DP: DvX1_8MHz : : : : : #Drv8MHz : 0 : #Drspc8MHz
DP: DvX2_8MHz : : : : : #seg_len : 0 : #Drspc8MHz
DP: DvX3_8MHz : : : : : 0 : 0 : #Drspc8MHz

** Antenna ball points
DP: ball_8MHz : : : : : #Drv8MHz+0.5 : 0 : #Drspc8MHz
DP: ball2_8MHz : : : : : #Drv8MHz+0.5 : 0.5 : #Drspc8MHz

** ----- **
** Create Geometry **
** ----- **

** Create dish
KU  D1  D2  D3  1          0          0          #adeg  360

```

```

** Construct ground shield
KK  GS1  GS2  GS3  GS4          360          1          0

** ----- **
** Construct 5.1 MHz antenna
** ----- **
LA   1
BL:  DvX2_5MHz : DvX3_5MHz

LA   201
BL:  DvX1_5MHz : DvX2_5MHz
KU:  ball_5MHz : DvX1_5MHz : ball2_5MHz : : : 0 : 0 : 180 : 360 : #tri_len/75

** translation
** Create 3 additional parts for 1st crossed dipole
TG   3   1   1   1   0          90
TG   3   201 201 1   0          90

** Shift Dipole
TG:  0 : 1 : 4 : : 0 : : : : : -#shiftA5MHz
TG:  0 : 201 : 204 : : 0 : : : : : -#shiftA5MHz

** Create 2nd and 3rd crossed dipoles
TG   2   1   4   4   0          120
TG   2   201 204 4   0          120

TG   0   1   12   0          #angshift
TG   0   201 212   0          #angshift

** ----- **
** Construct 8.175 MHz antenna
** ----- **
LA   1001
BL:  DvX2_8MHz : DvX3_8MHz

```

```

LA 1201
BL: DvX1_8MHz : DvX2_8MHz
KU: ball_8MHz : DvX1_8MHz : ball2_8MHz : : : 0 : 0 : 180 : 360 : #tri_len/75

** translation
** Create 3 additional parts for 1st crossed dipole
TG 3 1001 1001 1 0 90
TG 3 1201 1201 1 0 90

** Shift Dipole
TG: 0 : 1001 : 1004 : : 0 : : : : : -#shiftA8MHz
TG: 0 : 1201 : 1204 : : 0 : : : : : -#shiftA8MHz

** Create 2nd and 3rd crossed dipoles
TG 2 1001 1004 4 0 120
TG 2 1201 1204 4 0 120

TG: 0 : 1001 : 1012 : : 0 : : : : #angshift8MHz
TG: 0 : 1201 : 1212 : : 0 : : : : #angshift8MHz

IP #seg_rad #tri_len #seg_len

LA 100
** Create reflector
IN 8 31 "subreflectorSmall.cfm"

TG: 0 : Split_back3.Face1 : Split_back3.Face1 : : 0 : : : : : : #subscale
TG: 0 : Split_back3.Face1 : Split_back3.Face1 : : 0 : : : : : : #subhght

** Create upper platform
IN 5 1 "UP_PLT_2.NEC"

** Geometry for the Gregorian sphere
LA 103

```

```

KU  104 105 106 0          #GrAngS  0          #GrAng  360      5

** Geometry for the Gregorian sphere cap on bottom
LA  104
KK  111 112 113 114      360      6      6      0

** Geometry for the Gregorian sphere for the flat top
LA  105
KR  115 116 118          360      6      6
KR  115 116 117 118     360      6      6

** Connect points for connecting the sphere to the azimuth arm
BL  126 115              0.335    0.335

** Apply the scaling factor
SF  1                    #scaling

** ----- **
** End of the geometrical input                               **
** ----- **
EG  1  0  1  0
0

** Set the frequency
** FR  11  0          5.0e6          5.2e6 ** used for frequency sweep
FR  1          5.1e6

** ----- **
** Voltage gap excitation at a segment for 5.1 MHz          **
** ----- **

A1  0  1          1  0
A1  1  2          1  90
A1  1  3          1  180
A1  1  4          1  270

```

A1	1	5	1	120
A1	1	6	1	210
A1	1	7	1	300
A1	1	8	1	390
A1	1	9	1	240
A1	1	10	1	330
A1	1	11	1	420
A1	1	12	1	510

```

** ----- **
** Voltage gap excitation at a segment for 8.175 MHz
** ----- **

```

```

** Comment out 'LD' cards for closed passive array
** no voltage, 10e10 impedance for open on passive array

```

LD	1001	10e10
LD	1002	10e10
LD	1003	10e10
LD	1004	10e10

LD	1005	10e10
LD	1006	10e10
LD	1007	10e10
LD	1008	10e10

LD	1009	10e10
LD	1010	10e10
LD	1011	10e10
LD	1012	10e10

PW	1	0	6e5
----	---	---	-----

```

** surface currents
OS 1 1

```

```

** ----- **
** Far Fields
** ----- **
** horizontal pattern
FF  1  1  361  0  90  0  1
** vertical pattern Phi = 0
FF  1  361  1  0  0  0  1
** vertical pattern Phi = 90
FF  1  361  1  0  0  90  1
** 3D pattern
** FF  1  361  361  0  0  0  1  1
** ----- **
** Near fields
** ----- **

#n=120

** Inside Gregorian
#ymin = -1/#scaling
#ymax = 1/#scaling
#xmin = 29/#scaling
#xmax = 31/#scaling
#zloc = 132.29/#scaling
#deltax = (#xmax-#xmin)/#n
#deltay = (#ymax-#ymin)/#n
FE  1  #n  #n  1  0  #xmin  #ymin  #zloc  #deltax  #deltay

** Visitor Center
#ymin = 123.66/#scaling
#ymax = 125.66/#scaling
#xmin = 215.4/#scaling
#xmax = 217.4/#scaling
#zloc = 340
#deltax = (#xmax-#xmin)/(#n-1)

```

```

#deltay = (#ymax-#ymin)/(#n-1)
FE 1 #n #n 1 0 #xmin #ymin #zloc #deltax #deltay

** Upper Platform Walkway
#zmin = 138.5/#scaling
#zmax = 140.5/#scaling
#xmin = -1.5/#scaling
#xmax = 1.5/#scaling
#yloc = 0
#deltax = (#xmax-#xmin)/(#n-1)
#deltaz = (#zmax-#zmin)/(#n-1)
FE 1 #n 1 #n 0 #xmin #yloc #zmin #deltax #deltaz

** Dipole end 5.1 MHz
#ymin = 40.248/#scaling
#ymax = 42.552/#scaling
#xmin = -3.46/#scaling
#xmax = -1.16/#scaling
#deltax = (#xmax-#xmin)/#n
#deltay = (#ymax-#ymin)/#n
FE 1 #n #n 1 0 #xmin #ymin #Drspc5MHz#deltax #deltay

** Subreflector tip 5.1 MHz
#xmin = 83.664/#scaling
#xmax = 85.664/#scaling
#zmin = 143.159/#scaling
#zmax = 145.159/#scaling
#yloc = 48.881/#scaling
#deltaz = (#zmax-#zmin)/#n
#deltay = (#xmax-#xmin)/#n
FE 1 #n 1 #n 0 #xmin #yloc #zmin #deltax #deltaz

** Subreflector trough 5.1 MHz
#xmin = -1/#scaling
#xmax = 1/#scaling
#zmin = 100/#scaling

```

```

#zmax = 102/#scaling
#deltaz = (#zmax-#zmin)/#n
#deltay = (#xmax-#xmin)/#n
FE 1 #n 1 #n 0 #xmin #yloc #zmin #deltax #deltaz

** Dipole end 8.175 MHz
#ymin = -16.087/#scaling
#ymax = -18.392/#scaling
#xmin = 7.623/#scaling
#xmax = 9.933/#scaling
#deltax = (#xmax-#xmin)/(#n-1)
#deltay = (#ymax-#ymin)/(#n-1)
FE 1 #n #n 1 0 #xmin #ymin #Drspc8MHz#deltax #deltay

** End
EN

```

Appendix B

Feko Model Input File for Dual Array Design with 8.175 MHz Active

```
** Arecibo reflector as a cassegrain system fed by crossed dipoles.
** Both Antenna Arrays Present (5.1 and 8.175 MHz)
** Active array 8.175 MHz

**
** Kyle Labowski
** Created: 9/29/2008
** Updated: 2/11/2009

** ----- **
** Variables **
** ----- **

** Scaling factor
#scaling = 0.3048          ** meters to feet

** Frequency and wavelength
#freq8MHz = 8.175e6        ** freq in Hertz
#lam8MHz = #c0/#freq8MHz  ** minimum wavelength for segmentation
#lam8MHz = #lam8MHz/#scaling ** scale the wavelength as desired

#freq5MHz = 5.1e6         ** freq in Hertz
#lam5MHz = #c0/#freq5MHz  ** minimum wavelength for segmentation
#lam5MHz = #lam5MHz/#scaling ** scale the wavelength as desired

** Dish variables
```

```

#Dr = 870          ** Radius of the spherical reflector
#Rr = 300          ** Distance between sub-reflector and main dish
#Rr2 = 300         ** Radius of reflector for surface at dish focal point
#SRad = 145        ** Radius of sub-reflector area
#Rz = #Rr2+#Rr     ** Center of Reflector sphere (Rz > Dr/2 (435))

** Ground screen variables
#GSHgt = 50        ** Height of ground screen above main dish
#GSLen = 34.2      ** distance of tip from dish edge in x direction
#sang = ARCSIN(#SRad/#Rr2) ** angle from center of sub-reflector to edge off z axis
#sadeq = (#sang*180)/#pi ** angle in degrees
#adeg = 35         ** angle from center of main dish to edge off z axis
#ang = (#adeg*#pi)/180 ** angle in radians
#GSBasz = #Dr*(1-COS(#ang)) ** height from bot of main dish to bot of gnd screen
#GSTopz = #GSBasz + #GSHgt ** height from bot of main dish to top of gnd screen
#GSBasx = #Dr * SIN(#ang) ** lateral distance center to dish to bot of gnd screen
#GSTopx = #GSBasx + #GSLen ** lateral distance center to dish to top of gnd screen

** Point calculations for reflector
#Href = #Rr2*(1-COS(#sadeq*#pi/180)) ** Height of the reflector
#HdTop = #Href + #Rr ** Height of the top of the reflector

#yloc = -#SRad*COS(30*#pi/180) ** y-location of 2nd tie point of reflector
#xloc = -#SRad*SIN(30*#pi/180) ** x-location of 2nd tie point of reflector

** Antenna Variables 5.1 MHz
#Drv5MHz = 0.217*#lam5MHz ** half the length of a driven element
#Drspc5MHz = 0.1757*#lam5MHz ** distance from gnd (reflector) to driven
#Fd5Mhz = 0.0124*#lam5MHz ** Center of feed segment for each driven half
#aspace5MHz = 0.8414*#lam5MHz ** Array spacing

** Antenna Variables 8.175 MHz
#Drv8MHz = 0.214*#lam8MHz ** half the length of a driven element
#Drspc8MHz = 0.2*#lam8MHz ** distance from gnd (reflector) to driven
#Fd8Mhz = 0.0124*#lam8MHz ** Center of feed segment for each driven half
#aspace8MHz = 0.83814920*#lam8MHz ** Array spacing

```

```

#angshift = 63.19
#angshift8MHz = 3.19

** Subreflector Variables
#subscale = 1.106
#subhght = 299    ** subreflector height for 8.175 MHz
** #subhght = 284    ** subreflector height for 5.1 MHz

** Translation Variables
#shiftA8MHz =#aspace8MHz*TAN(#pi/6)
#shiftA5MHz =#aspace5MHz*TAN(#pi/6)

** Variables for defining the Gregorian housing
#GrX=30*3.28084    ** X location of Gregorian center
#GrY=0            ** Y Location of Gregorian Center
#GrZ=128*3.28084  ** Z Location of Gregorian Center
#GrRad=12.8016*3.28084  ** Radius of Gregorian Center
#GrTop=#GrZ+#GrRad  ** Top location of the Gregorian sphere
#GrSide=#GrX+#GrRad  ** Side location of the Gregorian sphere
#GrAngS=27        ** The angle to start the curve of sphere
#GrAng=110        ** The angle measured from Z axis to complete the sphere

** Variables for bottom cap of Gregorian sphere
#GrCpBas=#GrZ-#GrRad*cos((180-#GrAng)*#pi/180)  ** Height of base of the cap
#Cap_of_st=#GrCpBas-0.5*3.28084  ** Height of hole in cap offset value from cap edge
#GrB_rad=#GrX+#GrRad*sin((180-#GrAng)*#pi/180)  ** Radius for the base of the cap
#Gr_V_X=#GrX+3*3.28084  ** X location of hole in the cap (vertex)
#Gr_V_rad=6.5532*3.28084  ** Radius of the hole in the cap
#Gr_V_sid=#Gr_V_rad+#Gr_V_X  ** Point for the radius with offest
#Gr_V_Y=#GrY+0  ** Y location of the Gregorian cap vertex hole

** Variables for top cap of the dome
#GrCp_top=#GrZ+#GrRad*cos((#GrAngS)*#pi/180)  ** Height of the flat top of the sphere Z
#GrCp_sid=#GrX+#GrRad*sin((#GrAngS)*#pi/180)  ** Radius of the cap of the dome top X
#GrCp_nor=#GrCp_top+1*3.28084  ** Normal Position for the top cap
#inner=#GrX+0.3*#GrRad*sin((#GrAngS)*#pi/180)  ** X location for inner circle

```

```

** ----- **
** Segmentation parameters **
** ----- **
#seg_rad = 0.166667      ** segment radius
#tri_len = #lam8MHz/4   ** triangle size for 8.175 MHz
#seg_len = #lam8MHz/40  ** segmentation length for 8.175 MHz
** #tri_len = #lam5MHz/6    ** triangle size for 5.1 MHz
** #seg_len = #lam5MHz/40  ** segmentation length for 5.1 MHz

IP                      #seg_rad #tri_len #seg_len

** ----- **
** Define Points **
** ----- **
** Define dish points
** Define points for a quarter of the main dish
DP   D1                  0          0          #Dr
DP   D2                  0          0          0
DP   D3                  #Dr       0          #Dr

** Define ground screen points
DP   GS1                 0          0          #GSTopz
DP   GS2                 0          0          #GSBasz
DP   GS3                 #GSTopx  0          #GSTopz
DP   GS4                 #GSBasx  0          #GSBasz

** User defined points for the construction of the Gregorian sphere
DP   104                 #GrX     #GrY     #GrZ
DP   105                 #GrX     #GrY     #GrTop
DP   106                 #GrSide  #GrY     #GrZ

** User defined points for the construction of the Gregorian sphere cap
DP   111                 #GrX     #GrY     #GrCpBas  ** S1
DP   112                 #Gr_V_X  #Gr_V_Y  #Cap_of_st ** S2
DP   113                 #GrB_rad #GrY     #GrCpBas  ** S3

```

```

DP 114 #Gr_V_sid #Gr_V_Y #Cap_of_st ** S4

** User defined points for the construction of the Gregorian sphere top cap
DP 115 #GrX #GrY #GrCp_top ** S1
DP 116 #GrX #GrY #GrCp_nor ** S2
DP 117 #GrCp_sid #GrY #GrCp_top ** S3
DP 118 #inner #GrY #GrCp_top ** S4

** Define a point to connect gregorian sphere to azimuth arm NEC file
DP 126 105 0 464

** Define antenna points for 5.1 MHz
** Define points for half driven element on x axis for 5.1 MHz
DP: DvX1_5MHz : : : : : #Drv5MHz : 0 : #Drspc5MHz
DP: DvX2_5MHz : : : : : #seg_len : 0 : #Drspc5MHz
DP: DvX3_5MHz : : : : : 0 : 0 : #Drspc5MHz

** Antenna ball points
DP: ball_5MHz : : : : : #Drv5MHz+0.5 : 0 : #Drspc5MHz
DP: ball2_5MHz : : : : : #Drv5MHz+0.5 : 0.5 : #Drspc5MHz

** Define antenna points for 8.175 MHz
** Define points for half driven element on x axis for 8.175 MHz
DP: DvX1_8MHz : : : : : #Drv8MHz : 0 : #Drspc8MHz
DP: DvX2_8MHz : : : : : #seg_len : 0 : #Drspc8MHz
DP: DvX3_8MHz : : : : : 0 : 0 : #Drspc8MHz

** Antenna ball points
DP: ball_8MHz : : : : : #Drv8MHz+0.5 : 0 : #Drspc8MHz
DP: ball2_8MHz : : : : : #Drv8MHz+0.5 : 0.5 : #Drspc8MHz

** ----- **
** Creat Geometry **
** ----- **

** Create dish

```

```

KU   D1   D2   D3   1           0           0           #adeg       360

** Construct ground shield
KK   GS1  GS2  GS3  GS4           360           1           0

** ----- **
** Construct 5.1 MHz antenna
** ----- **
LA   1
BL: DvX2_5MHz : DvX3_5MHz

LA   201
BL: DvX1_5MHz : DvX2_5MHz
KU: ball_5MHz : DvX1_5MHz : ball2_5MHz : : : 0 : 0 : 180 : 360 : #tri_len/75

** translation
** Create 3 additional parts for 1st crossed dipole
TG   3    1    1    1    0           90
TG   3    201  201  1    0           90

** Shift Dipole
TG: 0 : 1 : 4 : : 0 : : : : : -#shiftA5MHz
TG: 0 : 201 : 204 : : 0 : : : : : -#shiftA5MHz

** Create 2nd and 3rd crossed dipoles
TG   2    1    4    4    0           120
TG   2    201  204  4    0           120

TG   0    1    12           0           #angshift
TG   0    201  212           0           #angshift

** ----- **
** Construct 8.175 MHz antenna
** ----- **
LA   1001

```

```

BL: DvX2_8MHz : DvX3_8MHz

LA 1201
BL: DvX1_8MHz : DvX2_8MHz
KU: ball_8MHz : DvX1_8MHz : ball2_8MHz : : : 0 : 0 : 180 : 360 : #tri_len/75

** translation
** Create 3 additional parts for 1st crossed dipole
TG 3 1001 1001 1 0 90
TG 3 1201 1201 1 0 90

** Shift Dipole
TG: 0 : 1001 : 1004 : : 0 : : : : : -#shiftA8MHz
TG: 0 : 1201 : 1204 : : 0 : : : : : -#shiftA8MHz

** Create 2nd and 3rd crossed dipoles
TG 2 1001 1004 4 0 120
TG 2 1201 1204 4 0 120

TG: 0 : 1001 : 1012 : : 0 : : : : : #angshift8MHz
TG: 0 : 1201 : 1212 : : 0 : : : : : #angshift8MHz

IP #seg_rad #tri_len #seg_len

LA 100
** Create reflector
IN 8 31 "subreflectorSmall.cfm"

TG: 0 : Split_back3.Face1 : Split_back3.Face1 : : 0 : : : : : : : #subscale
TG: 0 : Split_back3.Face1 : Split_back3.Face1 : : 0 : : : : : : : #subhght

** Create upper platform
IN 5 1 "UP_PLT_2.NEC"

** Geometry for the Gregorian sphere

```

```

LA 103
KU 104 105 106 0 #GrAngS 0 #GrAng 360 5

** Geometry for the Gregorian sphere cap on bottom
LA 104
KK 111 112 113 114 360 6 6 0

** Geometry for the Gregorian sphere for the flat top
LA 105
KR 115 116 118 360 6 6
KR 115 116 117 118 360 6 6

** Connect points for connecting the sphere to the azimuth arm
BL 126 115 0.335 0.335

** Apply the scaling factor
SF 1 #scaling

** ----- **
** End of the geometrical input **
** ----- **
EG 1 0 1 0 0

** Set the frequency
** FR 11 0 8.075e6 8.275e6 ** used for frequency sweep
FR 1 8.175e6

** ----- **
** Voltage gap excitation at a segment for 5.1 MHz
** ----- **

** Comment out 'LD' cards for closed passive array
** no voltage, 10e10 impedance for open on passive array

```

LD	1	10e10
LD	2	10e10
LD	3	10e10
LD	4	10e10
LD	5	10e10
LD	6	10e10
LD	7	10e10
LD	8	10e10
LD	9	10e10
LD	10	10e10
LD	11	10e10
LD	12	10e10

** ----- **
 ** Voltage gap excitation at a segment for 8.175 MHz
 ** ----- **

A1	0	1001	1	0
A1	1	1002	1	90
A1	1	1003	1	180
A1	1	1004	1	270
A1	1	1005	1	120
A1	1	1006	1	210
A1	1	1007	1	300
A1	1	1008	1	390
A1	1	1009	1	240
A1	1	1010	1	330
A1	1	1011	1	420
A1	1	1012	1	510
PW	1	0	6e5	

```

** surface currents
OS  1      1

** ----- **
** Far Fields
** ----- **
** horizontal pattern
FF  1  1  361  0      90      0      1
** vertical pattern Phi = 0
FF  1  361  1  0      0      0      1
** vertical pattern Phi = 90
FF  1  361  1  0      0      90      1
** 3D pattern
** FF  1  361  361  0      0      0      1      1

** ----- **
** Near fields
** ----- **

#n=120

** Inside Gregorian
#ymin = -1/#scaling
#ymax = 1/#scaling
#xmin = 29/#scaling
#xmax = 31/#scaling
#zloc = 132.29/#scaling
#deltax = (#xmax-#xmin)/#n
#deltay = (#ymax-#ymin)/#n
FE  1  #n  #n  1  0  #xmin  #ymin  #zloc  #deltax  #deltay

** Visitor Center
#ymin = 123.66/#scaling
#ymax = 125.66/#scaling
#xmin = 215.4/#scaling
#xmax = 217.4/#scaling

```

```

#zloc = 340
#deltax = (#xmax-#xmin)/(#n-1)
#deltay = (#ymax-#ymin)/(#n-1)
FE 1 #n #n 1 0 #xmin #ymin #zloc #deltax #deltay

** Upper Platform Walkway
#zmin = 138.5/#scaling
#zmax = 140.5/#scaling
#xmin = -1.5/#scaling
#xmax = 1.5/#scaling
#yloc = 0
#deltax = (#xmax-#xmin)/(#n-1)
#deltaz = (#zmax-#zmin)/(#n-1)
FE 1 #n 1 #n 0 #xmin #yloc #zmin #deltax #deltaz

** Dipole end 5.1 MHz
#ymin = 40.248/#scaling
#ymax = 42.552/#scaling
#xmin = -3.46/#scaling
#xmax = -1.16/#scaling
#deltax = (#xmax-#xmin)/#n
#deltay = (#ymax-#ymin)/#n
FE 1 #n #n 1 0 #xmin #ymin #Drspc5MHz#deltax #deltay

** Dipole end 8.175 MHz
#ymin = -16.087/#scaling
#ymax = -18.392/#scaling
#xmin = 7.623/#scaling
#xmax = 9.933/#scaling
#deltax = (#xmax-#xmin)/(#n-1)
#deltay = (#ymax-#ymin)/(#n-1)
FE 1 #n #n 1 0 #xmin #ymin #Drspc8MHz#deltax #deltay

** Subreflector tip 8.175 MHz
#xmin = 83.664/#scaling

```

```

#xmax = 85.664/#scaling
#zmin = 147.759/#scaling
#zmax = 149.759/#scaling
#yloc = 48.881/#scaling
#deltaz = (#zmax-#zmin)/(#n-1)
#deltay = (#xmax-#xmin)/(#n-1)
FE 1 #n 1 #n 0 #xmin #yloc #zmin #deltax #deltaz

** Subreflector trough 8.175 MHz
#xmin = -1/#scaling
#xmax = 1/#scaling
#zmin = 104.6/#scaling
#zmax = 106.6/#scaling
#deltaz = (#zmax-#zmin)/(#n-1)
#deltay = (#xmax-#xmin)/(#n-1)
FE 1 #n 1 #n 0 #xmin #yloc #zmin #deltax #deltaz

** End
EN

```

Appendix C

NEC File for the Upper Platform

CM UPPER PLATFORM FOR ARECIBIO
CM LAST EDITED ON 13 Oct 2003 BY TURNER J
CM FOR FEKO IMPORT
CM MAJOR DIMENSIONS WERE VAIRIFIED WITH NUMBERS FROM
CM ARECIBIO ON 15 SEPT 2003
CM PLATFORM HEIGHT INCREASE FROM 480 FEET TO 496 FT
CM
CE
CM BUILD MAIN TRUSS HORIZONTAL MEMBERS
GW 6001,3, 108,62.353829,0, 36,62.353829,0, 1.005
GW 6002,1, 36,62.353829,0, 16.7077,62.353829,0, 1.005
GW 6003,2, 16.7077,62.353829,0, -16.7077,62.353829,0, 1.005
GW 6004,1, -16.7077,62.353829,0, -36,62.353829,0, 1.005
GW 6005,3, -36,62.353829,0, -108,62.353829,0, 1.005
CM BUILD BRACING TRUSS HORIZONTAL MEMBERS
GW 6006,4, 36,62.353829,0, 72,0,0, 0.3335
CM BUILD TIE-DOWN TRUSS
GW 6007,3, 108,62.353829,30, 165.16,95.353829,30, 0.1
GM 0 1 0 0 0 0 0 30 6001 1 6006 4
CM BUILD VERTICAL MAIN TRUSS MEMBERS
GW 6013,1, 108,62.353829,0, 108,62.353829,30, 1.005
GW 6014,1, 36,62.353829,0, 36,62.353829,30, 1.005
GW 6015,1, 16.7077,62.353829,0, 16.7077,62.353829,30, 1.005
GW 6016,1, 60,62.353829,0, 60,62.353829,30, 1.005
GW 6017,1, 84,62.353829,0, 84,62.353829,30, 1.005
GW 6018,1, 0,62.353829,0, 0,62.353829,30, 1.005
GW 6019,1, -36,62.353829,0, -36,62.353829,30, 1.005
GW 6020,1, -16.7077,62.353829,0, -16.7077,62.353829,30, 1.005
GW 6021,1, -60,62.353829,0, -60,62.353829,30, 1.005
GW 6022,1, -84,62.353829,0, -84,62.353829,30, 1.005
CM BUILD VERTICAL BRACING TRUSS MEMBERS
GW 6023,1, 0,-62.353829,0, 0,-62.353829,30, 0.3335
GW 6024,1, 18,-62.353829,0, 18,-62.353829,30, 0.3335
GW 6025,1, -18,-62.353829,0, -18,-62.353829,30, 0.3335
CM BUILD DIAGONAL MAIN TRUSS MEMBERS
GW 6026,1, 0,62.353829,0, -16.7077,62.353829,30, 1.005
GW 6027,1, -16.7077,62.353829,0, -36,62.353829,30, 1.005
GW 6028,1, -36,62.353829,0, -60,62.353829,30, 1.005
GW 6029,1, -60,62.353829,0, -84,62.353829,30, 1.005
GW 6030,1, -84,62.353829,0, -108,62.353829,30, 1.005
GW 6031,1, 0,62.353829,0, 16.7077,62.353829,30, 1.005
GW 6032,1, 16.7077,62.353829,0, 36,62.353829,30, 1.005
GW 6033,1, 36,62.353829,0, 60,62.353829,30, 1.005
GW 6034,1, 60,62.353829,0, 84,62.353829,30, 1.005
GW 6035,1, 84,62.353829,0, 108,62.353829,30, 1.005
CM BUILD SECONDARY BRACING TRUSSES

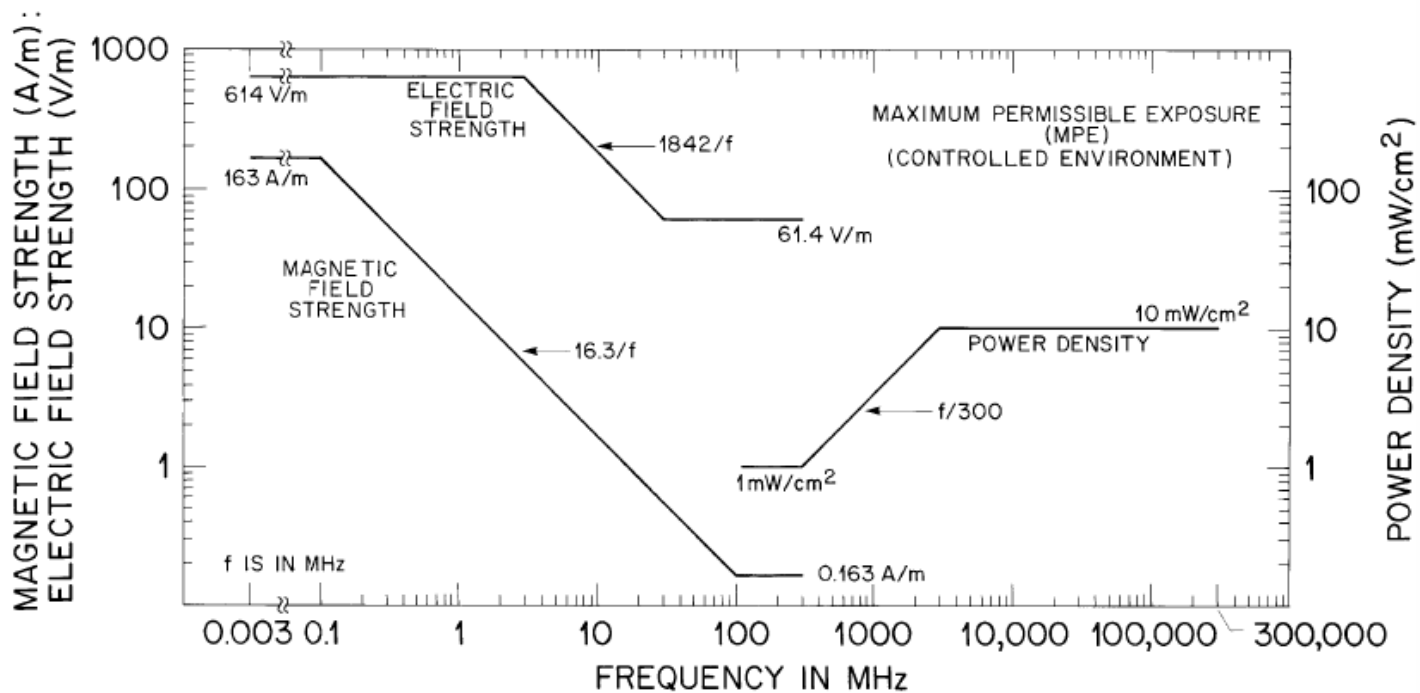
GW 6036,3, 0,0,0, 36,62.353829,0, 0.3335
 GW 6037,3, 0,0,0, 72,0,0, 0.3335
 GW 6038,3, 0,0,0, 36,62.353829,30, 0.3335
 GW 6039,3, 0,0,0, 72,0,30, 0.3335
 GW 6040,1, 24,0,0, 24,0,10, 0.3335
 GW 6041,1, 48,0,0, 48,0,20, 0.3335
 GM 0 5 0 0 60 0 0 0 6040 1 6041 1
 GM 100 2 0 0 120.00 0 0 0 6001 1 6039 3
 CM BUILD AZIMUTH FEED TRACK
 GA 6044 24 64.5534 0 359.999 1.005
 GM 0 0 90 0 0 0 0 -3 6044 1 6044 24
 CM CONNECT FEED TRACK TO PLATFORM
 GW 6045,1, -18,-62.35382843,0, -16.70732117,-62.35387802,-3, 0.3335
 GW 6046,1, 18,-62.35382843,0, 16.70732117,-62.35387802,-3, 0.3335
 GM 0 2 0 0 120 0 0 0 6045 1 6046 1
 GW 6047,1, -45.64583969,-45.64645004,-3, -45.64614868,-45.64620590,0,
 0.3335
 GW 6048,1, -62.35365295,-16.70816040,-3, -62.35385513,-16.70762062,0,
 0.3335
 GM 0 2 0 0 120 0 0 0 6047 1 6048 1
 CM CHANGED 480 Z TO 496
 GM 0 0 0 0 0 0 0 496 6001
 CM BUILD AZIMUTH ARM
 CM BUILD BOTTOM CHORD
 GW 6301,2, 0,6,0, 21.4246,6,0.5468, 0.3335
 GW 6302,2, 21.4246,6,0.5468, 42.8493,6,2.1914, 0.3335
 GW 6303,2, 42.8493,6,2.1914, 64.274,6,4.9472, 0.3335
 GW 6304,1, 64.274,6,4.947, 85.774,6,8.8519, 0.3335
 GW 6305,1, 85.774,6,8.8519, 105.774,6,13.5374, 0.3335
 GW 6306,1, 105.774,6,13.5374, 124.274,6,18.8068, 0.3335
 GW 6307,1, 124.274,6,18.8068, 139.274,6,23.7643, 0.3335
 GW 6308,1, 139.274,6,23.7643, 152,6,28.47001, 0.3335
 CM BUILD TOP CHORD
 GW 6311,6, 0,6,33.5, 64.274,6,33.5, 0.3335
 GW 6312,1, 64.274,6,33.5, 85.774,6,33.5, 0.3335
 GW 6313,1, 85.774,6,33.5, 105.774,6,33.5, 0.3335
 GW 6314,1, 105.774,6,33.5, 124.274,6,33.5, 0.3335
 GW 6315,1, 124.274,6,33.5, 139.274,6,33.5, 0.3335
 GW 6316,1, 139.274,6,33.5, 152,6,28.47001, 0.3335
 CM BUILD VERTICAL BRACES
 GW 6317,2, 21.4246,6,0.5468, 21.4246,6,33.5, 0.3335
 GW 6318,2, 42.8493,6,2.1914, 42.8493,6,33.5, 0.3335
 GW 6319,2, 64.274,6,4.947, 64.274,6,33.5, 0.3335
 GW 6320,2, 85.774,6,8.8519, 85.774,6,33.5, 0.3335
 GW 6321,2, 105.774,6,13.5374, 105.774,6,33.5, 0.3335
 GW 6322,1,124.274,6,18.8068,124.274,6,33.5,.3335
 GW 6323,1,139.274,6,23.7643,139.274,6,33.5,.3335
 CM BUILD ANGLE BRACING
 GW 6324,1,0,6,0,21.4246,6,17.0234,.3335
 GW 6325,1,0,6,33.5,21.4246,6,17.0234,.3335
 GW 6326,1,21.4246,6,0.5468,42.8493,6,17.8457,.3335
 GW 6327,1,21.4246,6,33.5,42.8493,6,17.8457,.3335
 GW 6328,1,42.8493,6,2.1914,64.274,6,19.2236,.3335
 GW 6329,1,42.8493,6,33.5,64.274,6,19.2236,.3335
 GW 6330,1,64.274,6,33.5,85.774,6,8.8519,.3335

GW 6331,1,85.774,6,33.5,105.774,6,13.5374,.3335
 GW 6332,1,105.774,6,33.5,124.274,6,18.8068,.3335
 GW 6333,1,124.274,6,33.5,139.274,6,23.7643,.3335
 CM BUILD CROSS BRACES
 GW 6334,2,21.4246,6,0.5468,21.4246,-6,0.5468,.3335
 GW 6335,2,42.8493,6,2.1914,42.8493,-6,2.1914,.3335
 GW 6336,2,64.274,6,4.947,64.274,-6,4.947,.3335
 GW 6337,2,85.774,6,8.8519,85.774,-6,8.8519,.3335
 GW 6338,2,105.774,6,13.5374,105.774,-6,13.5374,.3335
 GW 6339,2,124.274,6,18.8068,124.274,-6,18.8068,.3335
 GW 6340,2,21.4246,6,33.5,21.4246,-6,33.5,.3335
 GW 6341,2,42.8493,6,33.5,42.8493,-6,33.5,.3335
 GW 6342,2,64.274,6,33.5,64.274,-6,33.5,.3335
 GW 6343,2,85.774,6,33.5,85.774,-6,33.5,.3335
 GW 6344,2,105.774,6,33.5,105.774,-6,33.5,.3335
 GW 6345,2,124.274,6,33.5,124.274,-6,33.5,.3335
 GW 6346,2,139.274,6,23.7643,139.274,-6,23.7643,.3335
 GW 6347,2,152,6,28.47001,152,-6,28.47001,.3335
 GM 100 2 0 0 0 0 -6 0 6301 1 6316 1
 GM 100 1 0 0 0 0 -12 0 6317 1 6333 1
 GM 300 1 0 0 180 0 0 0 6301 1 6516 1
 CM TROUBLED AREA FOR FEKO
 CM GM 400 1 0 0 180 0 0 0 6417 1 6433 1
 CM END OF TROUBLED AREA FOR FEKO
 CM BUILD CENTER VERTICAL BRACE
 GW 6348,2,0,6,0,0,6,33.5,.3335
 CM CONNECT AZIMUTH ARM TO PLATFORM
 GW 6350,1,0,0,44,0,6,33.5,.3335
 GW 6351,1,0,0,44,0,-6,33.5,.3335
 GW 6352,1,0,0,44,0,0,33.5,.3335
 GW 6353,1,-64.55339813,-0.00057920,41,-
 64.27400208,0.00000156,33.5,.3335
 GW 6354,1,64.55339813,0,41,64.27400208,0,33.5,.3335
 CM CHANGED Z OF 436 TO 452
 GM 0 0 0 0 0 0 0 452 6301 1 6816 1
 CM END OF CHANGE
 CM TROUBLED AREA FOR FEKO
 CM GM 0 0 0 0 0 0 0 436 6348 1 6354 1
 CM GM 0 0 0 0 0 0 0 436 6717 1 6733 1
 CM END OF TROUBLED AREA FOR FEKO
 CM BUILD MAIN AND TIE-DOWN CABLES
 CM ADD 16 TO Z CORRIDENT OF THE NEXT TWO LINES
 GW 6361,20, 165.16,95.353829,526, 165.16,95.353829,30, .1
 GW 6365,30, 606.2177,350,626.372, 108,62.353829,496, .1
 CM END OF CHANGE
 GM 0 0 0 0 .25 0 0 0 6361 1 6361 20
 GM 1 1 0 0 -.5 0 0 0 6361 1 6361 20
 GM 1 2 0 0 120 0 0 0 6361 1 6365 30
 CM TROUBLED AREA FOR FEKO
 CM GM 1 2 0 0 120 0 0 0 6362 1 6362 20
 CM END OF TROUBLED AREA FOR FEKO
 CM BUILD CATWALK
 GW 6368,15, 108,62.353829,496, 606.2177,350,215, .3335
 CM BUILD CARRIAGE HOUSE
 GW 6371,2, -9,6,0, 9,6,0, .3335

GW 6372,2, -9,-6,0, 9,-6,0, .3335
GW 6373,2,-9,-6,0, -9,6,0,.3335
GW 6374,2,9,6,0,9,-6,0,.3335
GM 4 1 0 0 0 0 9.8 6371 1 6374 2
GW 6379,2,-9,-6,0,-9,-6,9.8,.3335
GW 6380,2,9,-6,0,9,-6,9.8,.3335
GM 2 1 0 0 0 0 12 0 6379 1 6380 2
CM BUILD LINE FEED
GW 6383,10, 0,0,0, 0,0,-96, 1
CM CHANGED Z VALUE FROM 430 TO 446
GM 0 0 0 15 0 -70 0 446 6371 1 6383 10
CM CONNECT TIE-DOWN CABLES
CM ADD 16 TO THE Z COODENT OF NEXT TWO LINES
GW 6390,1, 165.57449341,94.63227081,526, 165.16,95.353829,526, .01
GW 6391,1, 164.74237061,96.07356262,526, 165.16,95.353829,526, .01
CM END OF Z CHANGE
GM 0 2 0 0 120 0 0 0 6390 1 6391 1
CM CONNECT LINE FEED CARRIAGE HOUSE
GW 6400,1, -70,0,446, -78.6933,-6,448.329371, 0.55
GW 6400,1, -70,0,446, -78.6933,6,448.329371, 0.55
GW 6400,1, -70,0,446, -61.3066,6,443.6706, 0.55
GW 6400,1, -70,0,446, -61.3066,-6,443.6706, 0.55
CM CONNECT CARRIAGE HOUSE TO AZMUTH ARM
GW 6400,2, -58.7702,-6,453.136, -42.8493,-6,454.1914, 0.55
GW 6400,2, -58.7702,6,453.136, -42.8493,5.999,454.1914, 0.55
CM GW 6400,2, -76.1569,-6,457.7954, -85.7740,-6,460.8519, 0.1
CM GW 6400,2, -76.1569,6,457.7954, -85.7740,5.9999,460.8519, 0.1
CM MAKE A WIRE FOR CONNECTING TO GEORGIAN DOME
GW 6400,1, 105.7740,0,465.5374, 105,0,464, 0.3335
cm BUILD THE VERTICAL TIE DOWN SUPPORTS
GW 6400,4, -108,62.353829,526, -108,62.353829,566, 0.1
GW 6400,4, 108,62.353829,526, 108,62.353829,566, 0.1
GW 6400,4, 0,-124.70766,526, 0,-124.70766,566, 0.1
CM ATTACHE VERTICLE TIE DOWN TO CEN OF PLATROFM
GW 6400,8, 0,0,496, -108,62.353829,566, 0.1
GW 6400,8, 0,0,496, 108,62.353829,566, 0.1
GW 6400,8, 0,0,496, 0,-124.70766,566, 0.1
CM CONNECT HORIZONTAL TIEDWON TO VERTICEL TIE DOWN
GW 6400,4, -165.158838,95.3558,526, -108,62.353829,566, 0.1
GW 6400,4, 165.160,95.3538,526, 108,62.353829,566, 0.1
GW 6400,4, -0.00116,-190.70967,526, 0,-124.70766,566, 0.1
GE
CM SCALING IS DONE WITH FEKO
CM GS0 0 .3048
GE
EN

Appendix D

Graph of Maximum Permissible Exposure Levels for Controlled Environments in terms of Field and Power Density



Appendix E

Graph of Maximum Permissible Exposure Levels for Uncontrolled Environments in terms of Field and Power Density

